Novel recombinant varicella-zoster virus to study infection and induction of hypersensitivity in rat models of postherpetic neuralgia

by

Benjamin E. Warner

BA, University at Buffalo, 2013

MS, University at Buffalo, 2015

Submitted to the Graduate Faculty of the

School of Medicine in partial fulfillment

of the requirements for the degree of

Doctor of Philosophy

University of Pittsburgh

2021

UNIVERSITY OF PITTSBURGH

SCHOOL OF MEDICINE

This dissertation was presented

by

Benjamin E. Warner

It was defended on

October 8, 2021

and approved by

Kathryn M. Albers Ph.D.
Professor, Department of Neurobiology

Nara Lee Ph.D.
Assistant Professor, Department of Microbiology & Molecular Genetics

Sarah E. Ross Ph.D.
Associate Professor, Department of Neurobiology

Kathy H.Y. Shair Ph.D.
Assistant Professor, Department of Microbiology & Molecular Genetics

Dissertation Director, Paul R. Kinchington Ph.D.
Professor, Department of Ophthalmology

Novel recombinant varicella-zoster virus to analyze infection and induction of hypersensitivity in rat models of postherpetic neuralgia

Benjamin E. Warner Ph.D.

University of Pittsburgh, 2021

The mechanisms by which VZV causes pain during herpes zoster (HZ) and postherpetic neuralgia (PHN) are not well understood. Part of this stems from the lack of an animal model of reactivated HZ disease and the pain states that follow. However, primary inoculation of the rat foot- or whisker pad with VZV induces prolonged pain behaviors that resemble clinical PHN. To elucidate the infectious processes necessary for the induction of a pain state in this model, we have developed growth conditional VZV in which the turnover of essential proteins can be regulated by insertion of a degron. We report the degron system was effective for generating conditional knockout mutants for VZV proteins from immediate-early genes ORF4 and -63, and the late ORF9 gene. Inoculation of the recombinant viruses into the rat foot- or whisker pad revealed that VZV productive replication was dispensable for induction of hypersensitivity, whereas events early in the infectious process were essential. We then described a newly available transgenic reporter rat that conditionally expresses a tdTomato fluorescent gene which may help clarify VZV infection of rat tissues *in vivo*. The studies here characterize a recombinant VZV and methods for use in the reporter rat model. Finally, we described additional uses for the growth conditional VZV in two areas of VZV research that have proved difficult: the study of essential gene function and establishment of experimental latency in neuron cultures. The results established that the ORF9 growth conditional VZV may serve as a backbone for additional ORF9 gene mutations to determine essential protein functional domains, though further modifications to the system are required. The ORF4 growth conditional VZV was exploited for the establishment of a latent

infection in human embryonic stem cell derived neurons. We showed that infection of neurons with the ORF4 virus was quiescent, resembled experimental latency, and was reactivatable with a chemical stimulus. This work presents an alternative to current latent infection methods that rely on acyclovir which may damage VZV genomes and render them incapable of reactivation.

Table of Contents

List of Tables

List of Figures

1.0 Introduction

1.1 Virology

1.1.1 Classification, Genome, and Virion

Varicella-zoster virus (VZV) is one of nine distinct human herpesviruses and a member of the Alphaherpesvirus subfamily. Human and non-human Alphaherpesviruses are primarily distinguished from other subfamilies for their fast reproductive cycle, variable host range, and characteristic gene arrangement. VZV shares homology with human herpes simplex virus (HSV) -1 and -2, and non-human Alphaherpesviruses of the Varicellovirus genus including bovine herpesvirus (BHV), equine herpesvirus (EHV), Marek's disease virus (MDV), pseudorabies virus (PRV) [1], and is most closely related to simian varicella virus (SVV) [2]. VZV is one of the smallest herpesviruses with a double-stranded deoxyribonucleic acid (dsDNA) linear genome of about 125-kilobases [3]. The genome can be structurally divided into two unique regions, unique long (U_L) and unique short (U_S), that are separated by internal (IR) and terminal repeat sequences (TR) (**Fig 1**). The configuration of repeated sequences allows for efficient recombination and inversion of the unique regions that gives rise to isomers [4]. In VZV, these isomers are not found to be equally distributed and two forms predominate by inversion of U_S that occurs at an equivalent ratio with respect to the fixed U_L region [5,6]. In HSV, inversion of both U_L and U_S yields four equimolar isomer populations [7,8]. The VZV genome contains at least two origins of replication (*oriS*) located in the duplicated IR_S and TR_S sequences between ORF62 and -63 (**Figs 1 and 2**) [9]. Orthologous origins are found in HSV along with a third origin in the U_L region (*oriL*) between

the genes encoding DNA polymerase and ssDNA binding protein [10]. The encapsidated VZV genome is linear and contains a matching base pair overhang at each end to permit DNA circularization. The circularized DNA or episome is thought to be the primary configuration of Alphaherpesvirus genomes during neuronal latency [11,12].

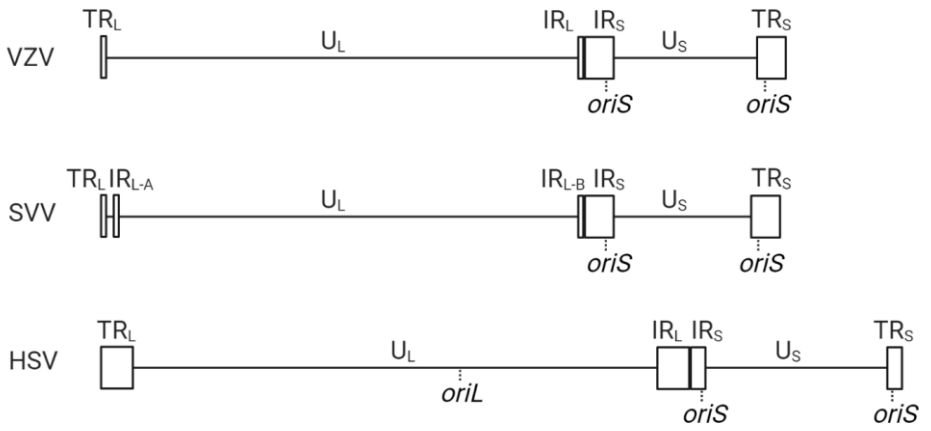

Figure 1: Organization of VZV genome compared SVV and HSV.

The VZV and SVV genome are aproximately 125- and 124-kilobases, respectively. The HSV genome is 152-kilobases. Each genome contains a unique long (U_L) and unique short (U_S) segment that include the majority of ORFs and are flanked by inverted repeat regions labeled according to their location: terminal repeat long (TR_L), internal repeat long (IR_L), and internal repeat short (IR_S), terminal repeat short (TR_S). The TR_L and IR_L sequences in VZV are only 88 bp. SVV contains an additional repeat, $IR_{L\text{-}A}$. The IR_S region contains an origin of replication (*oriS*) and three ORFs, which are duplicated and inverted in TR_S. A third origin, *oriL*, is located in the the U_L region of HSV. Genomes are representative and not to scale. Created with BioRender.com.

At least 70 unique ORFs are encoded by the VZV genome and 44 have been shown to be essential for replication in culture. Twelve other ORFs result in viral growth defects when deleted [13]. Several non-essential genes are recognized as having essential roles in pathogenesis or

specific cell types and organized tissues. A well-studied example is the putative VZV acidic protein kinase encoded by ORF47. It does not affect growth rates in culture, but has critical functions in T cell, skin, and dendritic cell tropism [14–17]. Most VZV genes are conserved across Alphaherpesviruses which allows for the prediction of gene function from HSV-1, which is easier to work with and better studied. The major transcriptional activator of VZV is encoded by ORF62 and is functionally equivalent to HSV-1 ICP4 [18]. ICP4 plays an essential role in the regulation of lytic gene expression for all HSV genes. Both ICP4 and ORF62 are located within the IR_S region and are therefore duplicated within the inverted TR_S region. Adjacent to ORF62 in the repeated sequence, ORF63 encodes an essential regulatory transactivator with host cell modulating activities and ORF64 encodes a non-essential tegument protein. Duplicates of the three genes are labeled as ORF71, -70, and -69, respectively (**Fig 2**).

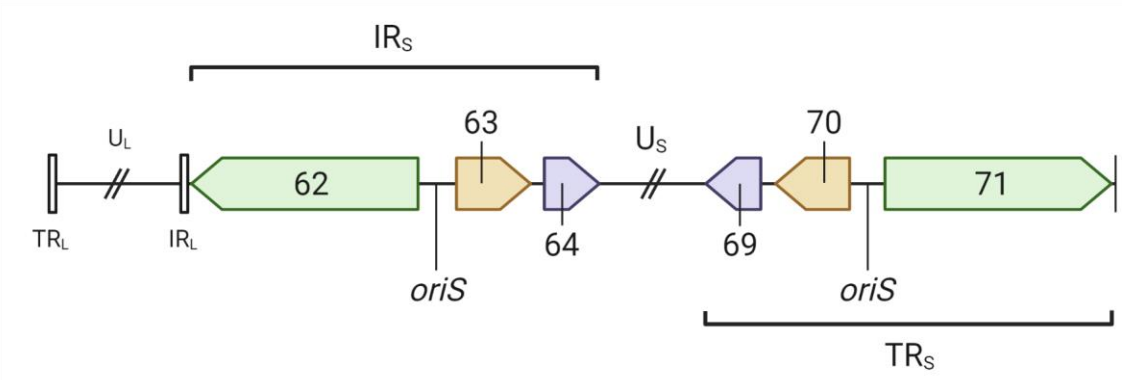

Figure 2: Organization of the IR_S and TR_S genomic regions containing major transcrptional activator protein from ORF62.

ORFs -62, -63, and -64 are found in the interal repeat short (IR_S), which is located at the 5' end of the unique short (U_S) segment. This region is inverted and duplicated at the 3' end of the U_S region, labeled terminal repeat short (TR_S), and contains identical ORFs -71, -70, -69, respectively. Origin of replication (*oriS*) is located between ORF62 and -63 or ORF71 and -70. Duplication of the region suggests evolutionary conservation of these sequences. Not to scale. Created with BioRender.com.

Six VZV ORFs do not have homologs in HSV-1 including, ORFS/L (ORF0), -1, -2, -13, -32, and -57 [3]. Only ORF13 that encodes a thymidylate synthetase [19,20] and ORF57 that encodes a tegument protein [21] have orthologs in other herpesviruses. All but ORFS/L [22] are dispensable for VZV replication in cell culture [21,23–26].

The structure of the VZV virion is indistinguishable from other herpesviruses with a T=16 icosahedral capsid containing the dsDNA genome. The capsid is surrounded by a proteinaceous tegument and enclosed in a lipid membrane envelope. The VZV capsid is composed of 162 capsomeres of major capsid protein from ORF40 and several other ORFs -20, -23, -33, -33.5, -41 that participate in its formation and structure [27–29]. In addition, the portal protein from ORF54 is located at one capsid vertex and it is thought to work with proteins from ORFs -25, -26, -30, -34, -43, -42/45 to package the linear VZV genome [30].

The surrounding tegument is composed of varying quantities of essential proteins from ORFs -9, -21, -22, -38, -44, -46, -53 and non-essential proteins from ORFs -3, -7, -8, -10, -11, -12, -36, -47, -49, -66 [31]. Many tegument proteins dissociate from the capsid upon cellular entry and envelope release, while the innermost tegument proteins do not completely dissociate and are thought to participate in capsid motility [32–36]. Tegument proteins have diverse functions throughout infection and many facilitate viral gene expression [31]. Proteins from ORF4 and ORF63 [37], ORF62 [38], ORF47 [39], ORF9, and ORF10 [40] are partly characterized for such functions and will be discussed in the results. Essential genes ORF4 and -63, which regulate gene expression, and ORF9 and -54 involved in virion assembly are important in these studies.

The VZV envelope is composed of a lipid membrane interspersed with an abundance of eleven essential (ORFS/L, gB, gE, gH, gK, gL) and non-essential (ORF39, gC, gI, gM, gN) viral glycoproteins that regulate membrane fusion, cellular entry, and egress [41].

1.1.2 Lytic and Latent Life Cycle

Alphaherpesvirus lytic replication is characterized by abundant transcription and translation of most viral ORFs. These include proteins that regulate viral and host gene expression, promote viral genome replication, alter the host cell for mass production of progeny virions, and facilitate VZV spread to new cells. The lytic cycle is thought to occur in all epithelial and some non-neuronal cells, as well as in some neurons whose subtype is only beginning to emerge [42,43]. The primary infection process in epithelia begins with receptor mediated fusion of the virion initiated by VZV gB, gH, and gL interaction with the host membrane inferred by experimental evidence from other herpesviruses [44–47]. Host receptors mediating entry may include myelin-associated glycoprotein (MAG), insulin degrading enzyme (IDE), mannose-6-phosphate (M6P), and other receptors that remain to be identified [41]. Fusion also involves pro-attachment factors such as heparin sulfate proteoglycans which interact with gB to initiate the process [48]. gB, gH, gL and gE have also been implicated in cell-cell fusion events between neighboring cells to form syncytia that contributes to virus spread [49]. Following entry, a portion of the tegument will dissociate from the capsid, while other tegument and capsid proteins facilitate dynein-mediated retrograde axonal transport for nuclear delivery [50]. The linear genome is then deposited into the nucleus where it associates with cellular transactivators and viral factors that were delivered as part of the tegument.

Lytic transcription of herpesviruses can be experimentally subdivided into three distinct kinetic classes based on gene transcriptional requirements. Immediate-early (α), early (β), and late (γ) genes were first described for HSV-1 [51] (**Fig 3**). Experimentally defined α-genes do not require *de novo* protein synthesis and may be transactivated by cellular factors alone or with viral proteins from the tegument [52–54]. VZV α-genes are thought to include ORF4, ORF61, ORF62, and ORF63 based on HSV homology, but this has been hard to experimentally define because high multiplicity of infection (MOI) with cell-free VZV has proved difficult. The α-genes encode gene regulators and transactivators that are required to transcribe β-genes that encode proteins involved in genome replication. Viral DNA replication licenses γ-gene transcription, which mostly encode structural proteins that are required for assembly of progeny virions. Recent VZV transcriptome analyses have begun to redefine some evidence inferred by HSV homology such as possible late expression ORF62, rather than immediate-early [55]. During the regulated transcription process, the VZV DNA genome is replicated and packaged into capsids that are assembled within the nucleus [56], requiring the essential portal protein from ORF54 to package the genome [30]. The incomplete virion associates with some tegument proteins and is then trafficked out of the nucleus where it undergoes a transient membrane envelopment during transport across the nuclear membrane [57]. The nucleocapsid and associated tegument then undergoes secondary envelopment at the *trans*-Golgi network (TGN) [58] facilitated by several tegument proteins including the essential ORF9 protein [59]. Experimental evidence suggests secondary envelopment is often coupled with vacuole envelopment which facilitates cellular exit [60].

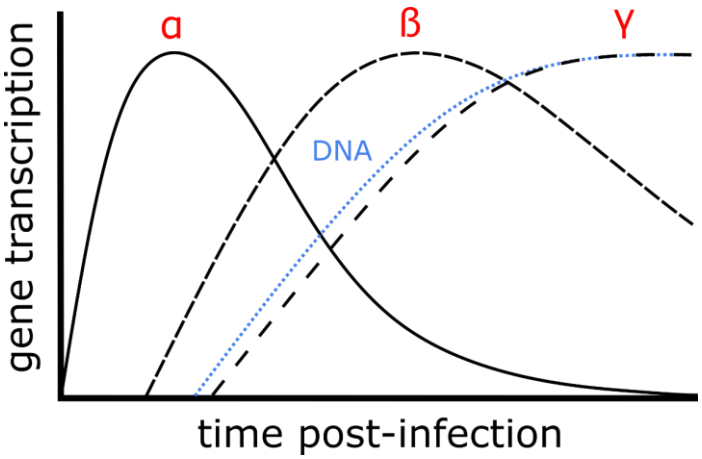

Figure 3: Approximation of canonical herpesvirus transcription cascade.

Immediate-early gene (α) transcription initiates after delivery of viral DNA into the nucleus of a permissive cell with or without *de novo* protein synthesis. The α-gene products initate the expression of early genes (β) that are are involved in genome replication. DNA replication licenses the transcription of late genes (γ) that mostly encode structural components of the virus.

In contrast, VZV latency is characterized by a program of heterochromatin-mediated transcriptional silence of most lytic genes. While the exact mechanisms of establishing latency in neurons is still largely uncharacterized, the VZV genome has been shown to associate with promyelocytic leukemia protein nuclear bodies (ND10s) and repressive chromatin upon nuclear entry [61–63]. ND10s are functionally promiscuous and have been implicated in regulation of transcription by protein sequestration and promotion of cellular stress responses [64,65]. The establishment of a herpesvirus lytic or latent cycle is likely a multifaceted balance between surmounting genomic repression and promoting viral transcription. For instance, VZV immediate-early protein from ORF61 has been shown to be involved in disruption of ND10s [63]. Its function may contribute to preventing latency, or promoting the transition from latency to lytic replication upon reactivation [66,67]. In the absence of ORF61, the default association with ND10s may result in the assembly of chromatin modifiers and heterochromatin that represses the VZV genome to a

silenced episomal state. Another example is that the trafficking of nucleocapsids in neurons from axonal termini to the nucleus may occur over a great distance, and it has been postulated that the dissociation of tegument transactivators upon cellular entry results in their poor delivery to the nucleus. VZV tegument protein from ORF10 (HSV-1 VP16 homolog) has been shown to associate with cellular factors Oct1 and HCF in the nucleus to initiate ORF62 transcription [68]. If ORF10p does not reach the nucleus, the balance may be tipped towards establishing latency.

What VZV makes during latency has been of recent interest. Many initial studies indicated that there was some expression from multiple genes, but these studies were confounded by the lack of a strong model of latency; non-specific and cross-reactivities of antibodies [69,70]; and the detection of VZV transcription and translation artifacts in post-mortem cadaver studies [71–79]. HSV-1 latency is now characterized by the transcription of latency-associated transcripts (LATs), which may work to suppress lytic reactivation in neurons through regulation of viral gene transcription, the production of miRNAs, and the promotion of survival of latently infected neurons [80–82]. Similar VZV latency transcripts (termed VLT) have been detected in human ganglia that are antisense to ORF61, a region homologous to HSV LAT [83]. The function of VLT requires further characterization, but recent work has revealed the detection of fusion transcripts between ORF63 and VLT that may be involved in reactivation [84]. The similarity of VLT to RNAs found in other latent neuronal Alphaherpesviruses is suggestive of strong evolutionary conservation of LAT function, but the functions of these RNAs remain largely uncharacterized.

The molecular mechanisms of VZV reactivation have not been elucidated in part because there is no animal model of reactivation. However, human embryonic stem cell (hESC)-derived neurons cultures provides a method for understanding the reactivation process at a single cell level [85,86]. Reactivation likely results from stimulus-driven heterochromatin reorganization during

physiological stress or injury that affects both cellular and latent VZV DNA. Evidence suggests that maintenance of alphaherpesviruses latency requires continued signaling from peripheral and central systems, and that disruption of these may lead to changes in chromatin states and viral gene expression patterns [87,88]. If so, any VZV gene expression may initiate a cascade capable of overcoming repressive heterochromatin and commence the initiation of productive VZV replication. Based on recent VLT function studies, a key component of this process might begin with expression of the VLT-ORF63 transcript and translation of a VLT-IE63 fusion protein [84]. IE63 may function to downregulate host expression of genes capable of inhibiting VZV replication and may also prevent nucleosome assembly by interacting with human antisilencing function 1 (ASF1) protein [89]. Preventing the re-silencing of VZV DNA may be a major step in achieving reactivation to allow for transcription and translation of the remaining immediate-early proteins and eventually all other lytic proteins. IE4 may promote the transport of viral intronless mRNA to the cytoplasm for translation, IE61 may disrupt ND10s to prevent chromatin repression as noted earlier, and IE62 functions as a transactivator of all other VZV genes. Inhibiting any of these crucial events would severely reduce reactivation efficiency and may force the VZV genome into latency once again.

1.1.3 VZV Limitations in the Laboratory

Although it is well recognized that VZV and HSV genes share considerable homology, the two viruses show different properties in tissue culture, experimental systems, and animal models of pathogenesis. In general, HSV is easy to grow and replicates on numerous cell types in tissue culture to generate high-titer cell free virus (often $>10^{10}$). HSV has a broad animal host range and the diseased states that result from primary, latent, and reactivated infections can be modeled in

several species, of which mice and rabbits for HSV-1 and guinea pigs for HSV-2 are most used [90]. VZV is much more limited for reasons not mechanistically understood. First, relatively few cell types support robust VZV replication, and most are human in origin. Examples of permissive cell types include human cell lines such as retinal pigmented epithelium (ARPE-19 and hTert RPE-1), a continuous skin melanoma line (MeWo), human foreskin fibroblasts (HFFs), and lung derived diploid fibroblasts (MRC5). Second, VZV replication in culture is inefficient and infectivity is almost completely cell-associated [91]. The generation of cell-free virus is problematic, as lysing of infected cells results in considerable loss of infectivity such that most studies use cell-associated virus stocks to achieve infections. The inclusion of uninfected cells as a negative control is consequently made necessary. Finally, VZV human specificity has resulted in few animal species used to study pathogenesis. The only laboratory animal that appears to model any characteristics of VZV disease is the guinea pig in which host-adapted VZV may induce exanthema and establish latency in neurons, though *in vivo* reactivation has not been achieved [92–94]. Immune compromised mice grafted with human skin, thymus, and ganglion tissues (SCID-hu) have provided much of our understanding of T cell tropism and skin cell homing properties [17,95–97]. The cotton rat has been described as a model of VZV latency in which VZV transcripts are detectable in ganglia [24,98,99], though this does not explicitly rule out the possibility of an abortive infection. Importantly, laboratory rat models develop prolonged pain behaviors resembling postherpetic neuralgia (PHN) after subcutaneous VZV inoculation as discussed in detail later [100].

The cell-associated nature of VZV and limited permissive cell lines makes generation of recombinant virus by homologous recombination and complementation difficult. Manipulation of the VZV genome has been aided by the development of isogenic bacterial expressed systems,

initially through the use of large overlapping cosmids covering the entire genome [25], and most recently through use of bacterial artificial chromosomes (BACs) containing the entire genome as one complete DNA copy [101–104]. BACs allow for "recombineering" or site-directed mutagenesis of the VZV genome by targeted recombination events. The BACs are maintained by insertion of sequences necessary for upkeep in bacteria so VZV can first be genetically modified, then infectious virus can be derived by transfection of isolated VZV BAC DNA into human cell lines. While HSV BACs present limitations in certain animal models that often preclude their effective use [105,106], VZV BACS have simplified mutagenesis and remain critical tools. However, VZV essential gene knockouts and mutations require complementation, or the ectopic insertion of a wild-type gene into a permissive cell line to allow efficient growth of recombinant VZV. Complementation is thus limited by available VZV permissive cells lines and few complementing cell lines have been generated [30,101,107]. Our lab has made novel use of a degron system for conditional protein degradation and virus growth [108], which has proved effective for probing the roles of certain essential genes as discussed below [109].

1.2 Clinical Disease

1.2.1 Primary Infection and Varicella Disease

Prior to widespread use of the varicella vaccine in the US and Europe, about 80% of children contracted varicella by their eighth year [110,111]. Primary infection initiates after respiratory transmission, which is followed by a prolonged incubation period of up to 21-d. This is commonly accompanied by prodromal symptoms of fever, malaise, headache, and abdominal

pain. Symptomatic varicella is characterized by cutaneous, pruritic lesions that stipple the skin. In less severe cases, lesions and associated symptoms may only last one to two weeks or even remain subclinical [112]. More severe complications of primary infection are generally limited to two cohorts: children with weakened immunity and seronegative adults (≥ 20 years old) [113]. Complications in immunocompromised children include bacterial infection of cutaneous vesicles, pneumonia, hemorrhagic conditions, and in rare instances, encephalitis [114]. Hospitalization is regularly required in severe cases, but this is limited to particularly susceptible populations of children in the post-vaccine era [113]. While seronegative adults comprise a very small minority in the U.S. and other industrialized countries in temperate regions, primary infection may have severe clinical outcomes that account for a considerable portion of VZV-associated deaths [115]. Outside the U.S., populations in tropical regions, especially those living in rural areas, have a greater tendency to remain seronegative into adulthood likely due to climate and reduced exposure [112,116]. Though adults present many of the same symptoms as children, they may be exacerbated by delayed medical attention, comorbidities, or pregnancy resulting in increased risk of developing complications such as pneumonia, which is frequently associated with a poor prognosis [117].

Transmission of VZV to seronegative populations is typically respiratory [118,119], a characteristic that separates VZV from HSV which spreads almost exclusively by direct contact [120]. Evidence suggests aerosolized droplets containing infectious VZV particles from skin lesions are inhaled [121] and is thought infect mucosal tissues of the upper respiratory tract near Waldeyer's tonsillar ring, a collection of lymphoid tissues within the pharynx [122]. Within the mucous membrane reside immature dendritic cells (DCs) and thymus-matured lymphocyte cells (T cells) that are susceptible and permissive for VZV. Immature DCs may migrate to regional

lymph nodes where they encounter and efficiently spread VZV to more T cells, a major step in achieving systemic dissemination [123,124]. More specifically, VZV has a defined T-cell tropism where it preferentially infects CD4+ T-cells expressing C-C motif chemokine receptor 4 (CCR4) and cutaneous lymphocyte-associated antigen (CLA) [14,95]. Together, CCR4 and CLA promote the homing of T-cells to skin, allowing VZV to disseminate to peripheral tissues, possibly homing to the stem cells of hair follicles where infection initiates and viral spread to keratinocytes of the dermis and epidermis [125]. The infection eventually erupts at the surface generating the systemic rash that defines primary varicella.

Replication in the skin often occurs near hair follicles where myelinated nerves of the peripheral nervous system (PNS) are densely populated [126,127], providing VZV with a convenient location to enter peripheral nervous tissue. Exposure of cutaneous neurites to VZV is one of the purported ways in which the virus gains access to sensory ganglia where it establishes lifelong latency. This is achieved by retrograde axonal transport along sensory nerve axons which has been demonstrated in hESC-derived neuron cultures [86,128]. Accessing sensory ganglia may also occur by a hematogenous route, which provides VZV access to ganglia that do not innervate the periphery. Hematogenous dissemination has been observed in SVV [129], but is supported for VZV by evidence in humans such as the seeding of ganglia that do not innervate the skin including geniculate ganglia [130], vestibular and spiral ganglia [131], nodose and celiac ganglia [132], enteric neurons [133,134], and other autonomic ganglia in the head, neck [135], and thoracic region [136]. Thus, it is highly likely VZV can access virtually any ganglia in the body, though conditions of latency and reactivation may vary.

1.2.2 Maintenance of Latency

The maintenance of VZV latency over an exceptionally long period between primary infection and reactivation is a continuing debate. While there is no doubt host immunity plays a substantial role in preventing reactivation, the molecular aspects of VZV latency have not been resolved, partly because modeling reactivatable latency *in vivo* has debatably not been achieved. Following primary infection by wild-type VZV or the vaccine strain, strong humoral and cell-mediated immunity is established that is predicted to participate in the long-term prevention of reactivation [137,138]. In addition, VZV is hypothesized to self-regulate by production of regulatory VLT transcripts which may contribute to the maintenance of latency [83]. Recent data suggests alternative forms of VLT may participate in reactivation [84], reiterating the concept that maintaining latency appears to be a careful balance between viral and host factors.

Investigators have relied heavily on clinical and epidemiological evidence to determine risk factors associated with HZ, and to develop new reactivation hypotheses [139]. A range of contributors have been identified from patient genetics to comorbidities that inform on an individual's likelihood of reactivation [139–143]. One concept which all agree is that age is one of the most significant risk factors. About 68% of HZ cases occur in patients that are 50 years or older and lifetime incidence rises to 50% in those that live to 85 years [144]. A contributing factor to age related disease is immune senescence or the gradual deterioration of the immune system with age [145,146], indicating an important role for adaptive immunity for maintaining VZV quiescence [147–149]. This is well substantiated by the Shingles Prevention Study, which indicated that boosting VZV immunity by vaccination significantly decreased risk of reactivation and burden of illness [150]. Additionally, cases of iatrogenic reactivation following tissue [151–

153] and solid organ transplantation [154–156] have revealed immune suppressive treatments substantially increase the likelihood of reactivation.

VZV reactivation was previously thought to be infrequent based on observations that herpes zoster normally occurs only once in a lifetime, whereas HSV reactivation can occur frequently [120]. However, it was discovered that not all reactivation events result in clinical symptoms. Asymptomatic shedding has been described as quite common for HSV [157], and was also found to occur for VZV in physiologically stressed individuals [158–160]. This alludes to the careful balance of both host and viral factors in maintaining latency, and small imbalances may occur regularly between clinical disease that allow for "bursts" of VZV activity. These bursts infrequently result in clinical reactivation and may instead endogenously boost host immunity to further delay HZ. Analyses of the gastrointestinal tract also indicate subclinical VZV activity [161], which supports the concept of endogenous boosting to replenish cell-mediated immunity [162]. Exogenous boosting theories have also been proposed in which adults exposed to children with varicella provides an immune boost that delays HZ onset [163]. The adoption of a universal varicella vaccination programs was predicted by some to increase HZ rates among adults carrying VZV, but this has not been substantiated with evidence [163–169]. Though the mechanisms of VZV latency and reactivation are unresolved, evidence strongly suggests a diverse process that relies on chance VZV gene expression leading to lytic replication that must overcome host immunity.

1.2.3 Reactivation and Herpes Zoster Disease

About 1/3rd of those carrying latent VZV will reactivate in their lifetime to develop HZ [139]. The chance of reactivation increases significantly with each decade over 50 years [168].

However, reactivation may occur at any time after primary infection and young adults under chronic physiological stress, but not psychological stress are known to reactivate at a higher frequencies than healthy peers [170,171]. Chronic comorbidities and immune suppression are important risk factors contributing to HZ in both aged and young adults [143,171]. Despite the diversity of affected individuals, most HZ cases will develop a painful rash that resolves over the course of weeks, and those at highest risk of disease often face troublesome chronic complications such as PHN that can last well-beyond visible signs of disease. Several factors including the severity of prodromal symptoms (e.g. fever, malaise, pain), location of reactivation, and severity of the cutaneous rash are reliable indicators of developing more serious complications [172,173]. It should be noted that HZ and subsequent complications can occur in the absence of a rash (zoster sine herpete) [174–176], indicating the importance of events within the ganglion for disease outcome.

It remains unclear if VZV reactivation originates in one or multiple neurons of the ganglion, but intraganglionic spread during reactivation is involved dissemination of VZV to adjacent neuronal and non-neuronal cells [97,177]. The considerable size of an HZ lesion is evidence for cell-cell spread before trafficking down axons to cutaneous sites where lytic replication forms a zosteriform rash. Human ganglia modeled in SCID-hu mice, and ganglia taken from patients with HZ at time of death, exhibit extensive syncytia between neuronal and non-neuronal satellite cells [97,177,178]. This neuropathic damage stimulates an infiltrating immune response that might contribute to inflammatory tissue damage in the reactivated ganglion [178,179]. Once virus is delivered to the skin, VZV undergoes lytic replication within the dermis and epidermis to develop the characteristic zosteriform rash. In immune competent adults, a rash may take two to three weeks to heal, during which time acute pain and pruritis (itch) tend to be the

most distressing symptoms [180]. HZ symptoms in immune compromised individuals follow the same trend, but disease states are often more severe due to the inability to control viral replication and spread. If host immunity fails to mitigate VZV activity, unchecked dissemination may exacerbate HZ and contribute to severe acute symptoms (e.g., encephalitis, paresis, pneumonia) and onset of chronic symptoms [142].

1.2.4 Vaccines

VZV is currently the only human herpesvirus for which effective vaccines are available. A two-dose regimen of the live-attenuated varicella vaccine (Varivax) prevents >90% of childhood varicella in the US and shows greatly reduced severity, medical complications, and morbidity of breakthrough disease [181]. Reducing HZ incidence was first achieved using a more concentrated formulation of the live-attenuated virus (Zostavax) used in the Varivax, and it reduced HZ incidence by half and the "burden of disease", including PHN, by 2/3rds in the Shingles Prevention Study (SPS) [150]. The SPS and the Zostavax Efficacy and Safety Trial [182] established a role for cell-mediated immunity in the prevention of HZ and PHN. Protection efficacy of Zostavax waned significantly from 68% to 4% over 8-years [183]. Because live-attenuated vaccines have potential disease consequences in immune compromised populations, Zostavax could not always be recommended for those that were at substantial risk of HZ. Most recently, a subunit HZ vaccine (Shingrix) is now recommended in the US, which is based on the VZV major glycoprotein E and a new adjuvant AS01B [184]. It was FDA-approved in 2017 to be given in a two-dose regimen to people over 50-years [185]. It demonstrated higher efficacy and was safer for use in immune compromised individuals [186]. The protective efficacy of Shingrix appears to last longer than that to Zostavax [183,187]. Despite the success of the vaccines, childhood universal varicella

vaccination programs worldwide are still not implemented everywhere [188,189] and the uptake of the Shingrix vaccine is only now being reported [190].

1.3 Pain

1.3.1 Zoster-Associated Pain

Pain is the most noted complication of HZ. Prodromal pain, or pain that precedes visible signs of HZ, is often misdiagnosed or not recognized as the result of VZV reactivation until vesicles appear [191–193]. Pain from HZ is then typically grouped into two categories: zoster-associated pain (ZAP), defined as acute pain throughout symptomatic HZ; and PHN, a chronic neuropathic pain condition can that last well beyond visible signs of disease. Acute pain occurs in most HZ cases regardless of age or immune health, though symptom severity generally increases with age [194]. Descriptions of ZAP include constant or intermittent throbbing, stabbing, or burning sensations, and often include varying degrees of mechanical and thermal hyperalgesia or allodynia [180,193]. Hyperalgesia is characterized by enhanced sensitivity to painful stimuli, such as increased responsiveness to heat. Allodynia is defined as the occurrence of pain from normally innocuous stimuli, such as clothes brushing against skin. ZAP is predicted to be the combined result of pathologic damage from VZV reactivation and host inflammatory responses within the reactivated ganglion and the periphery [195]. ZAP normally resolves with healing of the rash or in the proceeding weeks [196].

1.3.2 Postherpetic Neuralgia

The transition from ZAP to the chronic pain states of PHN is poorly understood, but the mechanisms of ZAP are different from PHN. While ZAP is associated with almost all HZ cases, PHN incidence is generally reported between 10-35% [188], with higher rates correlating to elderly and immune compromised populations. PHN is commonly defined as pain that remains more than 90-days after eruption of an HZ rash [172,197]. Descriptions of chronic pain resemble ZAP and is most commonly associated with allodynia [198,199]. The severity of PHN positively correlates with HZ, and greater HZ symptoms typically indicate an increased likelihood of PHN [172,200]. Severity also is influenced by the site of HZ reactivation, with ophthalmic HZ often being associated with more severe and debilitating pain sequelae [196,201,202], though frequency of PHN at this location remains around 20% [203]. A key difference between acute and chronic pain states is that ZAP correlates with VZV replication and acute immune inflammatory responses. Most PHN cases do not appear to be the result of ongoing viral replication, though infiltrating T cells in the ganglion may have a role [204]. Polymerase-chain reaction (PCR) analysis of peripheral blood mononuclear cells (PBMCs) from patients with active PHN usually fail to detect VZV DNA [205,206], contrasting results from those with active HZ [207,208]. Most cases of PHN are unresponsive to treatment with acyclovir (ACV)-based antivirals that inhibit VZV replication, which corroborates the inability to detect circulating virus by PCR [209,210]. These data rather support the hypothesis that PHN is a consequence of damage inflicted to the sensory nervous system during HZ, which persist after virus clearance. Hypothesized morphological, transcriptional, and translational changes within neurons that survive reactivation may have long-lasting consequences on nociception. Some of these tissue changes were recognized in ganglia of

those with PHN at the time of death [204,211,212]. Whether infected neurons impact signaling of otherwise healthy neurons within the ganglion is unclear, but growing evidence suggests a complex network of communication between neuronal and non-neuronal cells (e.g., immune cells, glial cells) [213]. It is important to note that contradictory studies have reported the detection of VZV DNA and responses to antiviral treatment in cases of PHN [214,215], which reiterates the continued need for quantitative analyses of the chronic disease.

The fact that prodromal pain can develop without a visible rash and still progress to chronic pain states strongly indicates the contribution of neuropathic events within the ganglion. Skin biopsies of painful regions show a reduction of free nerve endings terminating in the dermis, suggesting cell damage or death within the ganglion [216–218]. While a reduction of peripheral innervation might be predicted to reduce regional sensation, there appears to be an inverse relationship between nerve innervation density and allodynia [218]. Indicators of neural tissue damage can also extend beyond the reactivated ganglion and along the ascending sensory pathway to the dorsal horn of the spinal cord [212,219]. It has been suggested that central sensitization has a role during PHN [220,221]. Central sensitization is a process associated with an increase in neural excitability from repeated stimulation or "wind up." Nociceptors may become responsive to normal or sub-threshold sensory input thereby releasing stimulatory neurotransmitters. This may work in combination with the alteration or loss of descending inhibitory interneurons that often function to quell overabundant signaling of sensory neurons [222,223]. The exact contribution of the CNS in ZAP and PHN remains poorly defined. VZV has been detected in the spinal cord after HZ [224] and the range of neurological complications associated with HZ require further examination [176,225].

1.3.3 Treatment of VZV Disease and Pain

HZ and PHN are both still in need of better therapeutics. ACV and its oral prodrugs valacyclovir and famciclovir are common first-line treatments against HZ that act to interrupt DNA replication by chain termination [226,227]. Early treatment with ACV can significantly improve recovery time by reducing acute symptoms, likely by limiting virus replication and spread [228]. Like many drugs that directly target viral components, instances of VZV with ACV resistance have been reported [229,230]. The pyrophosphate analog Foscarnet may be used as a second-line treatment, although it has higher levels of toxicity and side effects [231]. Treatment of pain can undertake several strategies, though success varies greatly between cases. ZAP can be treated with analgesics in combination ACV or corticosteroids to limit inflammation. Analgesics include acetaminophen, non-steroidal anti-inflammatory drugs (NSAIDs), and topical patches of capsaicin or lidocaine. In those with compromised immunity who may have difficulty controlling VZV propagation, the risk of more severe acute and chronic pain can warrant longer term therapies [232].

Treatment of PHN currently relies more on mitigating symptoms rather than addressing the enigmatic root causes of chronic pain. PHN treatments are often similar to ZAP, but without antivirals [209]. More active analgesics and pain therapeutics are often used including gabapentin, tricyclic anti-depressants, and topical analgesic patches. In extreme cases, opioids may be used, though this is unfavorable as course of PHN is difficult to predict and treatment may extend over a long duration or indefinitely. It is recognized that a significant fraction of PHN patients do not respond to any currently available therapies [233].

1.4 Rat Models of Postherpetic Neuralgia

1.4.1 Establishment

While mice and rats constitute the most common laboratory animals used to study neuropathic pain [234], VZV-induced pain has been almost exclusively studied in rats. Initial reports exploited variations of the rat footpad model [100,235,236]. Despite the apparent inability of VZV to progress through the natural stages of clinical disease, latency, and reactivation in the rat, the host develops measurable and prolonged behavioral indicators of pain after a single, high titer VZV inoculum into the footpad. Later, a facial model involving inoculation of the whisker pad was developed [237,238]. This model requires different approaches to assess affective pain, including the use of a place-escape-avoidance-paradigm (PEAP) method [239] or an Ugo Basile Orofacial Stimulation Test apparatus [240].

1.4.2 Footpad Model

The footpad model employs inoculation of the glabrous region of the hind footpad with VZV-infected cells or uninfected cell equivalents (**Fig 4a**), followed by testing for behaviors that indicate mechanical allodynia and thermal hyperalgesia [100]. Animals are evaluated for mechanical responses by von Frey monofilament stimulation (**Fig 4b**) [241], and for thermal responses with a Hargreaves apparatus (**Fig 4c**) [242]. Initial studies by Fleetwood-Walker *et. al.* showed behavioral indicators of pain were prolonged, lasting more than 33 days [100]. Pain was hypothesized to be the result of a chronic VZV infection established within lumbar ganglia that innervate the hind paw because earlier studies of rats inoculated with VZV along the spinal tract

showed that VZV DNA and mRNA from immediate-early genes ORF62 and -63 could be found [243]. Additional histological analysis of the infected lumbar DRGs detected protein from ORF63 (IE63) in neuronal and non-neuronal cell types, but not from ORF62 (IE62) [100]. Despite the indication of a VZV infection within sensory tissues, there was no evidence of skin infection (e.g., redness, swelling), inflammatory cell infiltrates within the skin or ganglia, or necrosis of neurons in the ganglion. A subsequent study established that pain behaviors were VZV dose-dependent and could not mitigated by blocking VZV DNA replication with ACV [235]. Thus, the development of allodynia and hyperalgesia was proposed to be the result of VZV within sensory tissues and production of viral regulatory proteins. The model has since been independently replicated and expanded by other groups including ours [109,244–246]. We showed that VZV nucleic acids and proteins are expressed in DRG at low levels and that infection induces changes in host gene expression [244,246]. VZV also induced the loss of neurite density within the afflicted skin region [246], which was described in clinical cases [216,218]. The model has been used to assess the efficacy of various novel and established treatments for pain relief [235,236,245,247–250], and anxiety behavior has also been studied using a field paradigm [247].

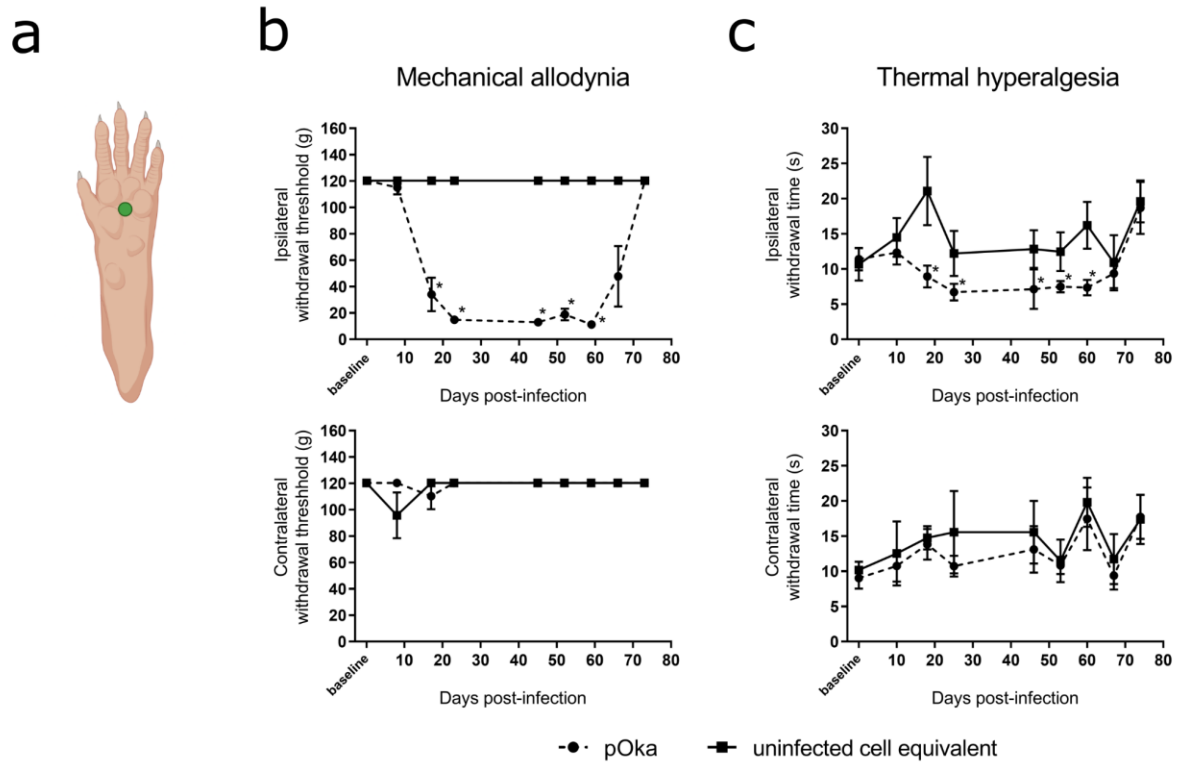

Figure 4: Representative mechanical and thermal pain behavior data from rat footpad model experiment.

(A) VZV injection and von Frey filament application site (green dot) of rat plantar hind footpad. (B) Male Sprague Dawley rats (n=6/group) were unilaterally inoculated with wild-type VZV (pOka, circle) or uninfected cell equivalents (square) and assessed for mechanical allodynia over a period of 74-d. The inoculated (ipsilateral) footpads from different rat groups are compared in the top graph, and the footpads that received no inoculation (contralateral) are compared in the bottom graph. (C) The same rats were assessed for thermal hyperalgesia. *, p<.05. Adapted from Warner *et al*. 2021. Part A created with BioRender.com.

Assessment of mechanical hypersensitivity has been well described but has many minor variations. Our approach has been well-detailed previously using calibrated von Frey monofilaments to determine the degree of tactile sensitivity (or gram-weight threshold) that stimulates a paw withdrawal response [109]. Rats are placed in a small enclosure that restricts

movement with mesh flooring that permits monofilaments to be applied upwards against hind footpads. Animals are distracted with a cereal treat ("Fruit Loops") given freely throughout testing. Beginning with a filament that exerts an upward force of 10-grams, the tip is applied to the injection site on the hind paw until the filament buckles, exerting an upward force which corresponds to the gram-weight tactile strength of the monofilament. A positive response manifests as immediate paw withdrawal followed by cupping or licking, while a negative response shows no obvious change in behavior. According to the up-down method, if a stimulus causes a response, the next von Frey filament applied will be a step down in gram-weigh force, while the next larger filament is applied if no withdrawal behavior is observed [241]. A minimum of six monofilaments are applied to each the ipsilateral (inoculated) and contralateral (uninoculated) footpad during one measurement period which are completed once or twice weekly. Paw withdrawal threshold is calculated as the filament gram-weight required to cause a positive response 50% of the time (**Fig 4b**).

Increased sensitivity to heat stimuli was determined by the Hargreaves method [242]. Briefly, rats are placed in a small Perspex enclosure on top of a thermal heated glass floor set to 32°C. Cereal treats are administered freely, and a brief 10-min acclimation period is observed. A concentrated light source from a standardized distance beneath the enclosure is directed at the injection site, and the time until paw withdrawal is recorded. All rats will eventually respond to the application of increasing heat, and a 30-second cut off is employed to prevent tissue damage. Control rats usually withdraw in a range greater than 10 seconds. Although temperature response between VZV and control groups are less dramatic than mechanical measurements, a distinguishable pattern forms and a difference in the time-to-withdrawal can be observed for VZV-inoculated animals (**Fig 4c**).

1.4.3 Facial Model

Facial models of affective pain have been used in orofacial pain research for decades, though application to the study of ZAP and PHN is recent [237,238]. About 1-in-5 cases of clinical HZ involve VZV reactivation from the trigeminal or fifth cranial nerve [251], which innervates the entirety of the face and can be further subdivided into three regions (ophthalmic, maxillary, and mandibular) based on nerve branching and tissue innervated. The facial model of VZV-induced pain analyzes development of mechanical and thermal sensitivities following VZV inoculation into the whisker pad (**Fig 5a**), which is analogous to the maxillary region in humans. Analysis of this sensory pathway is beneficial not only because of the frequency of facial HZ, but also because of an increased likelihood of complications during and after facial HZ, including pain [201,202]. In contrast, the footpad is innervated by nerves projecting from lumbar DRG and clinical HZ appears infrequently in the extremities [252]. Two methods have been used to investigate VZV-induced facial pain: a PEAP test in which rats avoid noxious mechanical stimuli (**Fig 5b**) [239], and Orofacial Stimulation Tests that measures perturbation of drinking activity when animals experience pain induced by either heat application or by mechanical stimulation using Ugo Basile chambers [240]. This model was employed to demonstrate the influence of sex on development of pain responses [237,253–256], since the development of clinical ZAP and PHN may be influenced by sex [139,173].

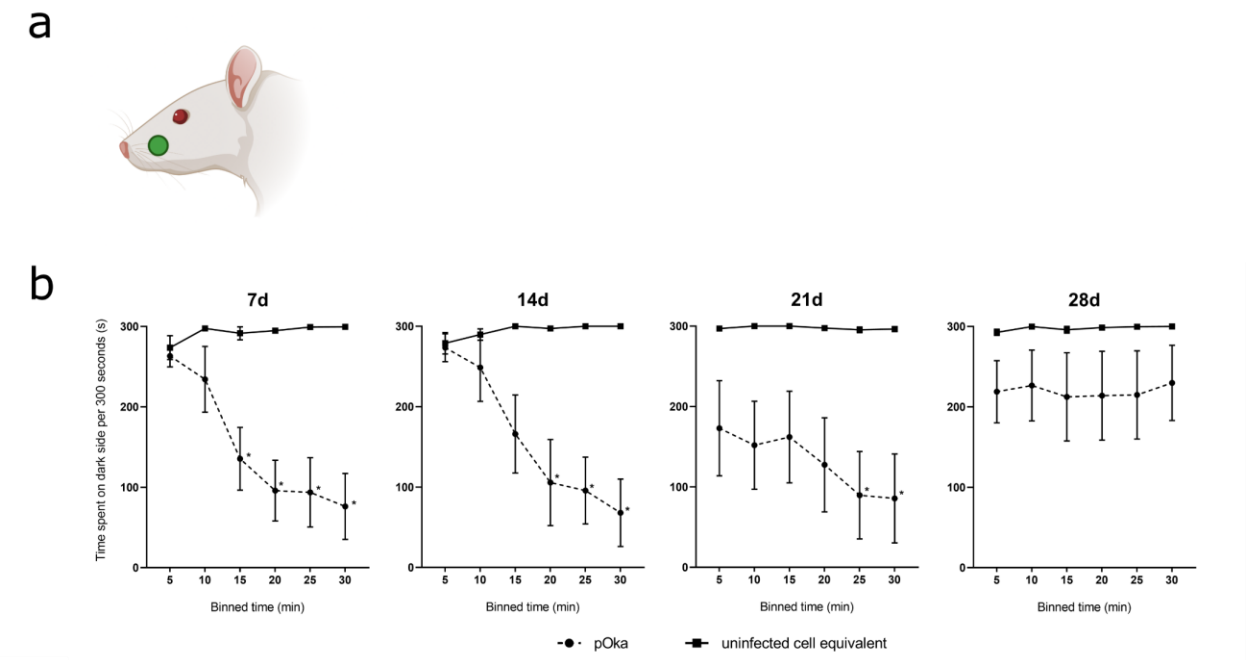

Figure 5: Representative PEAP assay data from rat facial model experiment.

(A) VZV injection site and application area (green dot) of 60-g von Frey monofilament during PEAP assay. (B) Male Sprague-Dawley rats (n=7/group) were inoculated with wild-type VZV (pOka, circle) or uninfected cell equivalent (square) and assessed for development of aversion to stimulation of the inoculation site if on the dark side. The uninoculated whisker pad was stimulated if on the light side. *p>.05. Adapted from Warner *et al*. 2021. Part A created with BioRender.com.

For assessment of facial affective pain responses in these studies, the Fuchs PEAP method is applied [237,239]. Rats are placed in a 30 x 30 x 30-centimeter clear, acrylic chamber in which half is made opaque by attaching a black covering to the exterior. Rats acclimate to the enclosure for 10-min, during which they unanimously choose to remain on the dark side of the enclosure. A 60-gram von Frey monofilament is applied to the left or right whisker pad every 15-seconds, depending on the location of the rat's head. The filament is applied to the ipsilateral whisker pad if the head is on the dark side of the enclosure and applied to the contralateral whisker pad if the

head is on the clear side. Uninoculated rats choose to remain on the dark side, while inoculated rats showed greatly reduced times on the dark side if stimulation by the filament is aversive. A positive nociceptive response is defined by avoidance of noxious stimuli to the inoculated whisker pad by preference for the clear side of the enclosure. Data is presented as time spent on the dark side in 5-min bins over a measurement period of 30-min (**Fig 5b**).

1.4.4 Mechanisms of VZV-induced pain in the rat

Although several independent groups have confirmed VZV-induced pain behaviors and the utility of the rat model in testing therapeutics, elucidation of viral and host mechanisms underlying the development of pain behaviors is lacking. Current hypotheses propose VZV gains access to nuclei of sensory ganglia and initiates an abortive infection to induce host physiological changes that propagate nociception. These may be changes in expression of host genes that participate in ascending and descending signal transmission, or immune responses to the presence of VZV. Essential VZV proteins of the immediate-early kinetic class IE62, IE63, and IE4 have been implicated in eliciting alterations in host gene expression because of their role in gene expression upon nuclear entry. VZV infection in rat cells appear to be severely limited and thus VZV pathogenesis may be limited to events preceding DNA replication [246]. The contribution of individual VZV proteins in pain development remain uncharacterized.

Naïve rats infected with VZV have been reported to seroconvert [243,257], however the inoculation of the foot- or whisker pad results in no visible signs of inflammation. Analysis of DRG sections after footpad inoculation corroborates the absence of any immune infiltrate [100]. This contrasts to the extensive inflammation observed in post-mortem analyses of human ganglia during or after HZ [178,258]. There is no evidence of infectious VZV in the PBMCs of inoculated

rats (Guedon and Kinchington, unpublished data). Several studies have detected expression of VZV immediate-early RNAs from ORF62 and ORF63 in ganglia of infected rats [246,259–261] and their proteins [100,237,243,244], though the signal level and number of positive ganglionic neurons appears low. The specificity of immunolabeling VZV proteins has been questioned, and may be complicated by cross and non-specific reactivities [69,70]. Nevertheless, VZV inoculated at the foot- or whisker pad is thought to traffic by retrograde axonal transport to access the innervating DRG or TG. Recently, it has been demonstrated that the development of pain behaviors can be elicited following direct stereotactic inoculation of the TG [238]. Behavioral measurements after whisker pad or direct TG inoculation were indistinguishable, indicating that some mechanisms of pain development were a result of ganglionic processes, and did not need to originate at peripheral nerve termini.

To better understand the response to VZV infection that might give rise to altered nociception, ganglia and the portions of the CNS have been studied for changes in host gene expression and markers of neuropathic damage [236,246,262]. Garry *et al.* reported upregulation of pain signaling neuropeptide Y (NPY) and antinociceptive galanin (Gal) in the footpad model, which have similarly been shown to upregulate in sensory ganglia in peripheral nerve injury models [263,264]. Additionally, they showed upregulation of voltage-gated sodium channels (VGSCs), which are implicated in neuropathic pain. Behavioral assessment with VGSC blockers in this study are consistent with antinociception from other studies [265]. The transactivator and marker of axonal damage, Activating Transcription Factor-3 (ATF-3) [266], can also be detected at higher levels in ganglia in the weeks following VZV inoculation. The similarity of these host physiological changes to related models of peripheral nerve injury are substantial because they indicate possible related pathways for nociception.

Guedon *et al.* analyzed the transcriptome of rat DRG following footpad inoculation with VZV or control cells using microarray analysis [246]. He identified statistically significant modulation of >200 genes in DRG at 10-days post-VZV infection, of which about 100 have been implicated as factors relating to nociception in DRGs according to the NCBI Gene database. Quantitative PCR validation of four genes known to be involved in immune function or pain established that VZV inoculation resulted in modulation of TNF receptor associated death domain (TRADD), neurotrophic receptor tyrosine kinase 2 (Nrtk2), vanilloid receptor 1 (Trpv1), and calcitonin gene-related peptide (CGRP). Upregulation of Trpv1 and Ntrk2, and downregulation of CGRP was previously described for an human immunodeficiency virus (HIV) gp120-induced model of neuropathic pain, possibly alluding to similar pathways of virally induced neuropathy [267]. In addition to the transcriptional changes, anatomical changes at the inoculation site showed reduced neurite density at the dermal-epidermal border compared to control cell inoculated rats. Reduced neuronal innervation is an important clinical characteristic of PHN and other peripheral neuropathies [216,218,268]. Neurite reduction in humans is likely the result of significant necrosis within the reactivated ganglion. Given the lack of immune infiltrate and cell death in infected rat DRGs [100], it is possible that the mechanism driving this phenomenon in rats is incomplete or alternative mechanisms are responsible. Incomplete mechanisms might reflect limited VZV permissivity in rat ganglia whereby innate or apoptotic responses are triggered and cause neurite retraction, but do not continue to neuronal death. Alternatively, retraction may by driven by events at the periphery following subcutaneous inoculation in which neurite receptors respond to foreign antigens to cause altered axon morphology The reduction of peripheral neurites in the rat was corroborated by similar tissue analyses following whisker pad inoculation [237].

Early studies assessing the detection of viral nucleic acids and proteins after VZV-inoculation of DRG or the footpad suggest there is at least some VZV gene expression in the rat that includes translation of IE63 [243,257]. However, because rats show no signs of clinical disease other than pain, a major question remains: does VZV replicate in the rat host? Surprisingly, this has never been fully resolved. The expression of viral genes during latency could be the consequence of an abortive infection in the rat host, rather than reflective of a latent state. This question was partly addressed by Guedon *et al.* who demonstrated that VZV did not undergo productive replication in primary cultures of several different rat tissues, but could initiate an infection that resulted in production of the IE62 protein [246]. Guedon reported that VZV infectious centers never expanded and there was no evidence of an increase in VZV DNA that would indicate DNA amplification. This *in vitro* study did not eliminate the possibility that VZV may replicate *in vivo* in cell types that were not assessed or could not be efficiently cultured. An additional but crucial observation by Dalziel *et al.* reported that development of hypersensitivity in the footpad model after VZV inoculation was not responsive to ACV treatment, while a similar mild hypersensitive response from HSV-1 infection was largely abrogated by ACV [235]. The data suggested that VZV is capable of infecting cells of the rat host and initiating a partial viral gene expression program, but that persisting chronic VZV replication as the cause of long-term hypersensitivity in the rat was unlikely. It was hypothesized that an abortive infection was sufficient for development of hypersensitivity and does not rely on progression past viral DNA replication. However, it is recognized that VZV pain induction is dose-dependent [236]. Furthermore, UV-irradiation of VZV-infected cell inoculates to block post-entry gene expression was shown to abrogate the development of MA and TH responses in the rat [245]. These data suggest that VZV enters cells of the rat host to initiate a partial gene expression program that

includes immediate-early and possibly early genes that is sufficient to alter sensory homeostasis and produce the pain phenotype.

Until recently, the contribution of sex in the development of hypersensitivity in the rat model had not been explored. Numerous clinical meta-analyses have indicated female sex as a significant contributing factor to the development of ZAP and PHN [173,269–271], while other studies have disputed such findings [272–274]. The discrepancy is not well understood, but population and cultural differences may have a role, such as pain tolerance and likelihood of seeking medical attention. Nevertheless, it is important to consider the physiological differences between males and females and the prospect that treatment efficacies may differ. Stinson *et al.* first reported the role of sex in the development of pain behaviors in the rat model of facial pain [237]. Significant differences between affective pain in female rats compared to males was reported, and female pain behaviors lasted longer in comparison to control groups. These results led to assessment of sex steroids in VZV-induced pain by analyzing the role of testosterone in the thalamus and hypothesized that aromatase conversion of testosterone to estrogen in the thalamus could reduce affective pain [254]. Inhibition of aromatase was shown to enhance pain behaviors, whereas concomitant inhibition of aromatase with activation of downstream receptors reestablished baseline pain responses. This study revealed that estradiol may modulate γ-aminobutyric acid (GABA), the principal inhibitory neurotransmitter of the mammalian CNS. In a follow-up study, the Kramer group showed that reducing the activity of GABAergic cells in the reticular thalamic nucleus increased pain responses excitatory activity in the ventral posteromedial nucleus [255]. These studies provide extensive evidence for sex differences in the rat model that can be further explored.

1.4.5 Testing therapeutics

ZAP and PHN have proved considerably difficult to treat. While ZAP can be partly addressed by antivirals to reduce viral replication and the damage that ensues if caught early, treatments for PHN have largely focused on mitigating chronic symptoms. The rat footpad model has been used as a preclinical model in several investigational pain therapeutic studies [235–237,245,247–250]. ACV administration had no significant effect on VZV-induced pain [235]. Garry *et al.* first showed the effectiveness of the anticonvulsant gabapentin in the model [236], which has shown efficacy in addressing clinical PHN [275]. Given the identification of upregulation in sodium channels that increase neuronal hyperexcitability in VZV-inoculated rats, the group also assayed sodium channel blockers mexiletine and lamotrigine which showed a short-term reduction in pain behaviors and have also shown pain reduction efficacy for clinical PHN treatment [276]. The authors used the similarity of the responses of human and rat pain to substantiate the validity of the rat as a model of neuropathic pain and concluded that VZV-induced pain may be acting through similar pathways to other neuropathic pain models. This suggests that drugs which have shown efficacy elsewhere may be tested in the rat model of PHN.

Hasnie *et al.* assayed a range of analgesic drugs for efficacy in reducing MA in the footpad model [247]. Morphine, amitriptyline, ibuprofen, and cannabinoid WIN55,212-2 all displayed some efficacy in mitigating mechanical pain behaviors over a 4-d testing period at 18-22-dpi post-VZV inoculation. Further, modulation of the cannabinoid pathway has shown efficacy for pain reduction in models of neuropathic pain, including the VZV footpad model. Other more experimental methods of pain relief have been assayed in the footpad model [245]. Guedon *et al.* showed the efficacy of using an HSV vector modified to express human preproenkephalin (PPE)

that is processed in neuronal termini and secreted to act locally at synapses in the spinal cord. PPE modulates pain perception by giving rise to endogenous opioids such as [Met]enkephalin, [Leu]enkephalin, and others which bind and activate opioid receptors. Expression of PPE from a herpesvirus vector based on HSV-1 ensured DRG delivery and may provide a long-term treatment option for PHN. Over a 56-d study in the rat PHN model, in which VZV-inoculated animals were secondarily inoculated with the PPE expressing vector, a dramatic reduction in MA and TH behaviors were observed that lasted throughout the testing period [250]. The footpad model has been addressed more extensively than the facial model for assaying therapeutics in part due to its earlier establishment, but Stinson *et al.* showed similar efficacy for gabapentin treatment in reducing affective pain responses following whisker pad inoculation [237]. Together, these models have shown numerous similarities in treatment efficacy to clinical studies despite VZV limitations in the rat.

2.0 Specific Aims and Rationale

The mechanisms by which VZV induces pain, and the shift to chronic pain states has not been resolved. We hypothesized that PHN may result from abnormal pain signaling by nociceptors that have undergone an abortive VZV infection during reactivation. While no animal can model reactivated VZV infection, subcutaneous inoculation of the rat foot- or whisker pad generates long-term nocifensive behaviors that resemble clinical PHN. We will show that VZV-induced pain in the rat results from an incomplete infection process and is dependent on the production of specific VZV regulatory proteins. We developed a novel method to generate conditional viruses to examine VZV growth requirements for pain induction. Additional uses for the growth conditional viruses will be discussed. We will also detail initial studies of a new transgenic reporter rat that can indicate cells that have become infected by VZV. The overarching goal of these studies was to understand the requirements for VZV-induced pain in the rat model, and to reveal the molecular components and tissues involved. The specific aims are:

Aim 1 To determine if productive VZV replication is required to induce hypersensitivity in rat models of PHN. Previous studies have indicated that VZV gene expression is essential for the induction of hypersensitivity in the rat, but infections of rat primary cultures have shown many cell types were not VZV permissive. The goal was to test the hypothesis that VZV-induced pain in the rat does not require the production of progeny virus, but certain early infection events involving gene and protein expression are crucial. Chapter 4 will detail the development of the viruses and their characterization. Chapter 5 will detail their evaluation in the rat host for the induction of pain behaviors. We targeted proteins involved in early and late VZV replication events

and their evaluation in the rat provides support for the hypothesis that VZV-induced pain results from abortively infected sensory neurons that have altered pain signaling due to VZV exposure. We propose the rat models events of human PHN despite the apparent limitations of VZV growth in this host.

Aim 2 To characterize the extent of VZV infection in vivo after rat foot- or whisker pad inoculation. Primary rat cultures infected with VZV is abortive. Because this likely represents only a subset of the tissues that can be infected by VZV upon subcutaneous inoculation, the extent of *in vivo* infection is unclear. A transgenic reporter rat has recently become available that expresses tdTomato following exposure to Cre recombinase. In chapter 6, we developed a Cre expressing recombinant VZV and used it to infect reporter rats. We sought to trace tissues that become infected after subcutaneous VZV inoculation. This rat model may bring tissue type context to the development of long-term VZV-induced hypersensitivity, and if neuronal or non-neuronal cells contribute to pain.

Aim 3 To explore use of growth conditional VZV in (a) gene function studies and (b) setting up the establishment of neuronal latency. Aspects of VZV pathogenesis have proved to be more difficult to study when compared to other herpesviruses. The highly cell-associated nature of VZV and limited cell types for growth have made it very difficult to generate recombinant viruses and complementing. The goal of this study was to explore the use of growth conditional viruses to simplify two areas of VZV research that are currently difficult, namely the study of essential gene function and the suppression of lytic infections in the establishment of neuronal latency without the use of genome-damaging antivirals. First, we explored essential gene function by inserting a

degron on a target gene, and then reinserting a second copy of the gene in the same virus background that contained potentially detrimental mutations. The logic was that the virus can be grown under permissive conditions for growth, then studied under nonpermissive conditions where only the ectopic mutant protein is functional. Second, the suppression of lytic infections in establishment of latency was addressed by initiating infections with a growth conditional VZV in which early lytic infection cannot progress without stabilization of the degron modified protein. This approach overcame two current obstacles in the establishment of latent infections: sporadic lytic infections and inadvertent damage to VZV genomes by ACV.

3.0 Materials and Methods

3.1 Cells and Viruses

3.1.1 Cell and Virus Preparation

VZV parental Oka (pOka) is a wild-type varicella isolate from which the current live attenuated vaccines were derived [277]. It has been established that pOka can induce both mechanical and thermal hypersensitivity in rat models of PHN [237,238,245,246,253–256] and was used as a positive control in all studies. Recombinant viruses were derived from a pOka bacterial-artificial chromosome (BAC) which contains a self-excisable BAC replicon [101] that was subsequently corrected for two spurious mutations in the VZV ORF40 and ORF50 genes (P. Kinchington and M. Yee, unpublished data). The virus was also modified to contain an N-terminal GFP fused to ORF23 as detailed previously [85].

Human telomerase (Tert) immortalized RPE-1 (TRPE, ATCC CRL4000) cells were grown in Dulbecco's Minimal Essential Media (DMEM, Gibco 10569-010) supplemented with 10% fetal bovine serum (FBS, R&D Systems S11150) and an antibiotic/antimycotic mixture (Caisson ABL02). TRPE cells were used for reconstitution of virus from BAC DNAs, VZV propagation, and stock preparation. VZV stocks were made as previously detailed [245]. Briefly, TRPE monolayers grown to 80-90% confluency at 37°C were infected, incubated 48-72 hours at 34°C, and underwent trypsinization and re-plating when needed, until >60% of cells showed visible cytopathic effect, or 95%+ fluorescence positivity where relevant. Virus infected cell stocks were generated by trypsin digestion, concentrated by low-speed centrifugation, then resuspended in cell

freeze media (DMEM, 20% FBS, 10% DMSO) and subjected to slow freeze at -80°C, followed by liquid nitrogen storage. Conditional VZV mutants were derived and grown in TRPE cells with the media additionally supplemented with 100 nM trimethoprim (TMP) (Sigma T7883) [108]. Prior to storage, all conditional VZV samples were washed extensively in cold DMEM without TMP to remove residual drug prior to freezing. Aliquots from liquid nitrogen storage were titrated to assess VZV cell-associated infectious center formation (taken as titer) by dilution and plaque assay in permissive conditions on ARPE-19 cells (ARPE, ATCC CRL2302) using supplemented DMEM as noted above, and TMP when necessary.

Primary rat cells from the tdTomato transgenic reporter rat [278] were prepared by harvesting ear tissue during necropsy followed by dissociation and plating. Briefly, ear tissue was minced and suspended in a dissociation buffer (.2% trypsin, .1% collagenase IV (Sigma C4-BIOC), 400 ug/ml DNase I (Roche 10104159001), in 1X PBS) and agitated at 37°C, 300 rpm, for 30-min. The solution was then strained through a 70 μm filter and remaining large tissues pieces were subjected to one additional round of dissociation and strained a second time. The filtrate was spun down at 600*xg* for 5-min and resuspended in DMEM supplemented with 10% FBS, 2X antibiotics, and GlutaMax (ThermoFisher 35050079). The suspension was added to 6-well plates precoated with .1% gelatin for 30-min at 37°C. Cells were passaged twice before storage and all cells used during experimentation were under 10 total passages.

Preparation of H9 human embryonic stem cells (hESCs) for derivation of neurons was described previously using a PA6 feeder-dependent method [85,279]. Bundles of neuronal precursor cells (neurospheres) were seeded in 24-well glass bottom plates for 21-d to allow for terminal differentiation into neurons and outgrowth of axons. VZV ORF4nDHFR infections were carried out with 1000 PFU cell-free VZV prepared by an established method [280]. Infections

were initially carried out in the absence of TMP for 15-d before supplementing growth media with 100 nM TMP alone or with 20mM sodium butyrate (NaB). Neurons were imaged over time by real time fluorescence microscopy.

3.1.2 Generation of Recombinant VZV

Recombinant VZV ORF54Δ and its complementing ARPE19-ORF54 (A54) cells were detailed previously [30]. Recombinants VZV ORF4nDHFR, VZV ORF63cDHFR, and ORF9cDHFR were constructed by two-step Red-mediated scarless recombination methods as previously described [102], using the VZV pOka BAC GFP-ORF23, as described previously [85]. Mutagenesis was performed in the GS1783 *E. coli* strain (gift of Dr. Gregory Smith, Northwestem University, IL) containing the heat shock-inducible (42°C) λRed recombination system and an L-arabinose inducible I-*Sce*I restriction enzyme. A transfer plasmid for the 480-bp degron domain derived from the *E. coli* DHFR gene [108] was generated by the insertion of the I-*Sce*I kanamycin resistance (kan^r) cassette flanked by 40-bp homologous sequences used for the scarless removal of the selective marker. PCR primers (**Table 1**) were designed to anneal at the end of the degron domain sequence and extend the cassette by 40-bp sequences homologous to the targeted insertion sequence in the VZV BAC. The fragment was amplified using the proofreading polymerase PrimeSTAR GXL (Takara Biochemicals, R050A). For generation of VZV ORF63cDHFR, the coding sequence of ORF70 (duplicated ORF63 gene) was replaced by a PCR amplified ampicillin resistance cassette before kan^r removal from ORF63cDHFR, and co-selected by growth on plates supplemented with chloramphenicol (to maintain the BAC) kanamycin and ampicillin. All BACs were subjected to extensive characterization by digestion with multiple restriction enzymes to

ensure no deletions of BAC DNA sequences, and all in frame gene-degron fusions were verified by Sanger sequencing of PCR amplified fragments across the respective junctions. Infectious virus was reconstituted by the transfection of the recombinant BACs using Lipofectamine 3000 (ThermoFisher) on TRPE cells grown in the presence of 100 nM TMP. VZV were passaged 3-5 times in permissive growth media (supplemented DMEM + 100 nM TMP) to allow self-excision of the BAC sequence, and master stocks were prepared and titrated as previously described. All mutant VZV used in these studies were grown from low passage master stocks with minimum of 8-10 additional passages. Integrity of the inserted DHFR sequences were confirmed by Sanger sequencing across the 5' and 3' insert junctions of both the BACs and of the resultant viruses.

Table 1: Primers to insert degron sequence at select genes.

Uppercase letters in all rows denote bases that share sequence homology with VZV for directional recombination. Lowercase letters are sequences homologous to the E. coli DHFR degron insert sequence (#1, 2, 3) or ampicillin resistance cassette sequence (#4).

#	Gene	Dir	Primer Sequence (5' → 3')
1	ORF4	Fwd	AGGCAACTGCAAACACGCAATTGTCAGATATTTTGCAGCCggatccgccaccatgatcagtctgattgcggcgttagcg
		Rev	TCACAAATAGTAGACACGTCTGGGTCGGTTGGAATTGAAGCAGAGGCGCAtgctcgccgctccagaatct
2	ORF9	Fwd	CGTGTTTGGATATTTCACGACCCTATCGTTTATTTACGTAggatccgccaccatgatcagtctgattgcggcgttagcg
		Rev	CATTAGAGCGACAAAGTCTGTCACCGTCGGAAGATGCCATtgctcgccgctccagaatct
3	ORF63	Fwd	AGCCCCGCGCCGGCATGATATACCGCCCCCCCATGGCGTGatgatcagtctgattgcggc
		Rev	AAGACACGAGCCAAACCATTGTATTTATTTATAAAGActatgctcgccgctccagaatct
4	ORF70 remove	Fwd	TATCCACAACACCCCACTCCCCCACAGACAGACATCAAAActtggtctgacagttaccaatgctt
		Rev	GTTTTGTTGTGCAGGGTTCGTCCGATTCATAACGCGACAGaaatgtgcgcggaacccctatttg

DNA of recombinant viruses generated from the BACs was Southern blot analyzed by extraction of nucleocapsid VZV DNA from 5 x 175 cm^2 infected cell flasks showing >70% cytopathic effect using the procedure detailed previously [281]. 1ug of DNA from each VZV recombinant DHFR virus and VZV from the VZV pOka BAC was assessed by restriction digestion

with multiple enzymes including *Kpn*I and *Sph*I, subjected to agarose gel electrophoresis, transferred to a nylon membrane (Millipore INYC00010), and then probed to identify the fragments that contain the degron element. The hybridization probe was generated by PCR amplification with oligos homologous to the DHFR degron using the primers 5'-CCTGGTTTAAACGCAACACC and 5'-GTGAGAGTTCTGCGCATCAG to amplify a 474-bp product, which was then labeled with a Biotin DecaLabel kit (ThermoFisher K0651). Probe hybridization (10 ng/mL) was completed overnight at 42°C and detected by binding fluorescent IRDye 800CW Streptavidin (LI-COR 926-32230) for 1-hr at room temperature at a 1:10,000 dilution. The blot was then imaged on a LI-COR Odyssey IR in linear range.

ORF9 ectopic mutants were generated in the VZV ORF9cDHFR BAC by directional recombination of a PCR generated cassette into the ORF56/57 locus. The final insertion cassette contained 40-bp of homology to ORF57 region, wild-type ORF9 promoter, ORF9 with a C-terminal V5-tag, the ORF9 poly(A) tail, a zeocin resistance cassette (Zeo^r), and 40-bp homology to ORF56 region. The cassette was recombined into the BAC and additional mutagenesis was carried out to delete portions of the N- or C-terminus of the ORF9 gene (**Table 2**).

Table 2: Primers to insert ectopic ORF9 mutants into VZV ORF9cDHFR.

Lowercase letters in row 5 denote bases homologous to VZV ORF9 promoter region (Fwd) or poly(A) tail (Rev) and uppercase letters to VZV ORF57 (Fwd) or to Zeo^r (Rev). Lowercase letters in row 6 denote bases homologous to Zeo^r and uppercase letters to ORF9 poly(A) (Fwd) or ORF56 (Rev).

#	Gene	Dir	Primer Sequence (5' → 3')
5	ORF9	Fwd	AGAGGATAGGTGTCTTCAAATTAAAAGCCGTTAAATATAAATTTTTTGTGccgcttcgttcatattaataacgatgc
		Rev	GTCAACACGGTCCGTTCCATTACTCGcggttcctaaattacactccatac
6	Zeocin	Fwd	ATGGAGTGTAATTTAGGAACCGcgagtaatggaacggaccgtgttgac
		Rev	AAGACAGATTCAAGACTAACATTTATCCCAACTGATTACATTTCATACGCctcaagtttcgaggtcgaggtg

VZV aT2C was derived from pOka BAC mutagenesis by insertion of a cassette at the ORF13/14 locus that contained a cytomegalovirus (CMV) promoter, fluorescent reporter gene Turquoise 2 (Turq2), a 2A peptide sequence (T2A), a Cre recombinase gene, and a kan^r cassette. The CMV.Turq2.T2A.Cre sequence was PCR amplified from a transfer plasmid and fused to a kan^r gene using primers as shown (**Table 3**), then recombined into the pOka BAC as described for the DHFR mutants.

Table 3: Primers used to generate VZV aT2C.

Lowercase letters in row 7 indicate bases that are homologous to the kan^r cassette and uppercase denotes bases homologous to CMV-Turq2.T2A.Cre fragment (Fwd) or to ORF14 region (Rev). Lowercase letters in row 8 denote bases homologous to CMV-Turq2.T2A.Cre and uppercase letters are homolgous to the ORF13 region (Fwd) or kan^r cassette (Rev).

#	Gene	Dir	Primer Sequence (5' → 3')
7	Kan^r	Fwd	TGACGAGCGCGATCCGGCCGGGATCgacgacgat
		Rev	AGAAACCAACCAAACGCGTCTGTGTATATCATTTTATTACaattaaccaattctgattag
8	CMV-Turq2.T2A.Cre	Fwd	GATTTTTAAATGTTGTCAAGACAGTAGATGTGTTGCGAATAGTAatcaattacggggtc
		Rev	CCTGTTATCCCTACTTATCGTCGTCgatcccggccggatcgcgctcgtca

3.1.3 VZV Growth Analysis

Growth of VZV recombinants modified with degrons were completed using an infectious focus assay as previously detailed [282] with modifications. Briefly, sub-confluent TRPE monolayers were plated in 12-wells (~$3.5x10^5$ cells/well) and infected with cell-associated, pre-titrated VZV at approximately 100 plaque forming units (PFU) per well, in duplicate. Infections were carried out in media containing 100 nM TMP (permissive) or no TMP (nonpermissive) conditions that was then maintained throughout the time of incubation. At times indicated, infected cells monolayers were harvested by trypsinization and then replated as dilutions of the cell suspensions in duplicate on ARPE cells under permissive conditions to quantify the number of infectious cells able to initiate formation of a plaque. Wild-type VZV pOka served as positive control. Titrated infections were fixed at 5-dpi, stained with crystal violet, and plaques were counted on a dissection microscope. Biological sample duplicates and technical duplicates were averaged and graphed.

3.2 Protein Analysis

3.2.1 Immunoblotting

Immunoblotting methods were previously described [283] and performed with minor modifications. Briefly, sub-confluent TRPE monolayers in 6-well plates (~1×10^6 cells/well) were infected with $1x10^4$ PFU VZV-TRPE cell-associated virus (1:100 infected to uninfected cells) and incubated in DMEM with or without 100 nM TMP for 24-, 48-, and 72-hpi. Cells were harvested

by washing twice in ice-cold 1x PBS and removed by mechanical dislocation into 1x PBS containing protease (ThermoFisher Halt) and phosphatase (Roche PhosSTOP) inhibitors. After concentration by centrifugation at 12,000*xg* at 4°C for 5 minutes, cells were resuspended in 100 µl 1x PBS with 2x protease inhibitors, to which 100 µl of 2X SDS PAGE lysis buffer was added for a final sample volume of 200 ul. Samples were briefly probe-sonicated, heated to 95°C for 5 min, then loaded onto precast 4 – 15% acrylamide gradient SDS-PAGE gels (Bio-Rad Criterion) and run at 65V until completion. Proteins were transferred by electrophoresis to a polyvinylidene difluoride membrane (Millipore Immobolin-FL 00010) overnight at 15V, and membranes blocked overnight at 4°C using LI-COR "Intercept" Blocking Buffer. Blots were incubated with dilutions of primary antibodies at 4°C for 4-24 h in diluted blocking buffer solution containing 0.1% Tween-20, washed extensively in the same buffer, and further incubated with secondary species-specific antibodies linked to near IR dyes (LI-COR, IRDye 680/800) at 1:20,000 dilution for 1-h at room temperature, washed, and imaged on a LI-COR Odyssey IR in a linear range.

3.2.2 Fluorescent Microscopy

For cell localization studies, TRPE monolayers prepared on 4-well chambered slides (Sigma-Aldrich Nunc Lab-Tek II C6807) were infected with 50 or 10 PFU VZV per chamber and incubated 4-days under TMP permissive and nonpermissive conditions at 34°C. Monolayers were fixed by incubation for 20-min in 4% paraformaldehyde at room temperature, washed in 1X PBS, and blocked overnight in 10% heat-inactivated goat serum (HIGS) in PBS. Samples were incubated in HIGS-PBS diluted primary antibodies overnight, washed, and incubated with Alexa Fluor-coupled secondary antibodies for 1-h at room temperature. After a final 10-minute incubation with DAPI, washed chambers were separated from the slides and coverslips mounted.

Slide imaging was performed on an Olympus IX83 inverted microscope using a 60X (NA 1.25) oil objective in a linear range. These images were processed using Olympus CellSens software and ImageJ, and comparative images were processed equally.

Plaque sizes were determined by imaging VZV infectious centers at 4-dpi prepared under permissive and nonpermissive conditions and grown at 34°C. Monolayers were fixed by 20-min incubation in 4% paraformaldehyde at room temperature, washed in PBS, and stored at 4°C in PBS until imaged. All viruses, except for pOka, produce a GFP fused ORF23 protein (ORF23p) that served to identify VZV infectious centers by fluorescent microscopy. To image pOka plaques under similar conditions, infected samples were probed with a primary antibody to ORF23p and detected with Alexa Fluor 488 secondary antibody as described in the localization analysis method. Images containing individual plaques were each acquired under identical acquisition settings with Cell Sens software on an Olympus IX83 inverted microscope with a 10X (NA 0.3) air objective. Images were exported from Olympus CellSens software and analyzed in Metamorph (Version 7.7, Molecular Devices, San Jose, CA). Data was reported as area in pixels (1 px = 1.024 μM).

Primary rat cell cultures from the transgenic reporter rat model were imaged under identical acquisition settings with on an Olympus IX83 inverted microscope with a 10X (NA 0.3) air objective. Primary rat cells were plated in 6-well dishes until confluent and infected with 1000 PFU TRPE-associated VZV aT2C in duplicate. Infected wells were fixed at 1-, 2-, and 7-dpi and imaged. Tissue cryosections were imaged on an Olympus IX83 confocal microscope with a 60X (NA 1.25) oil objective. All images were processed equivalently on Olympus CellSens and ImageJ software.

hESC-derived neuron cultures were imaged on an Olympus IX83 inverted microscope with a 10X (NA 0.3) air objective and processed with Olympus CellSens software.

3.2.3 Antibodies

Primary mouse antibodies to proteins IE4 (HR-VZV-20), ORF9p (HR-VZV-38), ORF23p (HR-VZV-12), and IE63 (HR-VZV-33) were acquired commercially from Center for Proteomics, University of Rijeka (CapRi). gE (SC-56995) was acquired from Santa Cruz Biotechnology (Dallas, TX, USA) and β-actin (A00702) was purchased from GeneScript (Piscataway, NJ, USA). NeuN (834501) were acquired from Biolegend (San Diego, CA). V5 (R960-25) was purchased from ThermoFisher (Waltham, MA, USA).

Primary rabbit antibody to α-Tubulin (600-401-880) and tdTomato (600-403-379) were purchased from Rockland Immunochemicals (Limerick, PA, USA). Cre (908002) was acquired from Biolegend (San Diego, CA, USA). Rabbit antibodies to IE62, ORF29p, and IE4 were reported previously [37,284,285].

Secondary IRDye antibodies for immunoblotting compatible with the LI-COR Odyssey were purchased from LI-COR: goat anti-mouse 680CW (926-32220), goat anti-mouse 800CW (926-32210), goat anti-rabbit 680CW (926-32221), goat anti-rabbit 800CW (926-32211). Those used for immunohistochemistry were purchased from Invitrogen: Alexa Fluor 488 goat anti-mouse (A11029), Alexa Fluor 546 goat anti-mouse (A11030), Alexa Fluor 488 goat anti-rabbit (A11034), Alexa Fluor 546 goat anti-rabbit (A11035).

3.3 Animal Studies

3.3.1 Ethics Statement

All animal studies were performed in accordance with protocols approved by the University of Pittsburgh Institutional Animal Care and Use Committee (IACUC, protocol #18022168). This protocol meets the standards for humane animal care and use as set by the Animal Welfare Act and the NIH Guide for the Care and Use of Laboratory Animals.

3.3.2 Behavioral Analysis

Male Sprague-Dawley rats (Charles River Laboratories) weighing 200 – 250 grams were acclimated to housing and mechanical and thermal behavioral measurement conditions for 1 - 2 weeks until establishing a consistent behavior baseline that was in accordance with historical records of previous studies. Animals falling outside the established parameters were excluded. To first establish the use of the recombinant VZV described in these studies and to simplify analysis, only male rats were assessed. Previous studies have indicated that the female estrus cycle can affect pain outcomes and would therefore require additional studies after pain behaviors are established using male rats [237]. All inoculations and behavioral assessments were blinded so the behavioral response recorder was ignorant of the inoculum source and injection location. Cell-associated VZV for animal inoculation was prepared by fast thawing pre-titrated virus aliquots stored in liquid nitrogen, followed by centrifugation at 150*xg* at 4°C for 10 minutes, an ice-cold 1x PBS wash to remove residual freeze media, and resuspension in 1x PBS for a final concentration of $4x10^6$ PFU/ml. Washed, intact cell-associated virus was maintained on ice for no more than 1-h prior to

foot or whisker pad inoculation. Uninfected cell equivalents were prepared identically. When TMP was included in the inoculum, virus infected cells were resuspended at the appropriate concentration in ice-cold 1x PBS supplemented to 500 nM TMP.

In the footpad model, inoculations were carried out as detailed previously [245] with slight modifications. Briefly, gently restrained rats were subcutaneously inoculated with 25-50 µl containing $2x10^5$ PFU VZV into the glabrous skin of the left or right rear footpad. Whisker pad inoculations were as detailed previously [237] using isoflurane anesthetized rats whereupon virus was injected subcutaneously in the right or left whisker pad. Animals were monitored for recovery and returned to housing. Mechanical and thermal responses of the footpad and mechanical responses in the whisker pad were performed as detailed in the introduction and previous studies [109,237,245].

3.3.3 Necropsy

Necropsies were performed on rats for the removal of skin from the foot- and whisker pad, for dorsal root ganglia adjacent to lumbar vertebrae 4, 5, or 6, and for trigeminal ganglia. Briefly, animals were euthanized by carbon dioxide asphyxiation until all movement ceased. Animals were then perfused with 4% paraformaldehyde if tissue was fixed or decapitated if tissue was taken fresh. Fixed tissues were stored in Zamboni's fixative at 4°C until processed for OCT compound (Tissue Tek) embedding and cryosection. Fresh tissues were snap frozen in liquid nitrogen and stored on dry ice until long-term storage in liquid nitrogen vapor phase, followed by nucleic acid extraction.

3.3.4 Tissue Analysis

Messenger RNA transcripts encoding ORF4, ORF62, ORF63, or DHFR sequences were quantified from rat DRG following footpad inoculation and tissue harvest as detailed previously [246], using reverse transcription quantitative real-time polymerase chain reaction (RT-qPCR) and TaqMan probes (S1 Table). Briefly, male Sprague-Dawley rats (n=24) were divided into four groups for inoculation (pOka, VZV ORF4nDHFR, VZV ORF63cDHFR, and uninoculated) and sub-divided into three timepoint groups for post-infection harvest at 4-, 5-, and 7-dpi. Rats (n=6/group) received injections of $2x10^5$ PFU VZV into the glabrous footpad. At each timepoint, rats (n=2/group) were necropsied, L4, L5, L6 DRG were micro-dissected and snap frozen in liquid nitrogen until nucleic acid purification. RNA was purified by mechanically disrupting tissues in TRIzol (ThermoFisher) reagent with a PT1200E tissue homogenizer (Kinematica, Bohemia, NY) for 10-s at ~75% power. RNAs were dissolved in nuclease free H_2O, DNase-treated (ThermoFisher EN0521) and converted into cDNA using a High-Capacity RNA-to-cDNA kit (Applied Biosystems 4387406). cDNAs were analyzed by thermocycling (95°C, 60°C, 40X) in an Applied Biosystems StepOne Plus qPCR system with PrimeTime Gene Expression Master Mix (IDT 1055770). Gene expression was detected by TaqMan assay and relative expression values were calculated by the $2^{-\Delta\Delta Ct}$ method with comparison to rat GAPDH (Applied Biosystems Rn01775763_g1) and displayed as fold-change over GAPDH (equal to 1). Data are averaged results from two similar qPCR assays. ORF62 and ORF63 TaqMan primer sets (**Table 4**) have been previously described [83].

Table 4: Primers used for RT-qPCR detection of VZV transcripts in rat DRG.

Fwd; Forward, Rev; Reverse, 6-FAM; 6-Carboxyfluorescein, BHQ1; Black Hole Quencher 1

#	Gene	Direction	Primer Sequence (5' → 3')	Probe
1	ORF62	Fwd	CCTTGGAAACCACATGATCGT	6-FAM-TGCAACCCGGGCGTCCG-BHQ1
		Rev	AGCAGAAGCCTCCTCGACAA	
2	ORF4	Fwd	CCTTCGGATGACTTTGCATT	6-FAM-CTCCAGGCGAGGACTCCACA-BHQ1
		Rev	TCGTTTGGAATACCGTGGAT	
3	ORF63	Fwd	GCTTACGCGCTACTTTAATGGAA	6-FAM-TGTCCCATCGACCCCCTCGG-BHQ1
		Rev	GCCTCAATGAACCCGTCTTC	
4	DHFR	Fwd	CCATACCTGGGAATCAATCG	6-FAM-ACGGACGATCGCGTAACGTG-BHQ1
		Rev	CTTCATCCACCGACTTCACC	

Tissue sections for imaging analysis were prepared post-necropsy by transfer from Zamboni fixative to 30% sucrose overnight, then embedded in OCT compound and frozen at -80°C. Foot- and whisker pad tissues were sectioned into 30 µm transverse sections using a cryostat at -20°C. TG and DRG samples were sectioned into 18 µm transverse sections and stored at -80°C until microscope imaging.

3.4 Statistics

All statistical analyses were performed using the Prism 9 software (GraphPad, La Jolla, CA). Specific tests and post-hoc analyses, including p-values, can be found in the figure legend where applicable.

4.0 Generation and Characterization of Growth Conditional VZV

This chapter was adapted from the published manuscript, "Varicella-zoster virus early infection but not complete replication is required for the induction of chronic hypersensitivity in rat models of postherpetic neuralgia," authored by Benjamin E. Warner, Michael B. Yee, Mingdi Zhang, Rebecca S. Hornung, Benedikt B. Kaufer, Robert J. Visalli, Phillip R. Kramer, William F. Goins, and Paul R. Kinchington [109]. It was written by BEW and PRKi and edited by WFG, PRKr, and BBK. All data in this chapter was collected, analyzed, and curated by BEW and PRKi.

4.1 Introduction

Recombinant VZV with essential gene mutations have been described by others [98,101,286], but their growth requires complementation. Genetically stable VZV-permissive cell lines harboring viral genes have proved difficult to generate. Complementation of VZV deleted for ORF9 [101] and ORF4 [107] was achieved by infection with high titer baculovirus containing a CMV-IE promoter-driven VZV gene, with concurrent treatment with sodium butyrate (NaB) to inhibit type I histone deacetylases. This approach that was not amenable for study in rat models of PHN because it did not yield the high infectious titers required in the models, and use of sodium butyrate may alter nociception [287,288]. Therefore, we adopted an alternative approach in which replication conditional VZV were generated using a degron system [108]. The 480-bp degron sequenced used here was derived from *Escherichia coli* dihydrofolate reductase (DHFR) and was added by recombination to several target VZV genes (**Fig 6a**). The DHFR degron facilitates

ubiquitin-dependent protein degradation unless it is stabilized by the cell-permeable ligand trimethoprim (TMP). In the absence of TMP, the protein is turned over by ubiquitin ligation to the degron, which initiates proteasome-mediated turnover of the fused protein (**Fig 6b**). The system overcame the need to generate complementing cells and was previously exploited to show that the protein from ORF63 is essential for SVV growth [289].

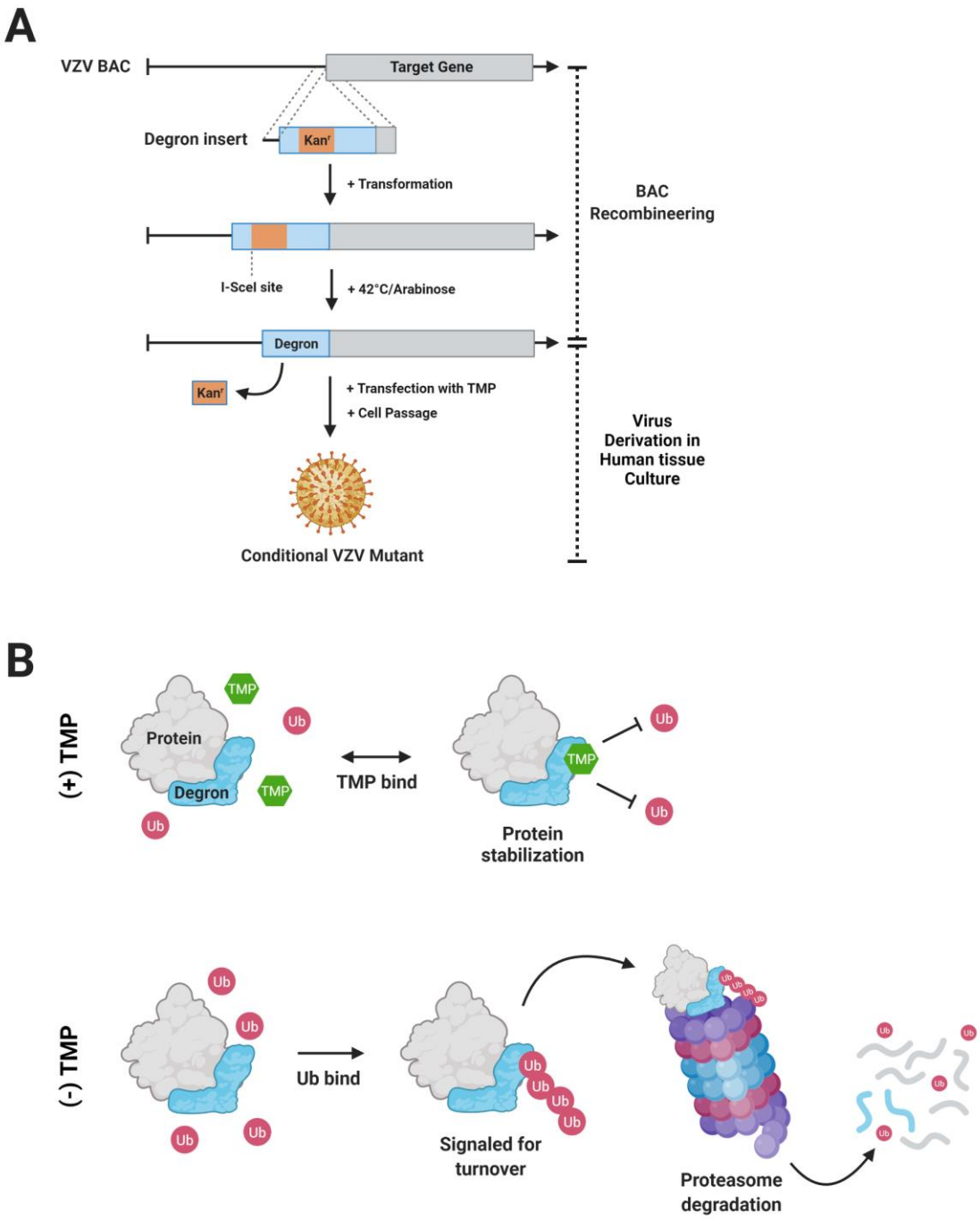
A
VZV BAC
Target Gene
Degron insert
Kan'
+ Transformation
BAC
Recombineering
I-SceI site
+ 42°C/Arabinose
Degron
Kan'
+ Transfection with TMP
+ Cell Passage
Virus
Derivation in
Human tissue
Culture
Conditional VZV Mutant
B
(+) TMP
Protein
Degron
TMP
Ub
TMP bind
Protein
stabilization
(-) TMP
Ub bind
Signaled for
turnover
Proteasome
degradation

Figure 6: Overview of VZV BAC development with a degron insertion and TMP-dependent protein turnover. (A) A target gene in the VZV BAC is engineered by recombining a degron sequence with an interrupting kanamycin resistance cassette (kanr) that allows for positive selection in *E. coli* GS1783 as detailed in the methods. A second induced recombination event in conjunction with expression of the homing endonuclease I-SceI results in markerless excision of the kanr cassette, so that the degron coding protein is fused to the target gene ORF. BACs are then transfected into human TRPE cell monolayers in the presence of the stabilizing ligand trimethoprim (TMP) to yield infectious VZV. (B) In the presence of TMP (top), TMP (green) is thought to bind the degron and prevent ubiquitin (Ub, red) ligation, thus stabilizing protein and halting turnover. In the absence of TMP (bottom), Ub is ligated to the degron, and the entire protein is targeted for degradation by ubiquitin-proteasome pathway. Created with BioRender.com.

We developed conditionally replicating VZV using the degron system by targeting essential genes from the VZV transcriptional cascade. Three recombinant VZV were generated by fusion of the DHFR degron sequence to ORF4, -9, and -63. Unexpectedly, VZV with the degron fused to ORF62 (with concurrent deletion of the reiterated ORF71) encoding the major transcriptional regulator protein IE62 were found to be unaffected by the degron. Several additional VZV BACs with the degron fused to candidate VZV proteins involved in DNA replication did not yield functional virus from multiple transfections of several independently developed BAC constructs (**Table 5**). This suggested that addition of the degron was not compatible with essential protein functions and not all VZV genes could be analyzed by the degron approach.

Table 5: Fate of reombinant VZV with degrons added to essential genes.

ORF; open reading frame, IE; immediate-early, N; amino-terminus, C; carboxy-terminus, Replication conditional; resulting VZV growth was TMP-dependent (or not), Not viable; resulting VZV failed to replicate in culture.

Gene	Protein	Function	Terminus attached	Resulting VZV
ORF4	IE4	regulator of mRNA export	N	replication conditional
ORF6	ORF6p	DNA primase	C	not viable
ORF9	ORF9p	tegument protein	C	replication conditional
ORF10	ORF10p	transcriptional activator	N or C	not replication conditional
ORF29	ORF29p	ssDNA binding protein	N or C	not viable
ORF52	ORF52p	DNA helicase	C	not viable
ORF55	ORF55p	DNA helicase	C	not replication conditional
ORF61	ORF61p	transcriptional regulator	N or C	not viable
ORF62	IE62	major transcriptional activator	N or C	not replication conditional
ORF63	IE63	transcriptional regulator	C	replication conditional

4.2 Results

4.2.1 Generation of replication conditional VZV with degron insertion at essential genes ORF9, ORF4, or ORF63

Three VZV recombinants were subsequently found to show TMP-dependent growth, one being VZV with the degron inserted at the 3' end of ORF9. This ORF encodes ORF9p, an essential phosphorylated late-expressed protein (orthologous to HSV-1 VP22) that predominantly localizes to the cytoplasm [290] and interacts with several structural proteins at the *trans*-Golgi network (TGN) during late infection [291]. Evidence suggests that ORF9p has key roles in tegument formation and secondary envelopment [59]. VZV ORF9cDHFR replicated similar to wild-type pOka VZV when grown in media supplemented with 100 nM TMP but showed a near 2-log reduction in the number of infected cell progeny by 48-h when TMP was withheld from the growth

media (**Fig 7a).** Growth of VZV pOka was not influenced by the presence or absence of TMP. A similar result was found for VZV with the degron attached to the 5' end of ORF4, which has been reported to be expressed as an immediate-early gene [292]. ORF4 is an essential gene and its protein (IE4) regulates VZV gene expression at the post transcriptional levels that involve the nuclear export of viral intronless mRNA [293,294]. IE4 has nuclear and cytoplasmic distribution in infected cells and interacts with SR nuclear shuttling proteins [294]. The virus (VZV ORF4nDHFR) showed a slight reduction of growth in the presence of TMP when compared to wild-type pOka virus (**Fig 7b**), but when grown in the absence of TMP, highly reduced progeny virus yields were detected at 1-d and longer times. This suggested that the addition of the degron to the protein may have a subtle effect on IE4 function but did not impair its essential functions. The third growth conditional VZV contained the DHFR degron domain inserted at the 3' end of ORF63, in a similar manner to that done previously with SVV IE63 [289]. ORF63 encodes the protein IE63, which has essential viral and host gene regulatory functions [295]. Since ORF63 lies within the reiterated genome sequences and is duplicated as ORF70, the BAC was deleted for ORF70 by replacing it with an ampicillin resistance cassette (Amp^r). The resulting virus (VZV ORF63cDHFR) showed significantly reduced virus replication and production of virus progeny over a 4-d time course in the absence of TMP, with approximately $2/3^{rd}$ to 1.2-log difference without TMP compared to virus growth with TMP (**Fig 7c**).

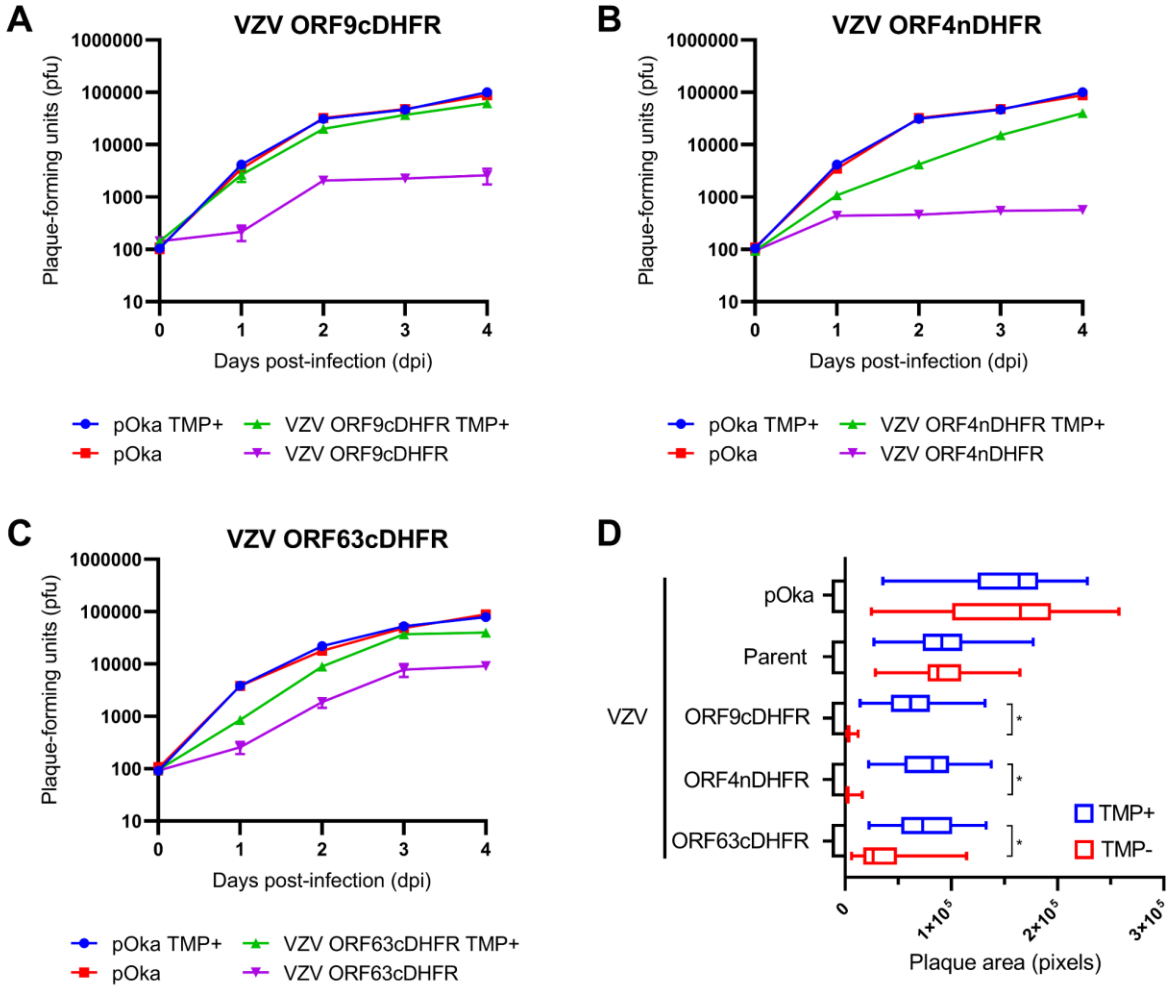

Figure 7: Growth of VZV containing DHFR degron sequence on specific genes confers TMP-conditional virus growth and formation of plaques.

(A-C) Conditional growth analysis of three VZV after initiating the infection on RPE monolayers at low multiplicity (1:100) with VZV degron virus or pOka. Cultures were grown in the presence or absence of 100 nM TMP maintained throughout the growth period from 0–4 days post-infection (dpi). Each day, cultures were then trypsinized and the infectious cell titer was determined by growth on new monolayers in conditions in which TMP was provided in the media. Shown are growth analyses for (A) VZV ORF9cDHFR, (B) VZV ORF4nDHFR, and (C) VZV ORF63cDHFR. (D) Plaque size of wild-type VZV (pOka) or VZV derived from the parental BAC (parent) or containing the degron

addition to the respective genes compared under permissive (100 nM TMP, blue) or nonpermissive (0 nM TMP, red) conditions on RPE cells at 4-dpi. Images (n = 28–35) were acquired for each virus/condition under identical settings and evaluated as detailed in methods and presented in pixel size estimated from images acquired under 10X (NA 0.3) air objective. Error bars: SD.

We next addressed growth by plaque size formation for the three degron viruses in parallel to pOka under identical conditions in the presence or absence of TMP (**Fig 7d**). Approximately 30 plaques per virus per condition were imaged for each virus/condition and analyzed by integrated morphometry analysis. Plaques formed by pOka and the parental BAC derived VZV (parent) were identical when grown with or without TMP, establishing that TMP does not affect WT VZV growth; parent plaque size trended to be slightly smaller than those formed by wild type pOka on TRPE cells. VZV plaques formed by the degron-containing viruses showed a similar marginally reduced average plaque size under permissive conditions compared to pOka, but under nonpermissive conditions, the plaques were barely detectable and involved only a few cells in the absence of TMP for VZV ORF9cDHFR and ORF4nDHFR. VZV ORF63cDHFR showed greatly reduced plaque size but appeared to show a slightly leaky growth restricted phenotype seen in the timed growth curve analyses (**Fig 7c**).

The three viruses were characterized to verify the expected degron insertion and its stability in the recombinant virus. This included DNA sequencing of a PCR amplified fragment spanning the fusion of each virus to confirm the in-frame fusion, and analyses of viral DNA obtained from nucleocapsids obtained from virus grown in the presence of 100uM TMP in the media. The DNA was subjected to gel analyses and Southern analysis using a DHFR degron-specific probe sequence. This was particularly important to characterize VZV ORF63cDHFR and show that ORF63 had replaced ORF70 by homologous recombination and removed the BAC replicon

sequences (**Fig 8**). The degron-specific probe hybridized to a large DNA fragment of the *Kpn*I digested VZV genomic DNA for ORF9cDHFR and ORF4nDHFR, but for VZV ORF63cDHFR, two *Kpn*I digested DNA fragments showed a 480-bp increase in size and hybridized the DHFR probe. These bands were of the sizes expected for not only ORF63, but also for its replacement of the ampicillin cassette in the ORF70 BAC used to derive VZV ORF63cDHFR. The blots and fragment sizes also demonstrated the expected recombinational removal of the BAC replicon from the virus, as originally designed [101]. The virus DNAs were likewise assessed by digestion with *Sph*I (**Fig 9**), which gave a novel fragment for each virus that confirmed the correct insertion of the degron sequence at the target site.

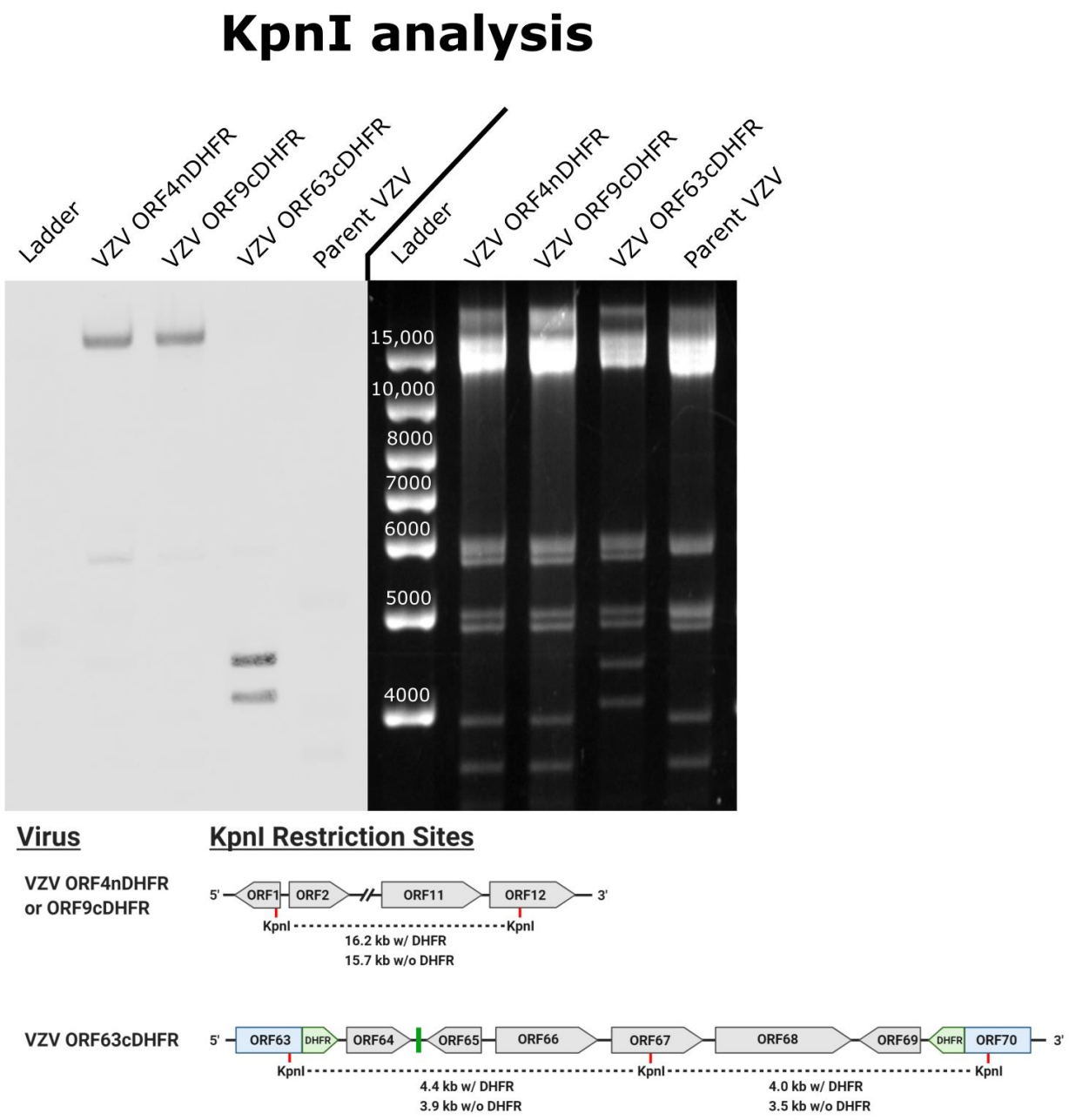

Figure 8: KpnI restriction enzyme analysis of viral nucleocapsid DNA and Southern blot with DHFR-specific probe to show expected insertion sites and VZV ORF63cDHFR homologous recombination to ORF70 within the TRs region.

Southern blots (left) are aligned with the ethidium bromide-stained 1% agarose gel electrophoresis image of separated fragments following KpnI digestion of purified VZV nucleocapsid DNA from each DHFR degron inserted virus, or

from virus derived from the parental VZV BAC (right). The DHFR probe generated by PCR predominantly hybridized to the same large DNA gel fragment for VZV ORF9cDHFR and ORF4nDHFR. For VZV ORF63cDHFR, two DNA fragments seen in other viruses (and not hybridizing the DHFR probe) increased in size by 480-bp and both hybridized the DHFR probe, with the larger representing ORF63 and smaller representing ORF70, respectively. A map of the regions of the DNAs for the expected KpnI DNA fragments in each virus is shown below the gel images with the expected fragment size indicated with and without the DHFR sequence insertion. The green vertical bar in the lower diagram for VZV ORF63cDHFR represents the position of the insertion of the BAC mini-F sequence (~8 kb) that self-excises with virus derivation and passage. A minor low abundance DNA fragment hybridizing the DHFR probe of ~6000-bp in size is present in every virus and was judged to be due to non-specific hybridization. Southern blot images were acquired on LICOR Odyssey in linear range. Created with BioRender.com.

SphI analysis

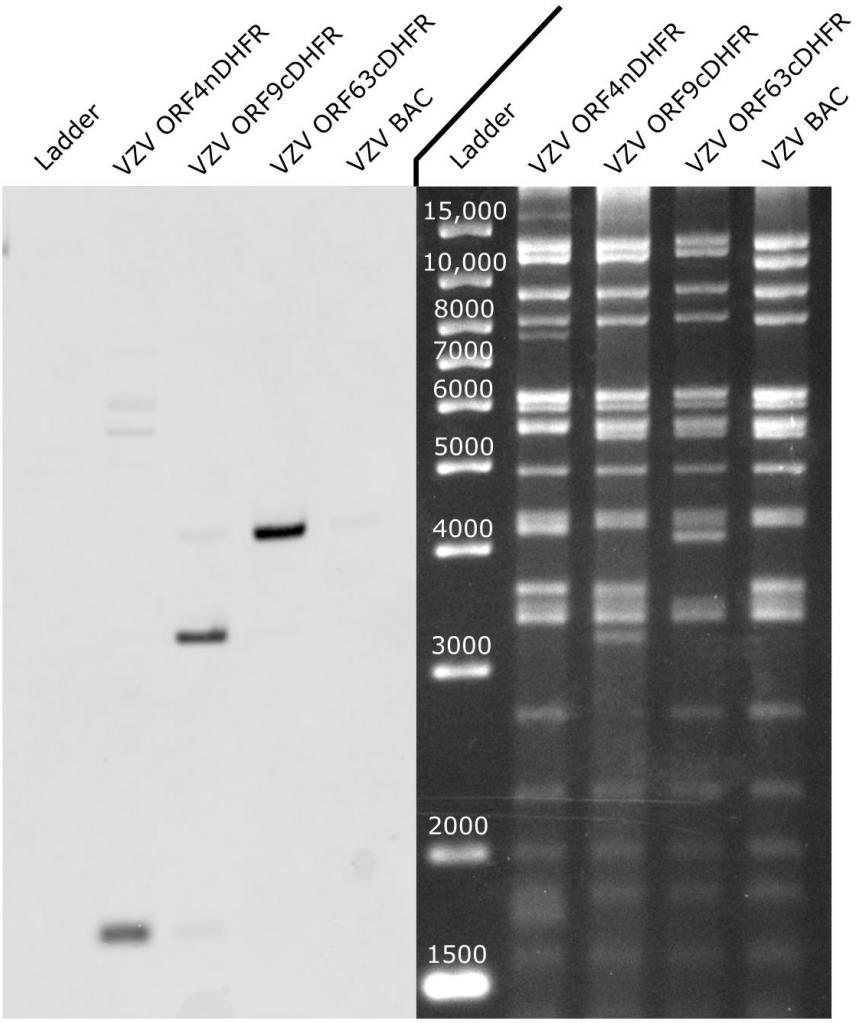

Virus **SphI Restriction Sites**

VZV ORF4nDHFR

VZV ORF9cDHFR

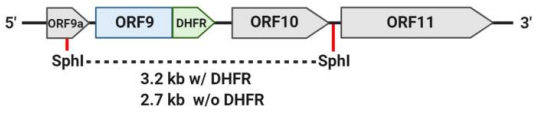

VZV ORF63cDHFR

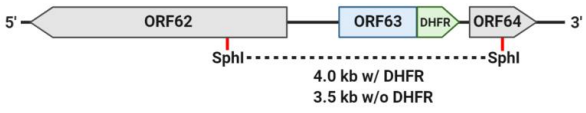

Figure 9: SphI restriction digestion and Southern blot analysis to show DHFR degron insertion.

Southern blotting of 1% agarose DNA-separated SphI digested fragments with a DHFR-specific probe (left) and the ethidium bromide-stained VZV nucleocapsid DNA after gel electrophoresis (right). A map of the DNA fragments is shown at the bottom for each virus DNA as predicted from insertion at the correct sites for each virus. The map shows the predicted DNA fragment size with and without the degron sequence insertion. The sizes of a DNA ladder are shown in the composite image. The blots reveal that the degron insertions for each virus result in the increase of specific DNA fragment by 480-bp that then are the main fragments hybridizing the DHFR probe as predicted. Two ~6000 bp fragments hybridizing the DHFR probe at low levels for VZV ORF4nDHFR DNA are of sizes expected from partial digestion products at low levels in which the expected fragment is not restriction digested from the adjacent SphI DNA fragment. Created with BioRender.com.

4.2.2 *In vitro* characterization of replication conditional VZV with degron insertion at essential genes ORF9, ORF4, or ORF63

We next assessed protein production by the three conditional VZV over a growth period of 72-h, in the presence or absence of TMP. Infections were initiated at low multiplicity (1 infected to 100 uninfected cells) so that multiple rounds of VZV infection could occur. For VZV ORF9cDHFR infections, protein levels made in the continued presence of TMP were similar to that made by wild-type VZV (pOka) (**Fig 10**), but in the absence of TMP, VZV protein accumulation was dramatically reduced in VZV ORF9cDHFR infections. Protein from ORF9cDHFR (ORF9cDHFRp) showed the expected size increase of about 18 kDa as a result of degron addition, and almost no unfused ORF9p in VZV ORF9cDHFR infections was detected. Of note, multiple forms of ORF9p and ORF9cDHFRp were detected, consistent with previous reports of this being a phosphoprotein [59].

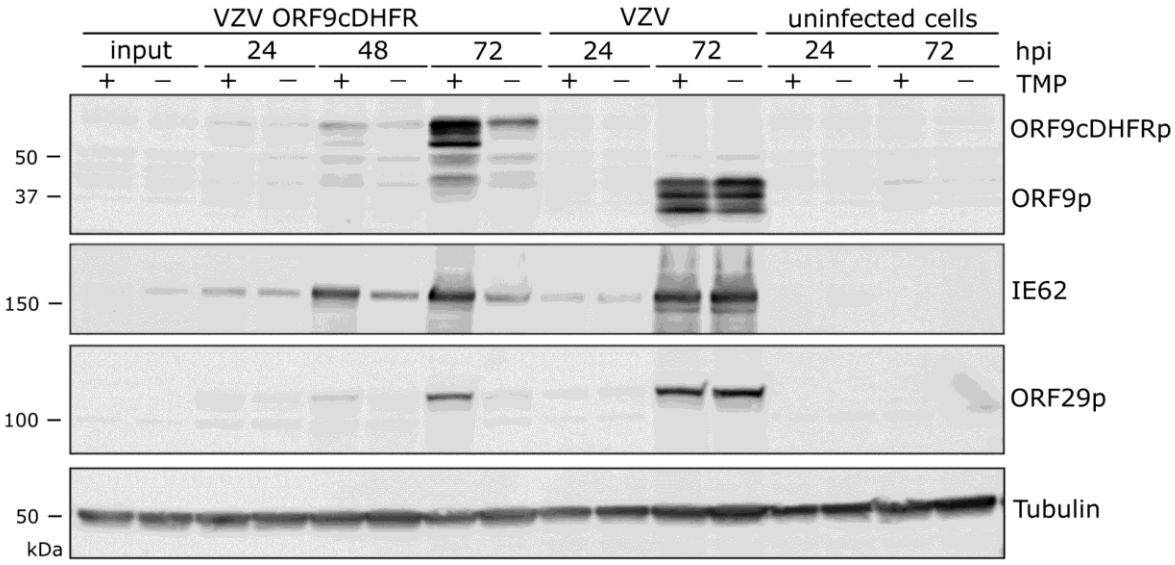

Figure 10: Proteins produced by VZV ORF9cDHFR and pOka grown in media containing or without TMP. (A) Cells were infected with titrated virus infected cell stocks as detailed in methods to allow multi-step virus growth analysis with VZV ORF9cDHFR or pOka. Proteins in infected cultures were harvested at times 24, 48 or 72-hpi in the presence (+) and absence (-) of 100 nM trimethoprim (TMP) and compared to uninfected cell extracts. SDS PAGE separated proteins were immunoblotted and probed with antibodies to ORF9, or proteins from other herpesvirus kinetic classes (IE62, ORF29p), and a cellular control (alpha-tubulin). Signals were determined using a LICOR Odyssey IR imager. ORF9 shows multiple species due to several recognized phosphorylated forms, and the expected size increase (~18 kDa) due to degron motif addition. The sizes of marker proteins (kDa) are indicated to the left of the blots. The blots are scanned in linear range and are representative of two identical experiments.

For infections initiated with VZV ORF4nDHFR, the expected IE4nDHFR size increase due to the addition of the degron was apparent, and TMP-dependent protein production increased over a 72-h infection in contrast to pOka and little protein accumulation was observed in the absence of TMP (**Fig 11**). VZV proteins from ORF29p and gE were greatly reduced in VZV ORF4nDHFR infections grown without TMP, consistent with impaired viral spread and

amplification, and the TMP-dependent loss of infectivity in growth curves (**Fig 7B**). Infections initiated with VZV ORF63cDHFR resulted in expression of the larger IE63cDHFR in the presence of TMP as expected (**Fig 12**), and it was the predominant form made by the recombinant virus. Substantially reduced levels of protein accumulated under nonpermissive conditions, although some accumulation of IE63cDHFR occurred in the absence of TMP over time. The increase in accumulation of other VZV proteins is consistent with a slightly leaky phenotype for this virus.

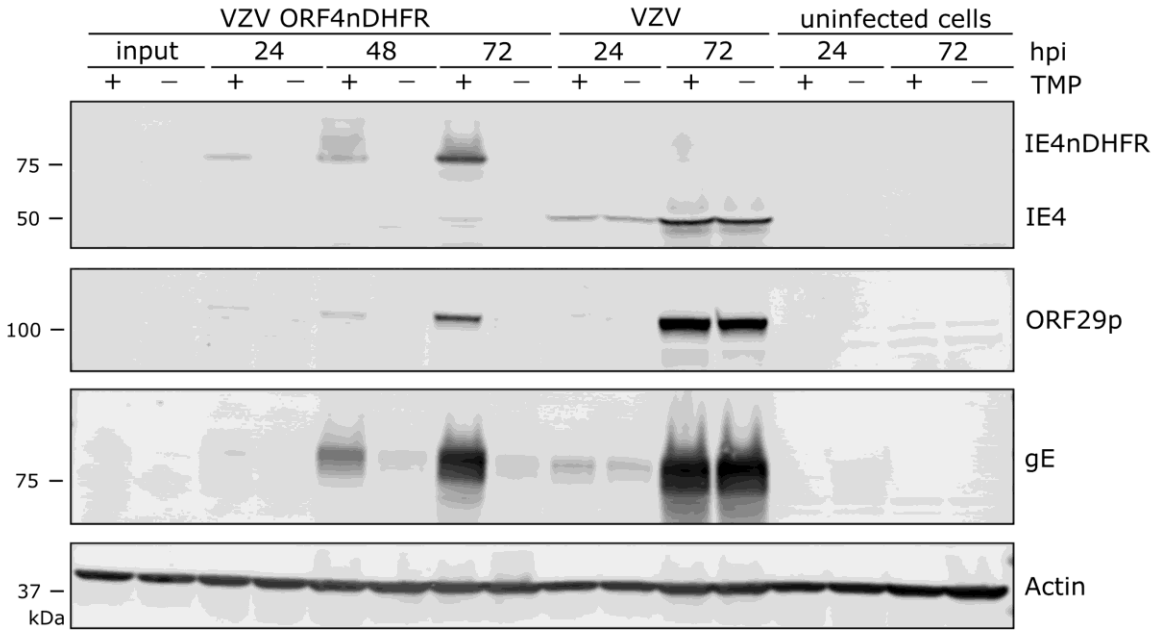

Figure 11: VZV IE4 is regulated by DHFR degron domain fused to amino-terminus.

VZV ORF4nDHFR was analyzed in a manner similar to that detailed for VZV ORF9cDHFR in the image and legend for Fig 3, with the exception that additional proteins were identified using antibodies to VZV gE and cellular protein actin. Proteins were from samples grown under TMP permissive (+) and nonpermissive (-) conditions and compared to wild-type pOka infections and uninfected cell equivalents. The blots are scanned in linear range and are representative of two identical experiments.

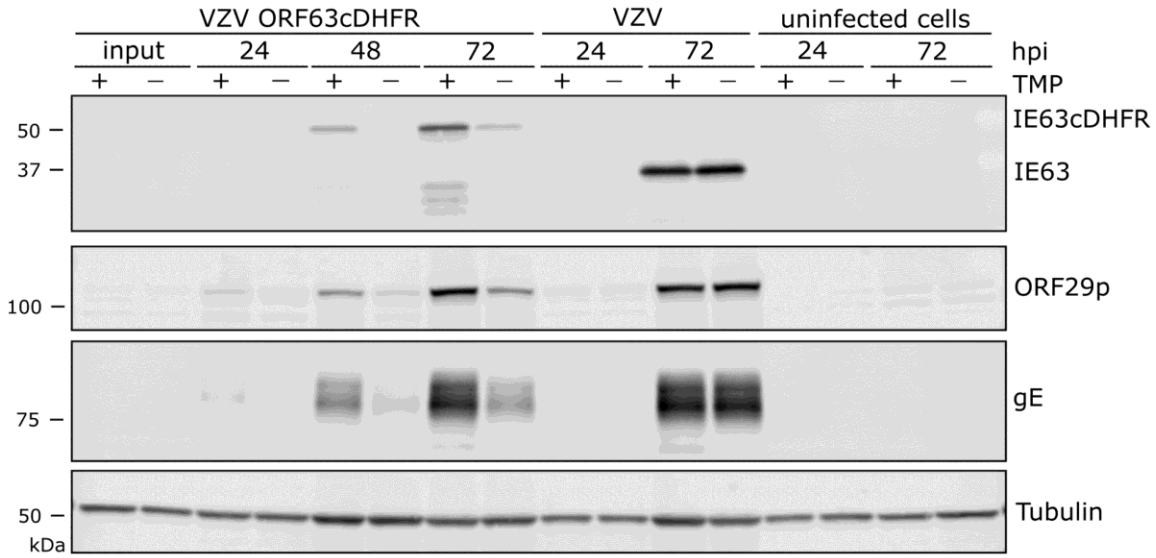

Figure 12: VZV IE63 is regulated by DHFR degron domain fused to carboxy-terminus.

Proteins were analyzed similarly to that shown in Fig 3 and 4. Protein samples were of cells infected with VZV ORF63cDHFR, pOka, or uninfected cell equivalents up to 72-hpi. Wild-type ORF63 (IE63) and DHFR modified (IE63cDHFRp) protein, proteins from alternative kinetic classes (ORF29p, gE), or cellular control (alpha-tubulin) were compared under TMP permissive (+) and nonpermissive (-) conditions. The blots are scanned in linear range and representative of two identical experiments.

Further characterizations were carried out to address if the degron addition had an influence on subcellular localization of the fused proteins. The nuclear localization (NLS) and/or nuclear export signals (NES) have been previously located for each protein [290,296–298]. The cellular localization of IE4nDHFR, ORF9cDHFRp, and IE63cDHFR were compared to the unmodified proteins made by wild type pOka infected cells, all grown in the presence of TMP. Images were acquired from edges of 2-dpi individual plaques showed that, in general, protein localization for each DHFR fused protein was similar to the distribution of the native proteins (**Fig 13**). IE4 and IE63 from pOka localized to both nuclear and cytoplasmic compartments, with IE4 showing a

more predominantly cytoplasmic distribution in most cells. IE63 was more nuclear localized in cells at the edge of plaques, which represent earlier stages of infection as compared to distributions at plaque centers. ORF9p was seen in both nuclear and cytoplasmic compartments in both DHFR and wild-type VZV infected cells. The similar distribution of the DHFR and wild-type proteins for each virus suggests that degron addition does not greatly affects subcellular distribution of the proteins.

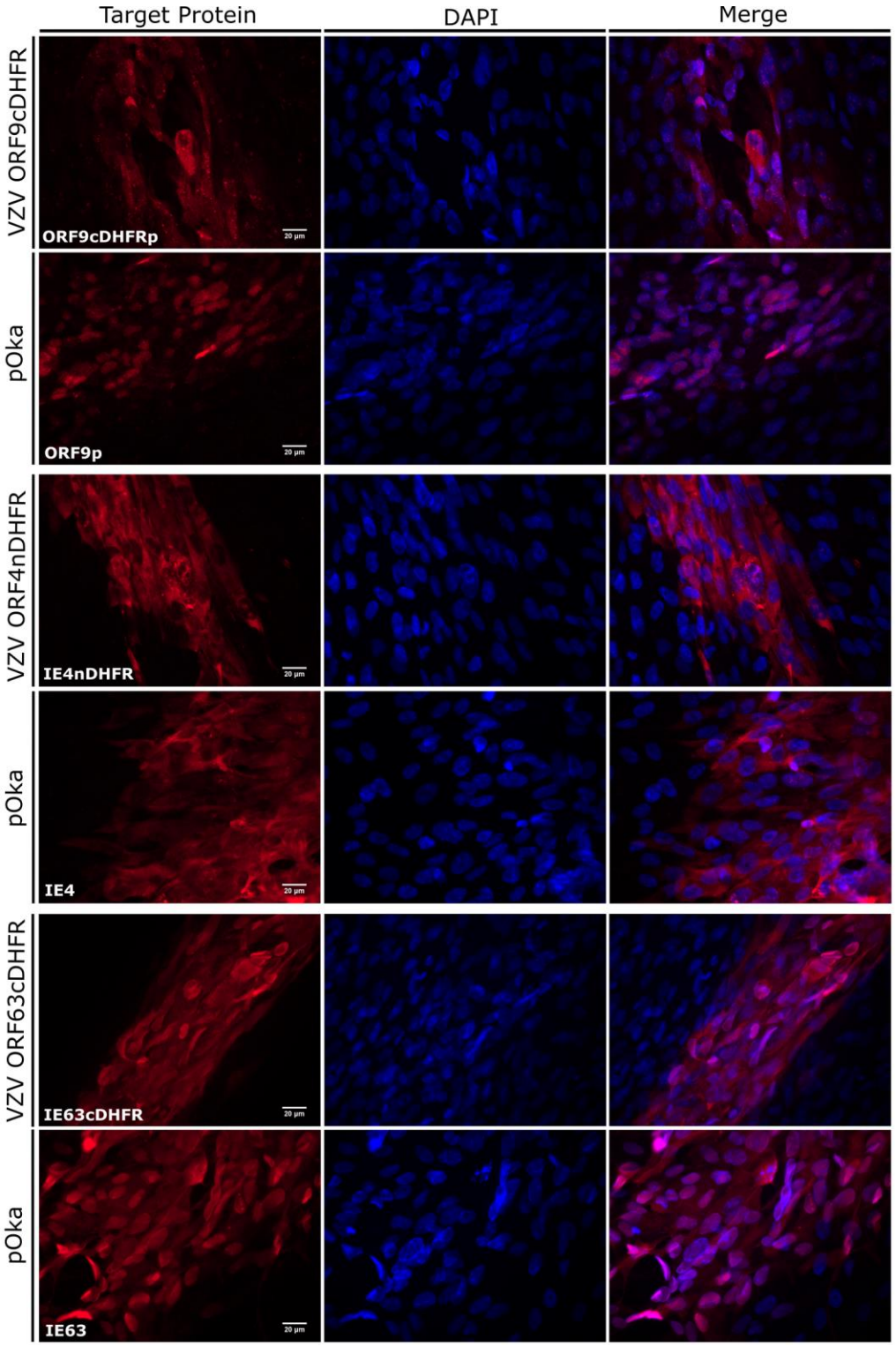

Figure 13: Localization of degron fused viral proteins compared to wild-type VZV proteins in infected cells.

(A) Images show the edges or small regions of plaques formed by wild-type VZV (pOka), VZV ORF9cDHFR (top), VZV ORF4nDHFR (middle), or VZV ORF63cDHFR (bottom) at 2-dpi. Protein cellular distribution in fixed cells was

imaged to represent the distribution seen in the cultures after staining with antibodies to ORF9p, IE4, or IE63. The 'target protein' column indicates the specific protein probed, as noted in the lower left corner of the column. The center column shows DAPI stained nuclei, and the rightmost column shows a merged panel of target protein immunofluorescence and DAPI staining. Magnification: 60X (NA 1.25) oil. Single images are representations of a minimum of 15 images analyzed for each virus.

4.3 Discussion

This is the first report of conditionally replicating VZV mutants, and was achieved by adopting a protein degron system that had been developed to study the consequences of protein turnover and removal in eukaryotic cells [108]. Viable VZV with ORFs -4, -9, or -63 containing the 160-amino acid degron were TMP growth regulated, so the degron addition had minimal overall effect on the function of the targeted proteins. Each virus showed similar levels of growth and protein production over time compared to wild-type VZV in growth-permissive conditions and formed plaque sizes that were only slightly reduced under permissive conditions. The degron did not strongly influence intracellular localization of the fused proteins, consistent with only a modest, if any influence on protein function. In the absence of TMP, each virus showed severely limited capacity in growth, viral spread, and protein production. ORF4 and -9 degron viruses showed tighter conditional regulation than VZV ORF63cDHFR. The degron system could clearly be useful to evaluate additional VZV essential genes. It has the advantage of permitting growth of mutant viruses in any permissible cell type. It also circumvents the need to derive complementing cell lines expressing the VZV gene-of-interest *in trans* in order to propagate VZV with a deleted gene, which has generally appeared to be more difficult for VZV in the limited human cell lines that support its growth. Previously developed VZV lacking ORF9 [101] and ORF4 [107] were

grown by complementing the absent gene in cells that had been transduced with high-titer baculoviruses expressing a cytomegalovirus (CMV) IE promoter driven VZV gene, which then required treatment with NaB to inhibit type-1 histone deacetylase activities and the chromatin-mediated silencing of the baculovirus. We attempted to prepare the VZVΔORF4 virus detailed previously [107], but could not obtain titers sufficient to exploit in the rat PHN models. The baculovirus approach is also complicated by the potential of the baculovirus itself and the sodium butyrate treatment required for transgene expression to affect behavioral responses [287,288,299]. The lack of success discouraged our pursuit of the VZVΔORF9 virus detailed previously [101]. VZV lacking the duplicated ORF63 and ORF70 has been reported by one group to replicate without complementation [300], but others report that deletion of ORF63 and ORF70 abrogated virus growth [13,301]. As far as we are aware, no ORF63 complementing cell line or system has been described. However, a caveat is that the conditional replication strategy is unlikely to be applicable to all VZV genes. Our attempts to target three DNA replication proteins did not result in viable virus, suggesting that the degron addition interfered with essential protein functions. We also found that degron addition does not guarantee regulation of protein stability, as found for VZV containing the degron added to the major transcriptional regulator encoded by ORF62 and ORF71. The reason for a lack of regulation is not clear, but it could be due to accessibility of the degron tag to ubiquitin-ligases as a consequence of cellular compartmentalization. For such genes, VZV deletion virus may require more classic complementation methods, and there has been some recent success in developing ARPE-19 based cell lines such as used here to grow the VZV Δ54S [30]. We are currently extending the degron system to evaluate additional VZV genes involved in DNA replication, to ask if VZV blocked at the DNA replication stage are able to induce hypersensitivity responses.

5.0 Replication-Conditional VZV in Rat Models of Postherpetic Neuralgia

This chapter was adapted from the published manuscript, "Varicella-zoster virus early infection but not complete replication is required for the induction of chronic hypersensitivity in rat models of postherpetic neuralgia," authored by Benjamin E. Warner, Michael B. Yee, Mingdi Zhang, Rebecca S. Hornung, Benedikt B. Kaufer, Robert J. Visalli, Phillip R. Kramer, William F. Goins, and Paul R. Kinchington [109]. It was written by BEW and PRKi and edited by WFG, PRKr, and BBK. All data in this section was collected, analyzed, and curated by BEW, RSH, WFG, PRKr, and PRKi.

5.1 Introduction

The lack of a reliable small animal model of VZV reactivation and HZ disease has precluded the study of VZV reactivation-driven pain. Rodent models show little to no clinical presentation after infection. Even non-human primate models using the closely related simian varicella virus (SVV) are difficult to employ for HZ and pain studies due to inefficient virus reactivation. Even then, animals do not routinely develop signs of PHN. Several groups have used the rat to investigate VZV latent states [257,259,260]. It was then demonstrated by multiple groups that Wistar and Sprague-Dawley rat strains inoculated with VZV at the footpad develop prolonged signs of pain that could serve as preclinical models for exploring mechanisms and treatment strategies for PHN [221]. The models involve subcutaneous inoculation of cell-associated VZV into the rat hind footpad [100,235,236,244–247] or more recently, the whisker pad [237,238,253–

256]. While animals show no outward signs of skin infection, inflammatory response, or disease, they develop nocifensive behaviors lasting several weeks. It has never been thoroughly resolved if VZV productive replication occurs within inoculated rats and if this is a requirement for nocifensive responses. Work from our group indicated that VZV did not replicate in rat primary cell cultures, suggesting VZV replication *in vivo* is unlikely [246]. One *in vivo* study indicated that VZV-induced hypersensitivity in rats was unresponsive to acyclovir administration [235]. Our group reported that rats inoculated with UV-irradiated VZV did not develop long-term nocifensive behaviors, suggesting a requirement for viral gene expression in the development of pain behaviors [245]. VZV has been shown to induce subtle changes in host gene expression within infected ganglia [246]. Ganglionic sections of rats with hypersensitivity show sporadic staining for the major VZV transcriptional regulatory protein, IE62 [236,237,244,247]. Taken together, these results suggest that VZV may initiate abortive infections in the rat that nevertheless induce nocifensive behaviors and hypersensitivity.

Here, we further addressed requirements of VZV replication and gene expression in development of pain indicators in the rat PHN models. Using the *Escherichia coli* DHFR degron system, we developed three conditionally replicating VZV that are expected to halt VZV replication at key points in the life cycle. These were used in conjunction with a cell-complemented VZV deletion mutant that did not express the essential ORF54 gene encoding the capsid portal protein [30]. The VZV recombinants were then assessed for their ability to induce behavioral hypersensitivities in rats when inoculated in the presence or absence of TMP. We show that VZV blocked at late stages of assembly and full productive replication (VZV ORF9cDHFR) in the rat still induced prolonged hypersensitive behaviors, establishing that productive replication is not required. In contrast, rats inoculated with conditionally replicating VZV with a degron attached to

IE regulated proteins (VZV ORF4nDHFR or ORF63cDHFR) only developed hypersensitivity when the inoculates were supplemented with TMP to stabilize the targeted degron proteins. This suggested that the production of essential IE transcriptional regulatory proteins IE4 and IE63 was required for the stimulation of persistent pain behaviors in the rat. These data are consistent with a hypothesized mechanism in which a limited VZV gene expression program in the rat results in altered host neuronal pain signaling. We discuss that this may occur in patients with PHN, in which an abortive VZV infection process occurs during HZ within sensory neurons that survive reactivation but go on to signal pain.

5.2 Results

5.2.1 Analyses of rats inoculated with VZV ORF9cDHFR indicate productive replication is not required for VZV-induced chronic hypersensitivity behaviors in rats

We used the conditionally replicating VZV to assess how reducing viral gene expression and replication influenced VZV induction of prolonged nocifensive behaviors in rat models of PHN. All TMP-dependent VZV were generated in cells supplemented with TMP. All viruses were managed identically for consistency, with the TMP-supplemented inoculant resuspended in PBS containing 500 nM TMP instead of PBS alone. Animals were then inoculated into the rear footpad as detailed previously [245], in a random left/right manner (n=6) so the inoculated paw and the nature of the inoculant was blinded from the behavioral assessors. Rat groups received equivalent infectious units of VZV ORF9cDHFR containing 500 nM TMP, the same virus without TMP, wild type pOka as the positive control, or uninfected cell equivalent as the negative control.

Development of mechanical allodynia (MA) and thermal hyperalgesia (TH) was assessed over a period 74-d (**Fig 14**). As predicted, pOka inoculated animals developed mechanical hypersensitivity responses by 14-dpi, consistent with previous studies [100,235,236,244–247]. Hypersensitivity was significant at multiple time points when compared to the contralateral (uninfected) footpad or rats that received uninfected cells, which none developed significant hypersensitivity over the course of the study. Importantly, VZV ORF9cDHFR induced significant hypersensitive states lasting over the testing period similar to that seen for pOka inoculated animals, whether or not a bolus of TMP was administered with the virus in the inoculate. Mechanical responses lasted several weeks and began to wane towards the end of this study, so that hypersensitive responses at 66-dpi were no longer significant for the pOka and VZV ORF9cDHFR groups compared to controls (**Fig 14a**). Measurements of thermal hypersensitivity followed a similar pattern, though the withdrawal time difference between positive and negative thermal responses was more subtle, so that significance in withdrawal times was not seen for every time point. By 18-dpi, significant differences were detected in all VZV inoculated groups when compared to the uninfected cell group or contralateral paw measurements (**Fig 14b**). The variability in thermal response is consistent with previous studies [100,236,245,247]. An average withdrawal time under 7-s was observed in hypersensitive rats, while responses for negative control animals remained above 10-s throughout most measurements in the 74-d study. Thermal hypersensitivity also waned during the later stages of the study. Given that VZV ORF9cDHFR replication is TMP-dependent and would be unable to spread when inoculated in the absence of TMP, we take these results to indicate that the development of hypersensitivity behaviors in the rat footpad model does not require productive replication, but is more the result of a single round, non-productive infection after inoculation.

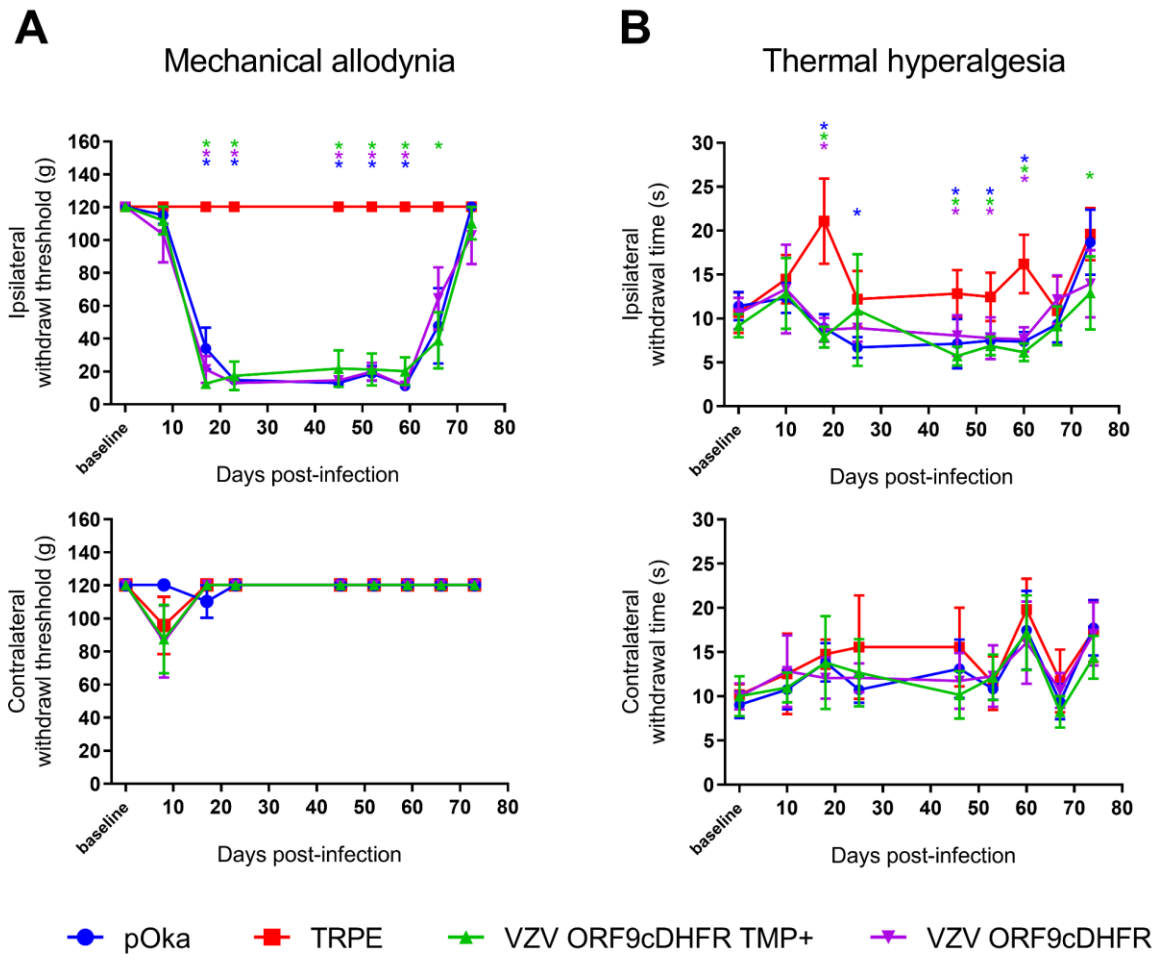

Figure 14: Development of mechanical and thermal hypersensitivity in rats after VZV ORF9cDHFR footpad inoculation under permissive and nonpermissive growth conditions.

Male Sprague-Dawley rats (n=6/group) were acclimated to measurement conditions and a baseline response was established the day of inoculation. Rats were inoculated in one rear footpad with $2x10^5$ PFU TRPE-associated pOka (blue circle), VZV ORF9cDHFR in PBS with 500 nM TMP (green triangle) or without TMP (purple triangle), or uninfected TRPE cell equivalent (red square). Mechanical hypersensitivity (A) was measured by von Frey monofilaments and the Up-Down method. MA assessment of the inoculated footpad was measured as 50% withdrawal threshold in grams (g) in the inoculated footpad (top) and the contra lateral, uninoculated footpad (bottom) of the same rats. Thermal hypersensitivity (B) was assessed by Hargreaves apparatus as detailed in the methods and is presented as time-to-withdrawal post-light activation (seconds). The responses of the inoculated footpad (top) and contralateral

footpad of the same rats (bottom) is shown. Error bars: SD. Statistics: Two-way ANOVA with Bonferroni multiple comparison to uninfected cell control, where *=p<.05 and is color coded by group.

We also evaluated the ability of these viruses to induce affective pain responses in the rat facial model (**Fig 15**). Rats were inoculated at the whisker pad in the same groupings as the footpad experiments, and rats were assessed for nocifensive behaviors in a fully blinded manner using the Fuchs' PEAP assay [237,239]. This physiological test evaluates animal behaviors resulting from noxious stimuli, in which rats show reluctance to locate to preferred locations if the stimulus evokes higher levels of pain or sensitivity. Animals receiving uninfected cells showed no behavioral indicators of aversion to stimulation of the inoculated whisker pad and remained predominantly on the dark or preferred side of the enclosure over the course of the experiment. However, stimulated animals that received pOka showed a considerable reduction of time spent on the dark side of the enclosure. Such behaviors began to return to baseline by 28-dpi and were no longer significant. While VZV-induced affective pain indicators at the whisker pad were shorter-lasting than the mechanical and thermal hypersensitivities detected at the footpad, the behavior of rats inoculated at the whisker pad with different viruses were consistent with the footpad data, in that VZV ORF9cDHFR induced hypersensitivity responses when inoculated with or without TMP. These data support the hypothesis that VZV ORF9cDHFR retains the ability to induce hypersensitivity with or without conditional replication and is consistent with the conclusion that ongoing replication of VZV is not required for the induction of pain behaviors.

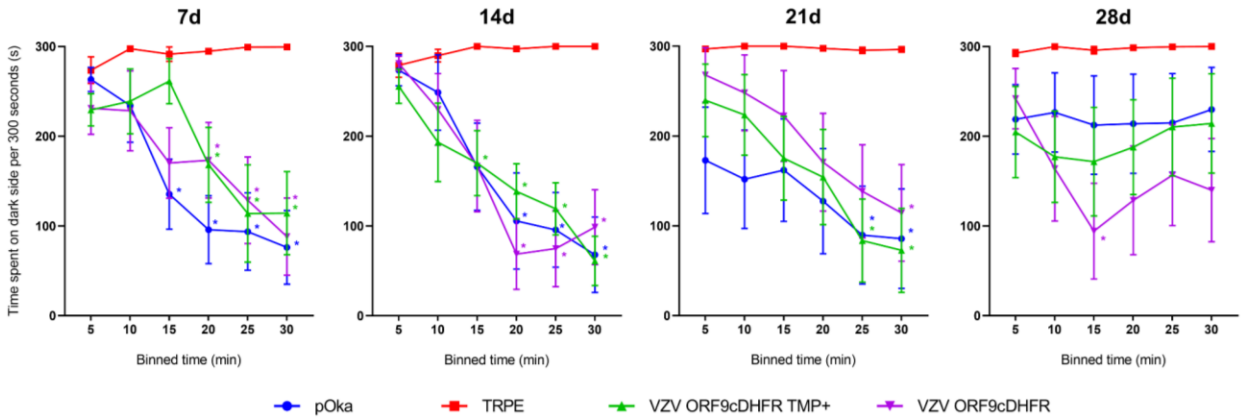

Figure 15: Affective pain develops in rat whisker pad following inoculation with replication conditional VZV ORF9cDHFR under both growth-permissive and nonpermissive conditions.

Male Sprague-Dawley rats (n=7/group) received inoculation into the whisker pad of $2x10^5$ PFU TRPE-associated pOka (blue circle), VZV ORF9cDHFR in buffer with 500 nM TMP (green triangle) or without TMP (purple triangle), or uninfected TRPE cell equivalent without TMP (red square). Hypersensitivity was measured at the times indicated by days (d) post-infection above each graph using a PEAP method detailed in methods. Time spent in the dark side (y-axis) of the enclosures is shown after repeated stimulation with a 60g (5.88) von Frey hair every 15 seconds, assessed over 5-min bin periods for a total of 30 min (x-axis). The side of the face stimulated depended on the position of the rat's head, with facial stimulation at the inoculated side if its head is in the dark side of the enclosure, and stimulation of the uninoculated side of the face if in the light side of the enclosure. Error bars: SEM. Statistics: Two-way ANOVA with Bonferroni multiple comparison to TRPE negative control where *p<.05 and color coded by group.

5.2.2 Analyses of VZV ORF4nDHFR indicates production of the VZV IE4 is required for development of VZV-induced hypersensitivity

A similar set of studies were performed in the footpad and facial models to examine how VZV ORF4nDHFR stimulates hypersensitivity when replication is permitted or prohibited. In footpad model studies (**Fig 16a**), responses indicating mechanical hypersensitivity developed by 22-dpi in pOka inoculated rats. The timing of onset of hypersensitivity was later than that seen in

the ORF9cDHFR study, but such variability has been seen previously [100,236,245,246]. No measurable hypersensitivity developed in rat footpads injected with uninfected cells or developed in the contralateral uninoculated footpads. In contrast to the results obtained from animals inoculated with VZV ORF9cDHFR, hypersensitivity developed in rats that received VZV ORF4nDHFR supplemented with 500 nM TMP, but animals did not develop hypersensitivity if TMP was not included in the inoculum. Rather, animals showed withdrawal responses similar to uninfected cell equivalent groups (**Fig 16a**). Hypersensitivity in animals inoculated with VZV ORF4nDHFR with TMP was detected throughout the entirety of the assessment period (the study was terminated at 55 dpi). Thermal hypersensitivity responses followed a similar pattern so that by 24-dpi, significant hypersensitivity was seen at select times in rat groups that received pOka or VZV ORF4nDHFR containing TMP (**Fig 16b**). Quicker withdrawal times did not develop in contralateral footpads, footpads inoculated with uninfected cells, or in footpads that received VZV ORF4nDHFR without TMP supplementation. Rat groups that developed hypersensitivity remained significant at most measurement times until to the end of the experiment when compared to the negative control. We did see some significant responses in the contralateral footpad at certain timepoints, but this is not unusual and has been observed at random and on occasion in previous thermal hypersensitivity assessments. However, these contralateral measurements did not form a consistent pattern of continued hypersensitivity, as observed on the ipsilateral side, and generally resembled the responses of the negative control group.

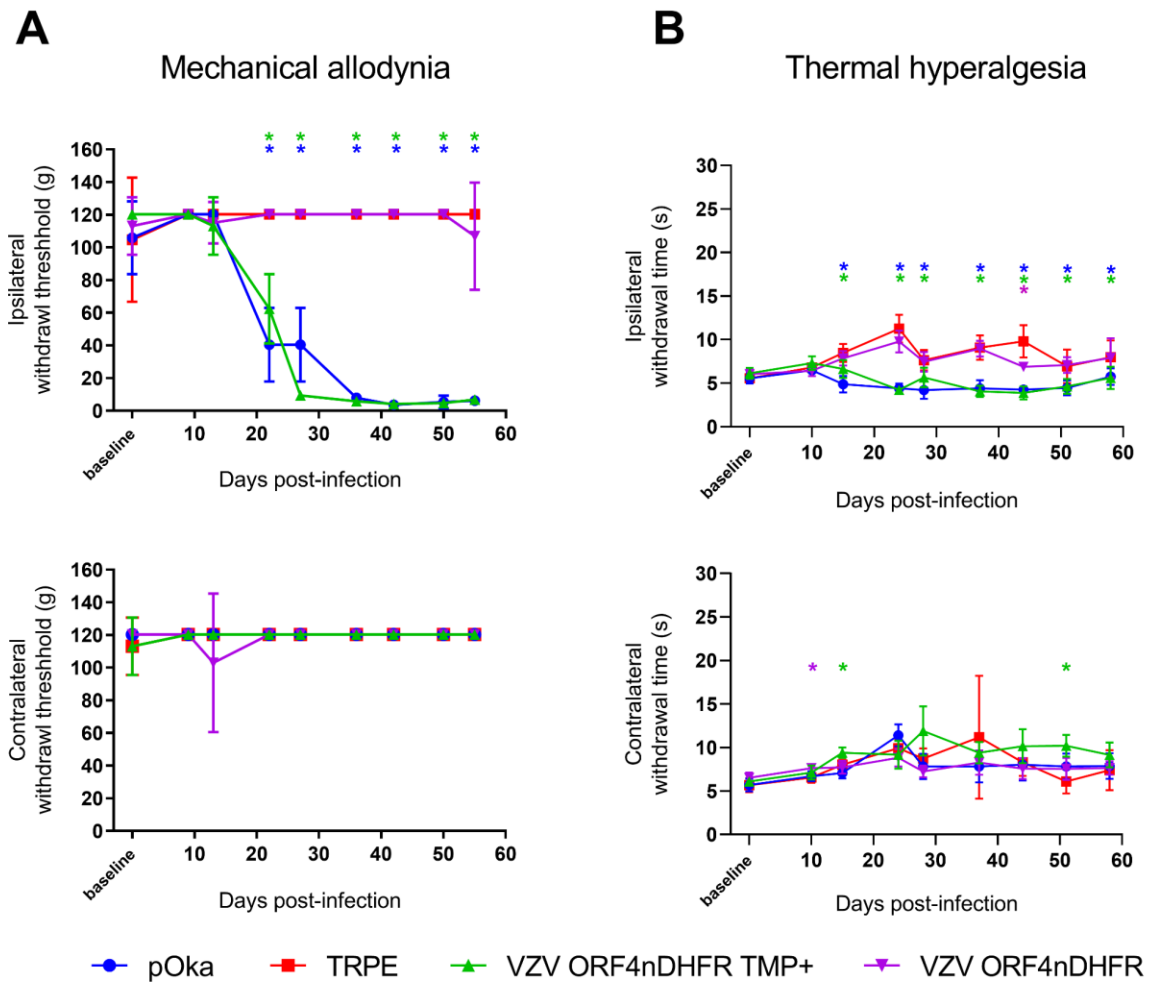

Figure 16: Footpad inoculation by VZV ORF4nDHFR induces mechanical and thermal hypersensitivity only if IE4 is stabilized under growth-permissive conditions.

Male Sprague-Dawley rats (n=6/group) were inoculated with $2x10^5$ PFU pOka (blue circle), VZV ORF4nDHFR with 500 nM TMP (green triangle) or without TMP (purple triangle), or uninfected TRPE equivalents (red square). (A) MA of inoculated footpad (top) vs contralateral (bottom). (B) The same group of rats were tested for TH of the inoculated footpad (top) vs contralateral, uninoculated footpad (bottom). Error bars: SD. Statistics: Two-way ANOVA with Bonferroni multiple comparison to TRPE negative control where *p<.05 and color coded by group.

In the rat facial model of affective pain, the pOka and VZV ORF4nDHFR with TMP groups were found to spend significantly more time on the light side of the enclosure at 7-dpi when

compared to the uninfected cell equivalent group (**Fig 17**). Consistent with the footpad studies, animals that received VZV ORF4nDHFR without TMP continued to spend a majority of time on the dark side as seen for the uninfected cell group. The trend continued over the course of the 5-week experiment, at which time nocifensive behaviors of the hypersensitive groups waned, as seen previously [237]. Post-hoc analysis indicates significance for the pOka group during all measurement groups, while the VZV ORF4nDHFR TMP supplemented group lost significance during the final measurement timepoint. At no point did the VZV ORF4nDHFR without TMP group show any significant indication of hypersensitivity. We highlight that these results contrast with the responses of animals receiving VZV ORF9cDHFR, in which pain behaviors developed with or without TMP. The results suggest that the degron mediated removal of IE4 prevents the development of pain behaviors and suggests that IE4 is necessary for the induction of pain responses after VZV inoculation.

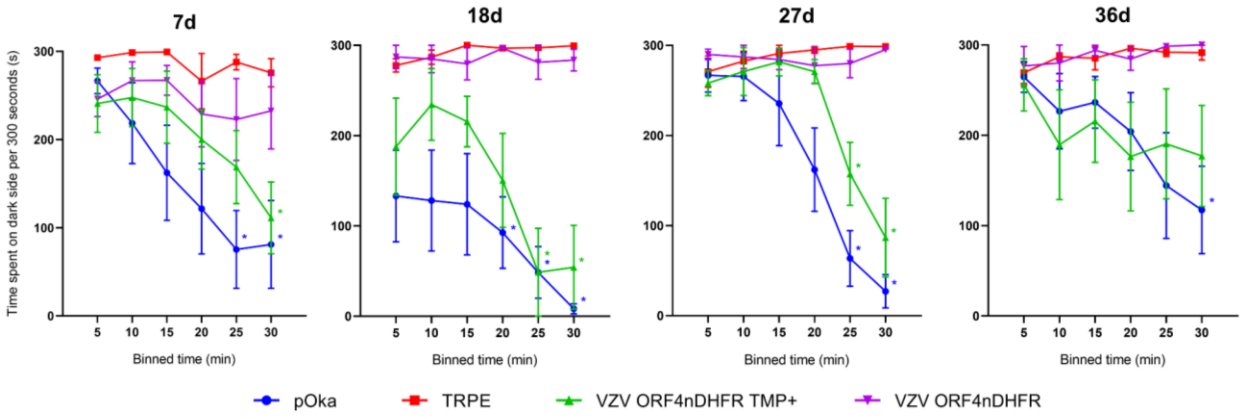

Figure 17: Affective pain develops following whisker pad inoculation with replication conditional VZV ORF4nDHFR only under permissive conditions.

Male Sprague-Dawley rats (n=6/group) received 2x105 PFU pOka (blue circle), VZV ORF4nDHFR with 500 nM TMP (green triangle) or without (purple triangle), or uninfected TRPE cell equivalent (red square). Hypersensitivity was measured at times post-infection (d) indicated above each graph using the same methods as Fig 7 and detailed in the methods section. Error bars: SEM. Statistics: Two-way ANOVA with Bonferroni multiple comparison to TRPE negative control where *p<.05.

5.2.3 Analyses of additional VZV mutants confirms the requirement for gene expression, but not full viral replication for the development of pain behaviors in rats

We sought to confirm the contrasting outcomes of the VZV ORF9cDHFR and ORF4nDHFR in the rat footpad model through the analyses of additional VZV recombinants containing mutations in different genes. We evaluated animals inoculated with VZV ORF63cDHFR in the same manner (**Fig 18**). In parallel, we examined the responses in the footpad model of animals that were inoculated with a recently described recombinant VZV that is deleted for expression of ORF54 (VZV Δ54S) [30]. ORF54 encodes the portal protein involved in the packaging of viral DNA into preassembled capsids in the nucleus, and VZV lacking ORF54 cannot replicate beyond the initial round of replication in non-complementing cells. To grow VZV Δ54S,

an ARPE-19 based complementing cell line was used (A54). Following footpad inoculation, the behavioral responses of rats receiving these viruses and controls were assessed for mechanical (**Fig 18a**) and thermal hypersensitivities (**Fig 18b**). In these studies, the negative control group was divided into two, with one group of rats inoculated with uninfected A54 (n=3) and the second with uninfected TRPE (n=3) cells. The behavioral responses of the two uninfected cell controls were indistinguishable from each other (and thus combined in the graph) or historical uninfected cell controls, indicating that the complementing cell line did not induce a significant pain response. pOka infected cell inoculated animals developed significant mechanical hypersensitivities from 18-dpi onwards that lasted through to the end of the study (**Fig 18a**). Thermal hypersensitivities for pOka inoculated animals also trended towards a response, although the measurements in this study were not significant at times other than 40 days (**Fig 18b**). Animals that received VZV ORF63cDHFR with a bolus of TMP at the footpad developed significant mechanical hypersensitivity at a time similar to those animals receiving pOka, but animals receiving the virus without TMP did not develop any significant hypersensitivity behaviors and showed responses similar to those of animals receiving uninfected controls at all timepoints. This result indicates that the production of IE63 is critical for the induction of a prolonged mechanical hypersensitivity response in the rat model. In contrast, significant and long-lasting mechanical pain responses developed in animals inoculated with the genetic mutant VZV Δ54S. While this virus was administered with its complementing cells, the subsequent infection of any cells in the rat host would not be expected to progress to infectious virus production. These studies further support our previous conclusions involving VZV ORF9cDHFR (**Figs 14 and 15**) and ORF4nDHFR (**Figs 16 and 17**) and denote that hypersensitivity in the rat models of PHN require early infectious

processes and the expression of regulatory proteins, but that this occurs during a single and abortive round of infection in the rat host.

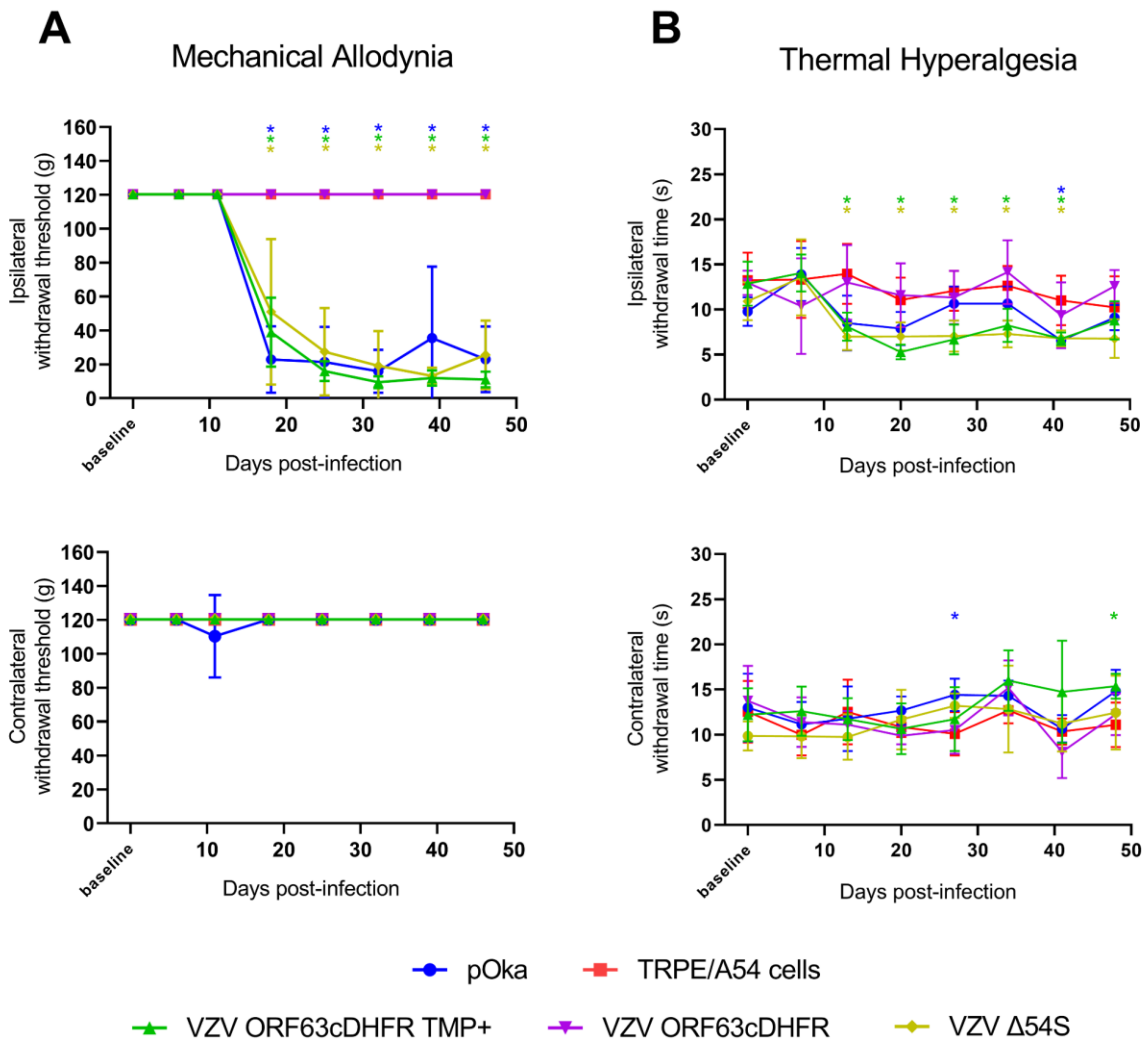

Figure 18: Induction of mechanical and thermal hypersensitivity by VZV with conditionally stabilized IE63 or by VZV lacking the production of the ORF54 portal protein.

Male Sprague-Dawley rats (n=6/group) were inoculated with 2x105 PFU pOka (blue circle), VZV ORF63cDHFR with 500 nM TMP (green triangle) or without TMP (purple triangle), VZV Δ54S (yellow diamond), or uninfected cell equivalents (red square) and subjected to the same testing methods in Fig 6. (A) Mechanical hypersensitivity of inoculated footpad (top) vs contralateral (bottom). (B) The same group of rats were tested for thermal hypersensitivity of inoculated footpad (top) vs contralateral (bottom). Error bars: SD. Statistics: Two-way ANOVA with Bonferroni multiple comparison to TRPE negative control where *p<.05. Note: The uninfected cell equivalents (red square) in this figure represent inoculated rats n=3 A54 cells and n=3 TRPE cells. This data has been combined for clarity and was deemed appropriate as the cell lines are from a common lineage.

5.2.4 Detection of gene expression following inoculation of rat footpads with replication conditional VZV

We next sought to determine if these genes were expressed at detectable levels in DRG of inoculated rats. Previous studies have found that VZV transcripts [260,261] and proteins [100,236,244] can be detected by *in situ* hybridization or immunohistochemistry in ganglia after inoculation. We used a set of described PCR primer/probes to detect ORF62 and ORF63 [83], and additional sets to identify ORF4 and the DHFR degron domain by RT-qPCR. The TMP-dependent virus stocks were generated as detailed in the methods and were the same used throughout all animal studies. Titrated virus was inoculated into rat footpads. The L4, L5, and L6 DRG of animals harvested at days 4-, 5-, and 7-dpi was used to prepare total RNA and then converted to cDNA for assessment of VZV gene expression in DRG (**Fig 19**). We were unable to obtain statistically significant increases in gene expression for the probed VZV genes. This indicates that levels of transcripts for ORF62, ORF4, and ORF63, or the DHFR sequence are too low for consistent detection by this approach in rats infected with wild-type VZV, VZV ORF4nDHFR, and VZV ORF63cDHFR. The lack of significance when compared to relative changes in GAPDH is similar to our previous study [246] and is generally consistent with sparse detection of VZV transcripts by *in situ* hybridization studies. Despite low detection levels for VZV ORF63cDHFR infected rats, the similar pattern that formed in the detection of ORF63 and DHFR, which should identify the same transcript, may suggest these data are consistent with the ORF63 transcript being detectable in rat ganglia at low levels [260].

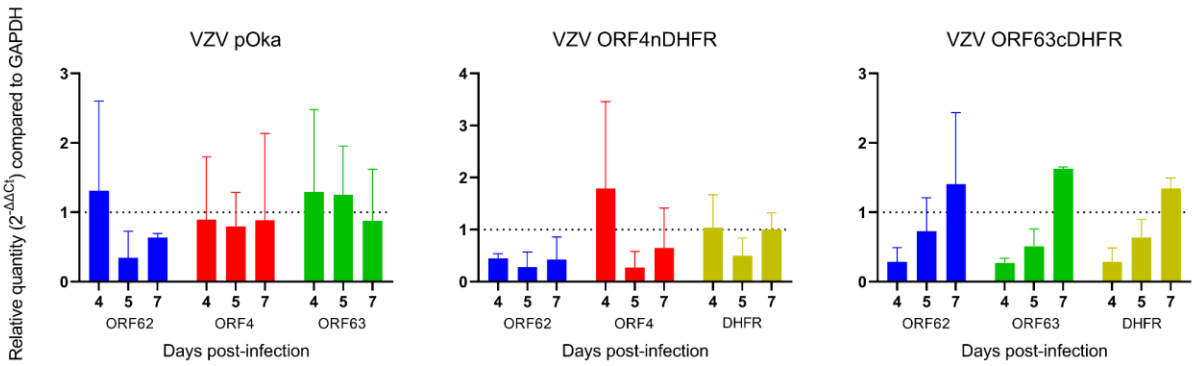

Figure 19: Detection of ORF4, ORF62 and ORF63 transcripts in rat DRG tissues after inoculation of wild-type VZV or VZV containing DHFR degrons.

L4, L5, L6 DRG were isolated from VZV pOka (left), ORF4nDHFR (middle), or ORF63cDHFR (right) inoculated rats at 4-, 5-, and 7-dpi and used to prepare total RNA. RNAs were quantified by TaqMan probe for expression of ORF62 (blue), ORF4 (red), ORF63 (green), DHFR (yellow) and GAPDH transcripts. RNA quantification was analyzed by the $2^{-\Delta\Delta Ct}$ method relative to GAPDH expression. The dotted line (=1) represents no change over the GAPDH control from naïve uninoculated animals. Data represents two similar experiments combined and averaged. Error bars: SD.

5.3 Discussion

In this work, we developed and exploited novel VZV mutants to dissect how components of the VZV infectious process contribute to the development of nocifensive behaviors in rat models of PHN. The data establish that presence of two VZV regulatory proteins, IE4 and IE63, are required for the development of hypersensitivity, but that production of infectious progeny virus in cells of the rat host is dispensable. The results imply that development of hypersensitivities in rats inoculated with VZV are the consequence of a single round, abortive infection in cells of the rat host but require some level of viral gene expression. These data also suggest that

hypersensitivities are not the result of a reaction to the VZV-associated cell antigens injected but require VZV to initiate an infection in cells of the rat host. The studies have implications for the induction of hypersensitivity and PHN in humans: we speculate that the partial VZV expression program could occur in human ganglia after an HZ event, in which infected but surviving neurons have a destabilized host neuronal homeostasis that leads to prolonged signaling of pain that may underlie PHN.

The data show that productive VZV replication in the rat PHN model is not required to cause VZV-induced pain in those models. This fits with our suspicion that the high species specificity of VZV prevents viral replication *in vivo* at some post-entry phase in rats. While rats have long been used as both models of pain and as models of latency, VZV permissivity in the rat has never been fully resolved. Numerous studies report the detection of viral transcripts and some proteins in VZV infected rat ganglia that were hypothesized to reflect the VZV latent state [100,236,246,260,261,302,303]. The long-term pain behaviors have been useful to examine potential pain alleviating drugs [100,235,236,245,247,249,304]. Dalziel *et al.* (2004) found that that pain induced by VZV infection was not alleviated by a 10-day treatment with systemic ACV administration to rats [235]. ACV inhibits herpesvirus DNA replication, and blocked pain responses generated in rats receiving HSV, suggesting these two related herpesviruses induced pain by different mechanisms. Our work showed that UV-irradiation of the VZV infected cell inoculate (to reduce infectivity by more than 2-logs) prevented development of most pain behaviors [245]. However, we reasoned that neither approach was definitive in determining if VZV replication was required for induction of pain behaviors. The minimum inhibitory concentration of ACV for VZV is considerably higher than for HSV and the results of Dalziel *et al.* may have reflected insufficient levels to block VZV. UV-irradiation may have caused considerable damage

to the inoculum. However, our finding that two mutants unable to fully replicate under our inoculation conditions (VZV ORF9cDHFR and VZV Δ54S) allows us to conclude that potential ongoing VZV productive replication, should it occur in rats, is not needed for development of nocifensive behaviors. Both mutants would likely be blocked at late stages of infection and express most VZV genes; ORF9p is essential and primarily involved in tegument assembly and secondary envelopment [59,101], while VZV lacking ORF54 would not be able to package DNA into capsids. Though VZV Δ54S was administered in complementing cells, the virus produced would be unable to form assembled virions in cells of the rat. A54 cells induced responses that were similar to uninfected cells in the same experiment and in historical studies [237,238,244–246]. Thus, the rat pain models appear to reflect a nonpermissive host in which abortive infection by VZV is sufficient for pain indicators.

In contrast, studies with the ORF4 and ORF63 conditionally replicating VZV establish that some VZV gene expression is essential for the induction of mechanical hypersensitivities. ORF4 is expressed as an IE gene based on classic cycloheximide-actinomycin D reversal experiments after cell-free VZV infections [292–294]. The protein has post-transcriptional regulatory activities suspected to be involved in nuclear export of intronless mRNA, in a manner similar to HSV ICP27 [305]. Removal of this protein from the infectious process would likely severely limit downstream VZV gene expression programs, as most VZV lytic transcripts are not spliced. Similarly, ORF63 was shown to be IE expressed using cycloheximide-actinomycin D approaches, and studies indicate it is a regulatory protein that is critically involved in early infectious processes [295]. Rats inoculated under conditions of TMP-permitted replication with each virus developed long-lasting hypersensitivities, establishing that the viruses themselves were not defective, but under nonpermissive replication conditions, neither induced significant behavioral responses in both the

footpad and facial models. The data solidifies that some VZV genes and proteins with regulatory function are needed in rats for prolonged pain indicators. Presumably, VZV lacking IE4 would not shuttle intronless VZV messenger RNA to the cytoplasm for translation [294]. What the consequences of ORF63 are on the rest of the VZV expression program is less clear. The lack of any response without permission to replicate also indicates that antigen load in the inoculate, and components contained in the infecting virus tegument and capsid, are not sufficient to drive the signaling processes associated with hypersensitivity.

At this stage, there are some questions that remain to be resolved. We do not yet know whether the production of IE4 and/or IE63 are the actual drivers of the pain responses, or if their roles are to permit the expression of downstream genes that induce nocifensive behaviors. The resolution of this would require the study of additional mutants, such as a mutant that would enable us to prevent DNA replication in the rat host. Based on our previous work, where we did not see DNA replication in primary rat cell cultures, we would predict that a VZV with conditional degron-controlled essential DNA replication protein might show the same type of hypersensitivity induction seen for VZV ORF9cDHFR and induce hypersensitivity without DNA replication. Such mutants are being developed. It is also not yet clear as to what tissues the VZV limited expression program is needed to induce the hypersensitivity responses. We hypothesized that VZV proteins are produced within a few neurons of a sensory ganglion that innervate the site of inoculation, and that these trigger altered neuronal signaling. However, studies to determine significantly increased expression of VZV transcripts in rat ganglia have not been successful here and in a previous report beyond 5-7 days [246]. This indicates that VZV gene expression within innervating neurons is low and could be transient. Others have reported the detection of IE62 and IE63 in ganglia obtained after *in vivo* inoculation at sparse levels [100,259–261] and gene array studies suggest there are

some changes in the respective ganglia [246]. We postulate that further studies of transcripts at the single cell level of the ganglia may allow the correlation of host with viral genes expression, but we considered them outside of the scope of the current work. It is even possible that the essential components of VZV gene expression is in non-neuronal cell types, such as glia and support cells proximal the sensory nerve endings at the periphery. These studies are planned or in progress.

Taken together, the data are consistent with the hypothesis that a partial gene expression program is required and sufficient for the induction of hypersensitivity in rat models of PHN. We speculate that this may be quite relevant to clinical HZ and the development of PHN, despite the fact that PHN follows reactivation whereas the rat model reflects events after a primary inoculation. However, when VZV reactivates in sensory ganglia, it probably starts within one or a small fraction of neurons, usually within a single ganglion. VZV then undergoes intraganglionic spread by cell-cell fusion, spreading to other neurons that are, therefore, newly infected [177,306]. These deliver virus to the periphery via innervating axons that terminate throughout the dermatome. There is neuropathic damage in many neurons and a reduction of nerve fibers in the afflicted dermatome [216]. Ganglionitis has been proposed to partly account for acute pain associated with HZ [191]. However, the ganglionic replication of VZV is usually limited, probably because of intrinsic, innate, and VZV-specific adaptive immune responses. We know that in HSV ganglionic infection models, ganglia resident CD8+ T cells limit virus gene expression and can suppress active neuronal replication through non-cytolytic means [307,308]. As such, the neuron survives, despite having initiated some viral gene expression. We propose this occurs on a much larger scale in the human ganglion hosting the HZ reactivation event, and clinical PHN may reflect the activity of neurons that have been infected, have made some VZV proteins (that induce host cellular changes) but then become subjected to multiple noncytolytic effectors such as mediated

by ganglion resident VZV-specific T cells that halt the full infectious program in a non-cytolytic manner. We postulate that a limited viral protein expression program (and/or the immune effectors targeting them) in surviving neurons may have undergone altered host gene expression programs that involve genes of pain signaling. We are currently examining how individual VZV gene products may induce development of PHN-like behaviors in the rat models and the host expression programs that result. This may identify mechanisms that can be therapeutically targeted to limit the development of PHN.

6.0 A Transgenic Reporter Rat to Study VZV Infection *In Vivo*

6.1 Introduction

Several questions remain about VZV infection in the rat host despite being used extensively as models of induced pain and latency. Early studies indicated that immediate-early VZV transcripts could be detected by ISH in ganglia of VZV inoculated rats at 9-months [243,257] and 18-months after subcutaneous inoculation [260,261]. VZV reactivation was achieved *ex vivo* by repeated passage of 30-dpi rat DRGs with human fibroblasts [243,257]. Subsequent studies using the cotton rat model supported many of these initial findings and characterized several VZV genes that were dispensable for establishing latency [24,99,303]. While these rat models appear to reproduce some aspects of VZV genome persistence observed in human cadaver ganglia, it is difficult to differentiate persisting VZV genomes as abortive or latent infections because reactivation has never been demonstrated *in vivo*. Previous studies from our lab suggested that VZV does not fully replicate in any primary rat cultures, but can support limited gene expression and protein translation [246]. *In vitro* infection of primary rat lung fibroblasts showed that the major transcriptional activator from ORF62 was detectable by 1-dpi. Despite initiating transcription and translation, rat cells cultured from the eye, paw, liver, kidney, and lung showed no increase in VZV DNA consistent with active DNA replication [246]. Much of these findings are consistent with the early rat studies. However, RT-qPCR analyses of rat ganglia after subcutaneous inoculation were unable to conclusively detect ORF4, -62, or -63 transcripts (**Fig 19**) [109,246] as previously reported by ISH detection. Our understanding of VZV latency has changed since many of the early infection studies in rats, such as the detection of VLT in latently

infected human ganglia [83] and detection of VLT-ORF63 isoforms upon *in vitro* reactivation [84]. Thus, evidence for VZV latent or abortive infection of the rat host *in vivo* remains inconclusive could benefit from reevaluation considering new evidence.

Recently, a Long-Evans transgenic rat was made commercially available that uses Cre-Lox recombination for conditional expression of a bright red fluorescent protein (tdTomato) [278]. Upon exposure to Cre recombinase, recombination at *loxP* recognition sites removes repressive DNA sequences to enable tdTomato gene expression and permanently marks tissues exposed to Cre. Here, we developed VZV that expresses a Cre recombinase gene to explore *in vitro* and *in vivo* infections in this rat model. Induction of tdTomato expression occurred readily in tissue culture but *in vivo* detection thus far has been limited to 28-dpi footpad tissue. While the experiments reported here are ongoing and will be expanded in the future, they establish the reagents in this reporter rat model. Further analyses may help clarify what tissues become infected and if VZV undergoes a latent or abortive infection in the rat ganglia.

6.2 Results

6.2.1 Development of VZV containing Cre recombinase

We first developed a recombinant VZV that expresses a Cre recombinase gene. An insertion cassette was generated by PCR amplification of a sequence that combined a CMV IE promoter with a turquoise2 (Turq2) fluorescent gene linked to Cre using an in-frame 2A peptide sequence (T2A) (**Fig 20a**). The addition of a T2A sequence between Turq2 and Cre provided a method to easily determine if Cre was being produced. The cassette is expressed as a single

message under the CMV promoter, but the T2A sequence allows Turq2 and Cre proteins to be translated as separate proteins due to ribosomal skipping at the T2A sequence and therefore Turq2 florescence should indicate Cre production. This cassette was recombined into a non-coding gap between two nonessential genes in tissue culture, ORF13 (thymidylate synthetase) and ORF14 (glycoprotein C), of the self-excisable VZV BAC [101] with or without the N-terminal GFP on ORF23 [85]. The resulting recombinant virus (VZV aT2C) was verified by Sanger sequencing and virus was derived by TRPE cell transfection. ARPE monolayers were then infected for 48-h with cell associated VZV aT2C to determine if Turq2 fluorescence was observable and if Cre protein could be detected by antibody probe. Turq2 fluorescence was abundant (data not shown), and the viruses produced Cre protein (~38 kDA) (**Fig 20b**). VZV aT2C.1 and aT2C.2 are technical replicates and aT2C.3 contains a GFP on the N-terminus of ORF23. Here forward, the experiments described were carried out with VZV aT2C.1.

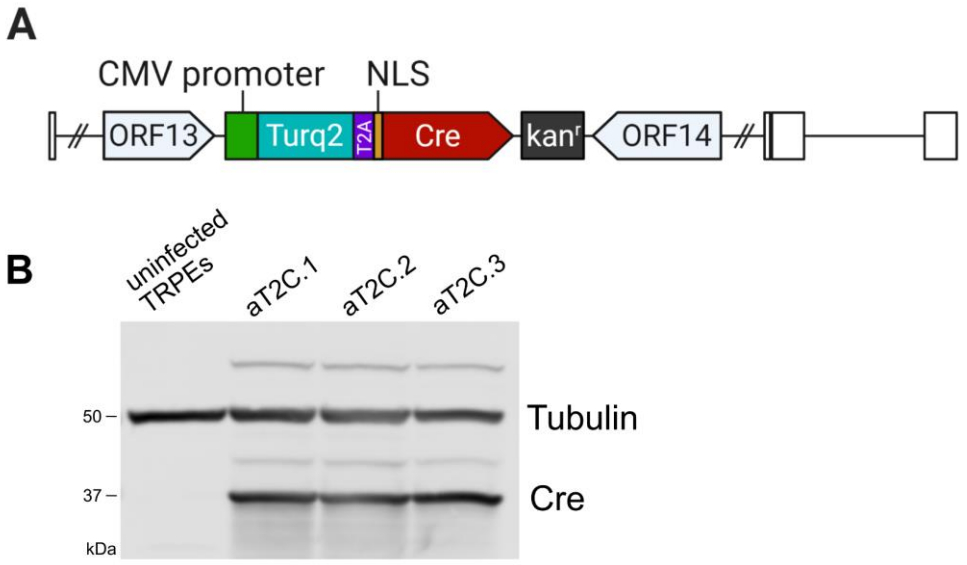

Figure 20: Construction of recombinant VZV containing Cre recombinase.

(A) A single cassette containing a cytomegalovirus (CMV) promoter, turquoise2 (Turq2) fluorescent gene, multicistronic linker T2A, a modified NLS-Cre recombinase from bacteriophage P1, and a kan^r cassette was inserted between VZV ORFs -13 and -14 in the self-excisable VZV BAC. (B) Recombinant VZV were derived, passaged in TRPE cells, and tested for production of Cre following a 48-h infection of ARPE-19 cells.

6.2.2 *In vitro* inoculation of primary rat cells harvested from tdTomato transgenic rat

We next tested VZV aT2C for Turq2 fluorescence and Cre recombinase activity in reporter rat cells. Skin cells were first harvested from the ears of reporter rats to establish primary cell cultures for *in vitro* infection studies. Cell associated infections were initiated at 1:1000 VZV to cell and were fixed for imaging at 1-, 2- or 7-dpi (**Fig 21**). Turq2 fluorescence was immediately observable because many of the infecting human cells were fluorescent. tdTomato fluorescence was visible after 1-d. Both Turq2 and tdTomato increased in fluorescence by 48-hpi. By 7-dpi, Turq2 fluorescence reduced to mostly single infected cells. This likely indicated that the VZV-infected TRPE cells used to initiate infections had succumbed to VZV infection and lysed, and

expression in the rat cells had ended. tdTomato fluorescence was abundant after 48-h and lasted throughout the 7-d experiment. Any loss of tdTomato was expected to be the result of cell death rather than inhibition of tdTomato gene expression as Cre-mediated recombination is not reversable in this model. While Turq2 fluorescent cells were regularly adjacent to tdTomato, cells producing both fluorescent proteins were infrequent. When found, tdTomato fluorescence was relatively weak suggesting low levels of expression, but this is consistent with our understanding of VZV infection of rat cells. This is most readily observed at the center of the 1-dpi images but will require a quantification study to determine the frequency of dual fluorescent cells. As these were plated from dissociated skin cells, there is likely an abundance of different cell types represented in the monolayer. This may indicate differences in susceptibility of rat cell types to VZV. As infections were initiated with cell associated virus, this analysis does not rule out the possibility Cre protein produced within the infected TRPE cells was taken up by rat cells and led to tdTomato fluorescence. Dual fluorescent cells are a better indication of VZV gene expression within the rat cells.

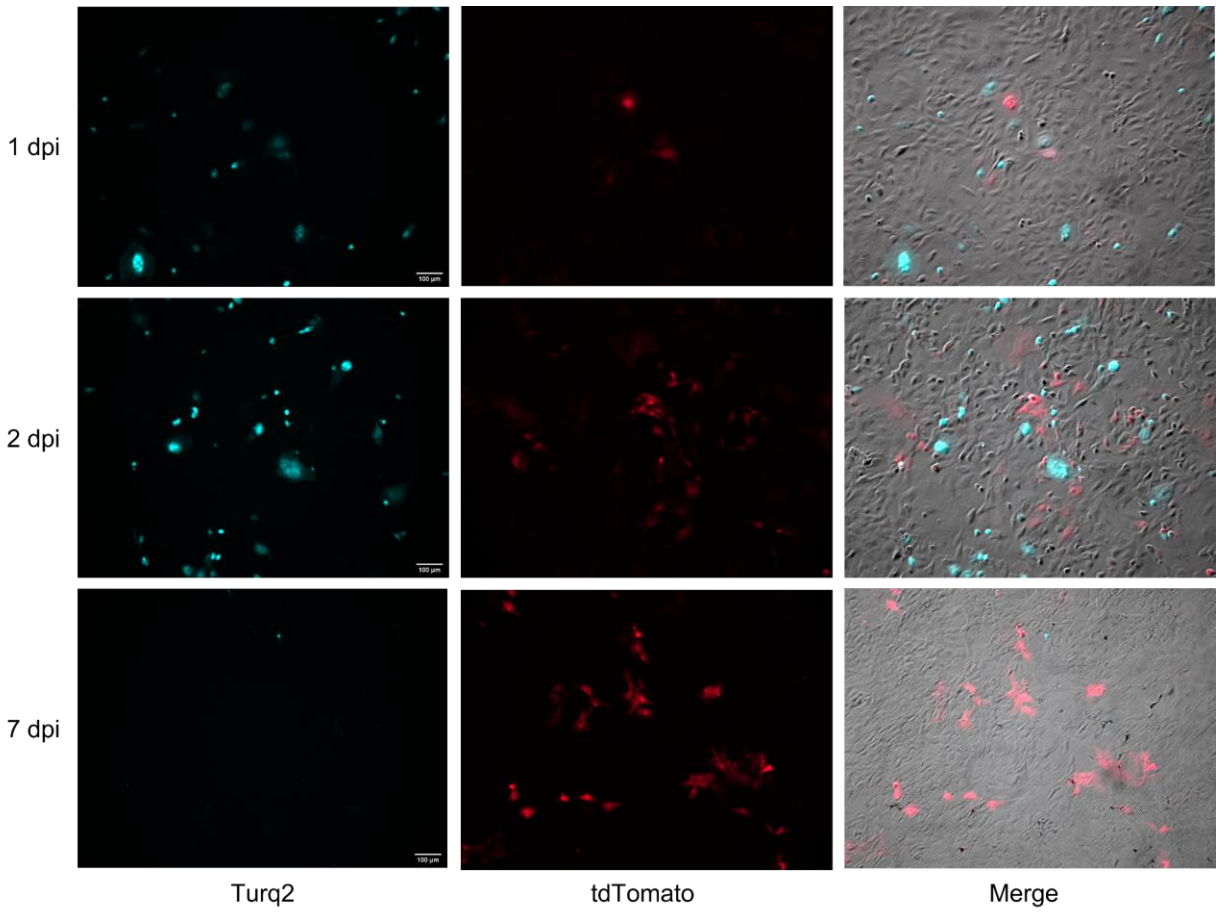

Figure 21: VZV aT2C infection of transgenic rat primary skin cultures induces tdTomato fluorescence.

Skin cells dissociated from reporter rat ears were cultured and infected at low multiplicity (1:1000) with VZV aT2C and fixed at 1-, 2-, or 7-dpi. Turquoise2 (Turq2) fluoresence is shown in the left column, tdTomato fluoresence in the center column, and a merge of the panels with the phase channel on the right. Images were acquired with a 10X (NA 0.3) air objective and are representative of at least ten images per infection sample. Scale bar = 100 µM.

We next sought to determine if our embedding and cryosection procedure could influence Turq2 and tdTomato fluorescence, and for optimization prior to *in vivo* infection analyses. Primary rat monolayers were infected for 48-h with VZV aT2C, pOka, or uninfected TRPE cells. Samples were then pelleted, fixed, OCT embedded, and cryosectioned. Observation showed that tdTomato fluorescence was a direct result of VZV aT2C and could not be influenced by wild type pOka or

associated TRPE cells (**Fig 22**). Cryosectioning did not inadvertently activate tdTomato expression but showed some increase in background fluorescence of the cell sections. This background did not surpass actual Turq2 or tdTomato fluorescence and suggested additional antibody detection of the reporter proteins should not be necessary after *in vivo* infection samples were harvested and cryosectioned. Also note that in many of the rat cells infected by VZV, the production of the tdTomato is readily visible, but the expression of Turq2 is not. This suggests that there is minimal VZV gene expression in rat cells, but it is sufficient to induce the recombination of the tdTomato gene and enable its expression.

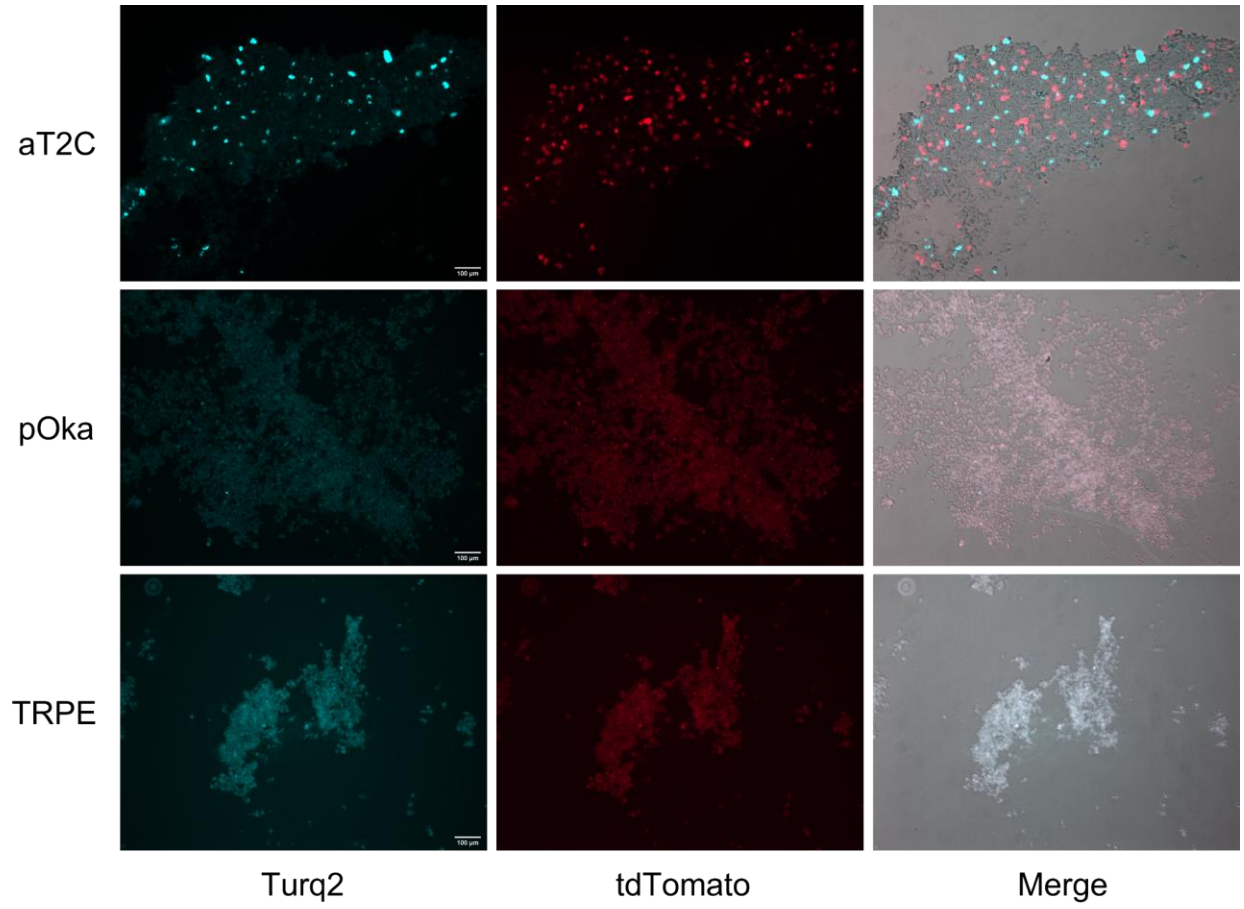

Figure 22: Cryosectioned cell pellets from VZV infected rat primary cultures show Cre is necessary to initate tdTomato production.

VZV aT2C (top), pOka (middle), or uninfected TRPE cells (bottom) were used to inoculate reporter rat primary skin cells for 48-h. Samples were then pelleted, crysectioned, and imaged with a 10X (NA 0.3) air objective. Scale bar = 100 µM.

6.2.3 Analysis of skin and innervating ganglia of transgenic rats inoculated with VZV aT2C at the foot- and whisker pad

We next sought to determine if VZV aT2C was able to initiate tdTomato production after foot- or whisker pad inoculation in the transgenic rat. Rats were inoculated with $2x10^5$ PFU VZV

aT2C in the foot- and whisker pad or left uninoculated for negative control tissue. Necropsies were performed at 14- and 28-dpi for skin from the site of inoculation and the innervating ganglion. Tissues were embedded and cryosectioned identically to the cell pellet experiment. Initially, all tissues were analyzed without additional antibody detection to look for Turq2 produced from the virus or tdTomato produced from the transgenic rat cells. Unfortunately, no Turq2 or tdTomato fluorescence was found in any tissues analyzed from either timepoint or tissue type. We considered that fluorescence may have been lost during tissue processing despite results from the cell pellet experiments, so we probed with a primary antibody to tdTomato with a red fluorescent secondary to amplify the signal and primary antibody to NeuN (Fox-3) with a green fluorescent secondary to identify neurons. Tissue sections were imaged on an inverted confocal microscope. In studies to date, we have located tdTomato fluorescence only in one 28-dpi footpad tissue sample and have not yet found tdTomato co-staining with NeuN in ganglia (**Fig 23**). The fluorescence attributed to tdTomato was obvious (**Fig 23a**) and control samples that received only 2° antibody showed little background fluorescence in the tdTomato channel (**Fig 23b**). NeuN antibody mediated fluorescence staining was less convincing for unclear reasons, and analysis of tissues stained only with 2° antibody showed substantial background florescence. Tissues that received no primary or secondary antibodies showed almost no background fluorescence (**Fig 23b**).

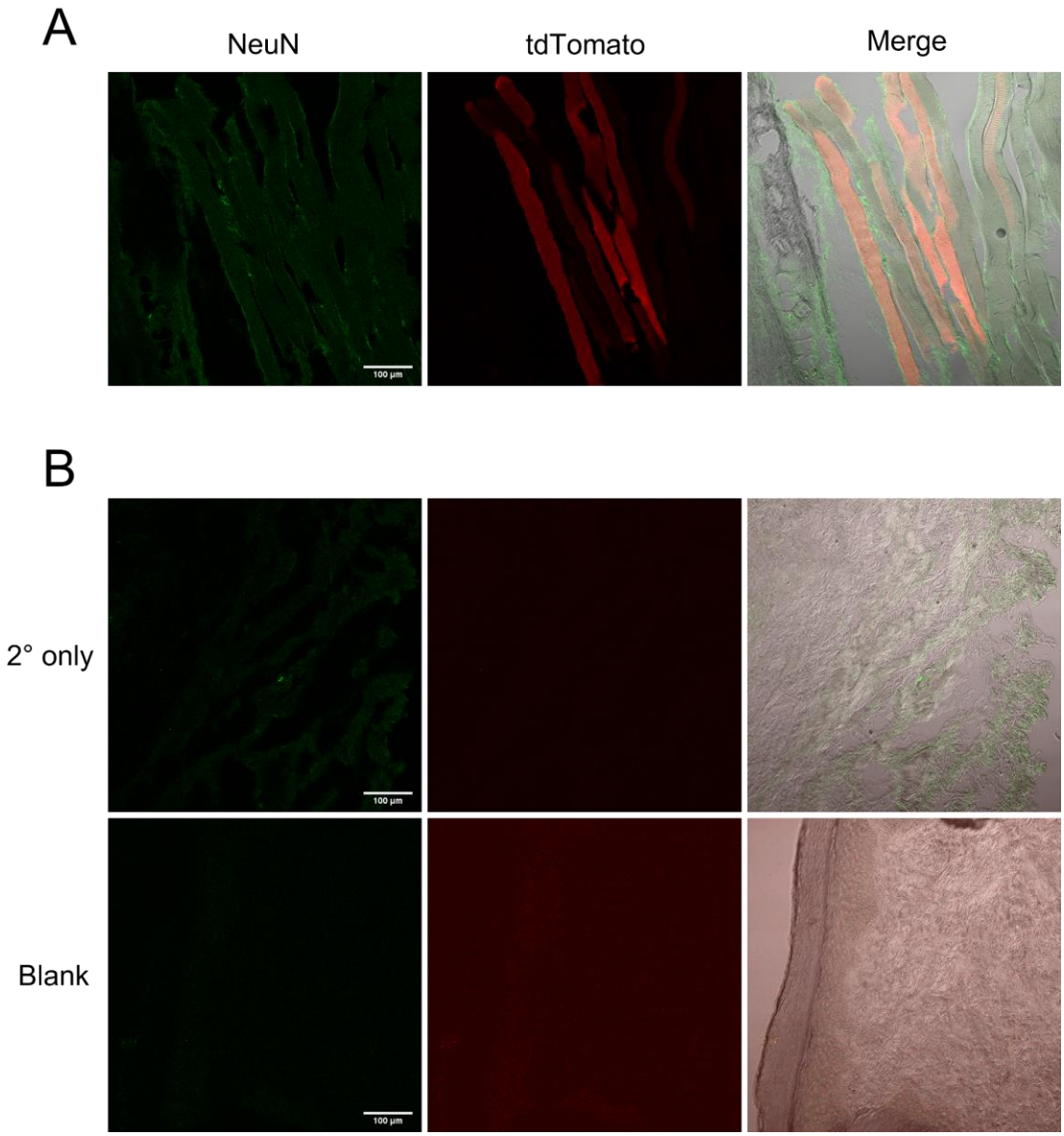

Figure 23: Footpad tissue from a transgenic rat infected with VZV aT2C and analyzed at 28-dpi.

(A) 28-dpi footpad tissues stained with primary antibodies against neuronal marker NeuN (left) and tdTomato (middle). The green and red fluorescent channels were merged with a phase image of the tissue section (right). (B) Tissues were alternatively stained with secondary antibody only (top) or no antibodies (bottom) to reveal possible tissue autofluoresence. Images were acquired at 60X (NA 1.25). Scale bar = 100 µM.

6.3 Discussion

In this continuing work, we developed the principal methods to examine the infection of reporter rats with a VZV capable of inducing reporter gene expression. We first developed a recombinant VZV that expresses the Cre recombinase gene. VZV aT2C derived from the self-excisable VZV BAC produced infectious VZV that reliably produced Turq2 and Cre recombinase from a cassette inserted at the ORF13/14 locus. We then demonstrated that primary rat cells cultured from the skin of the transgenic reporter rat conditionally produced tdTomato after VZV aT2C infection at 1-d and fluorescence increased by 2-dpi. At these timepoints, Turq2 fluorescence was abundant though only limited dual fluorescent cells were observed. After 7-d, Turq2 fluorescence was nearly absent and limited to mostly single infected cells. This suggested the infected human cells that delivered VZV to the primary rat cultures had died over the course of the infection, but the induction of tdTomato fluorescence remained throughout the 7-d experiment as a result of the virus induced expression. The loss of Turq2 suggested that VZV aT2C was not capable of a continued productive infection of the Cre gene in rat cells, which is consistent with past *in vitro* infection analyses [246]. However, it is clearly sufficient to switch on the expression of tdTomato. One caveat of this study is that since VZV can express the Cre gene in any infected cell that supports a CMV IE promoter, it is possible that Cre produced in human cells was secreted and influenced Cre-Lox recombination in the rat cells. This is a complication of cell associated infections detailed earlier and an NLS was added to Cre to ensure nuclear localization, but we have no proven Cre is not secreted from infected TRPE cells. The presence of dual fluorescent cells is a much better indicator of VZV aT2C infection of the rat cells and warrants quantification. *In vitro* infections with cell free VZV aT2C could also provide insight. A potential modification of this

system would be to replace the CMV IE promoter with a rat specific promoter so that Turq2 and Cre can only be expressed in rat cells.

We then showed that the Turq2 and tdTomato fluorescence was not influenced by our tissue embedding and cryosection protocol. The process did generate some background fluorescence, but this was easily discernable from the true fluorescence of Turq2 and tdTomato. Cryosectioning and infection with pOka or uninfected TRPE cells did not elicit any tdTomato production showing that presence of VZV aT2C was required for tdTomato production. We then inoculated rat foot- and whisker pads with VZV aT2C and harvested tissues from the site of inoculation and innervating ganglia at 14- and 28-dpi. Despite the simplicity with which tdTomato was detected after *in vitro* infection studies, we found no indication of Turq2 or tdTomato fluorescence from ganglionic tissues infected *in vivo*. Considering that internal fluorescence was found to be partially lost during tissue processing, we used a primary antibody against tdTomato combined with a red fluorescent secondary antibody. We additionally used a primary antibody against NeuN with a green secondary, a putative neuronal biomarker. We located tdTomato fluorescence only in 28-dpi footpads of one of our inoculated groups. While we expected that VZV infection would be sparse in the innervating ganglion, we expected to find much more fluorescence at the site of inoculation. About 120 tissue sections from all four tissue types (footpad, DRG and whisker pad, TG) have been analyzed so far and tdTomato was located from just three sections of 28-dpi footpad tissues from one rat. The contrast between the *in vitro* and *in vivo* experiments was unexpected. Again, secreted Cre protein from infected human cells may account for the fluorescence in foot pad tissues, but the scarcity of fluorescence indicates this is not likely a major concern. Alternatively, VZV aT2C may have initiated an immunologic response that quickly removed the infecting VZV and associated human cells from the rat.

As tdTomato was rare at the site of inoculation, finding fluorescence in the TG or DRG from this experiment is unlikely. Cre-mediated recombination in DRG and TG are expected to require VZV infection and *de novo* protein synthesis to induce tdTomato. Previous evidence has suggested VZV infection of the rat ganglion is sparse [109,246,257,260]. It may be beneficial to insert the CMV-Turq2-T2A-Cre cassette into an HSV or AAV vector for a positive control to determine if the lack of tdTomato production is a function of the infecting VZV. Stereotactic inoculation of cell-free VZV into the TG has also been previously shown to induce hypersensitivity and could be used here to study infection of the ganglion without waiting a month after inoculation for tissue analysis [238]. Analysis of inoculation site tissues at 1- to 3-dpi could determine if any Turq2 fluorescence can be located and may also give insight into how long the infected human cells remain present after subcutaneous inoculation. One of the greatest benefits of this system is that tdTomato fluorescence should be permanent after Cre-Lox recombination. This could help determine how widespread VZV infection is after subcutaneous inoculation without concern for timing tissue necropsies for maximal detection of VZV. These studies may also reveal rat tissues that are exposed to VZV that have not been previously explored such the spinal cord and brain. The reporter rats may also be used in pain studies as the Long-Evans strain has been characterized for VZV-induced hypersensitivity [237].

7.0 Development of Growth Conditional VZV for Gene Functional Domain Studies and Suppression of Lytic Growth in the Establishment of Latency in Neurons

This chapter contains ongoing work by Benjamin E. Warner, Michael B. Yee, and Paul R. Kinchington in collaboration with Marielle Lebrun and Catherine Sadzot at the University of Liège, Liège, Belgium and Biswajit Das, Punam Bisht, and Ron Goldstein at Bar-Ilan University, Ramat-Gan, Israel. The data presented in section 6.2.1 can be attributed to BEW, MBY, PRKi, ML, and CS. The data in section 6.2.2 can be attributed to BEW, PRKi, BD, PB, and RG.

7.1 Introduction

The highly cell-associated nature of VZV and limited breadth of fully permissive cell lines continues to complicate VZV infection and gene studies. Initiating a cell-associated infection delivers a large number of host and viral antigens to the newly infected cells that may influence the infection outcome. For instance, infections with VZV mutants that are deleted for an essential gene that have been generated using classical cell complementation also delivers associated cell contents with the capability of producing the wild-type protein of interest. The use of cell-free VZV is desirable but is hindered by difficulties in its generation, and a considerable loss of infectivity when infected cells are lysed [280]. This substantially reduces the utility of cell-free preparations when studies with high infectious titers are required as has been the case for rat models of PHN. The DHFR degron system provides a simplified method for studying essential gene mutations in virtually any VZV permissive cell line [108,109,289]. Here, we used VZV

ORF9cDHFR (**Fig 10**) as a strategy to investigate the genetic requirements of the essential ORF9 tegument protein in VZV growth. This is done by placing otherwise detrimental ORF9 mutants at a second locus within the ORF9cDHFR virus. Infectious VZV may be prepared under TMP stabilizing conditions to provide functional ORF9cDHFRp, and later withdrawn to study the effects of the ectopic ORF9 mutant. Such experiments have demonstrated the C-terminal residues of ORF9p are important for VZV growth.

Secondly, we evaluated the DHFR degron system as a method to prevent sporadic lytic infections that occur when establishing experimental latency with wild-type VZV in hESC-derived neuron cultures. Current methods for establishing VZV latency in hESC-derived neurons require the use of ACV or low-MOI infection of axon termini in microfluidic chambers to prevent most lytic infections [85,128]. Infections in the presence of ACV inhibits VZV DNA replication thus preventing a fully productive infection. However, the activation of ACV by thymidine kinase results in the molecule being incorporated into genomes where it acts as a DNA chain terminator [226]. This leads to an abundance of VZV genomes that are damaged and likely unable to reactivate, thus reducing the efficiency of the system. Low-MOI infections reduces the likelihood of VZV entering lytic replication upon reaching neuronal nuclei by minimizing the presence of VZV lytic transactivators and processes that overcome host DNA silencing mechanisms. However, achieving latency by these methods is not absolute, and lytic replication may initiate spontaneously or when acyclovir is withdrawn [128]. Here, we show that infection of hESC-derived neurons with VZV ORF4nDHFR in the absence of TMP strongly favors a quiescent infection. Addition of TMP alone is not sufficient to simulate reactivation suggesting the virus is not undergoing an abortive infection. Instead, a reactivation stimulus is required in addition to TMP to initiate lytic replication which implies experimental latency has been achieved.

7.2 Results

7.2.1 Development and characterization of recombinant VZV ORF9cDHFR with a second ectopic ORF9 copy downstream at the ORF56/57 locus

To determine if the DHFR degron system was amenable for use in gene function studies, we first developed a method of inserting a second copy of ORF9 within VZV ORF9cDHFR. The wild-type ORF9 promoter, ORF9 gene, and poly(A) tail were amplified from the VZV genome. ORF9 was fused in-frame with a C-terminal V5-tag as a method to detect this protein independently from ORF9cDHFRp, which has previously been shown to work in ORF9 studies [59,309]. A Zeo^r cassette was added downstream of the expression cassette for selection during BAC recombineering (**Fig 24a**). Several mutants were then constructed that included stepwise deletions from the carboxy-terminus and amino-terminus, or deletions from both termini (**Fig 24b**). These were generated by further modification of the wild-type ORF9 fragment that was recombined into the ORF56/57 locus. Mutant generation was guided by important features have been previously identified in ORF9p, including a nuclear localization signal (NLS) from amino acids (aa) 16-32 [290], an ORF47 kinase binding and phosphorylation consensus sequence from aa 84-87 [59,310], an acidic cluster from aa 85-93 [309], a nuclear export signal (NES) from aa 103-117 [290], an IE62 interaction region from aa 117-186 [311], a highly conserved region of homology to HSV-1 VP22 from aa 141-236 [311], and finally a predicted second NLS from aa 272-275 [290]. The exact function of these features requires further assessment as has been completed for the ORF9/ORF47 phosphorylation interaction and overlapping acidic cluster by Riva *et. al.* [59,309].

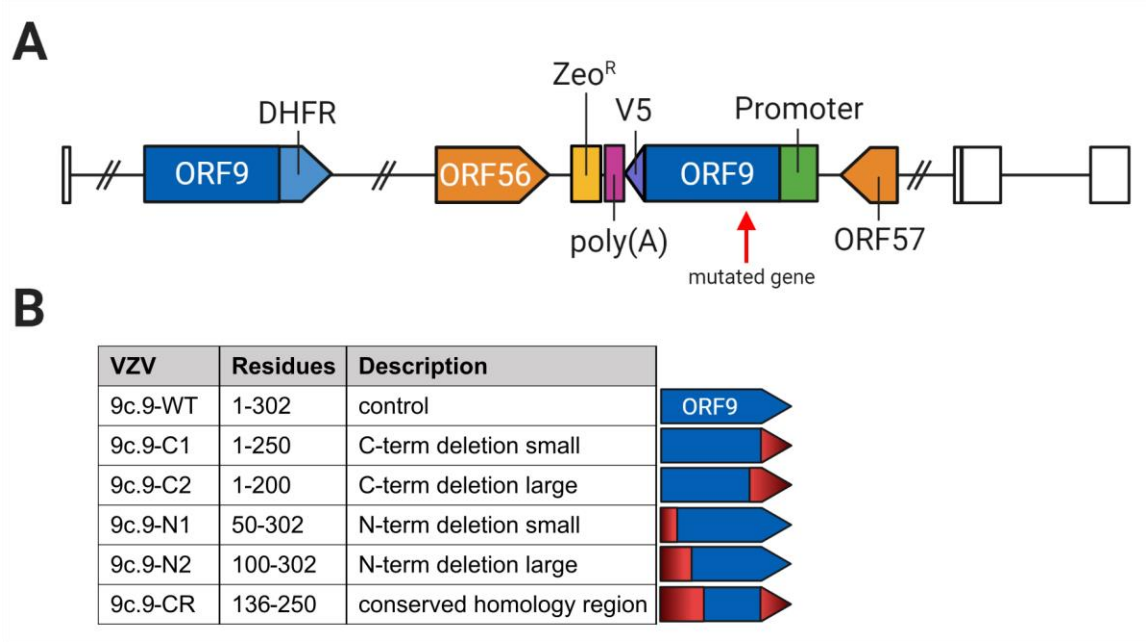

VZV	Residues	Description
9c.9-WT	1-302	control
9c.9-C1	1-250	C-term deletion small
9c.9-C2	1-200	C-term deletion large
9c.9-N1	50-302	N-term deletion small
9c.9-N2	100-302	N-term deletion large
9c.9-CR	136-250	conserved homology region

Figure 24: Ectopic insertion of ORF9 gene mutants in VZV ORF9cDHFR.

(A) A PCR generated fragment containing the ORF9 promoter, an ORF9 gene with an in-frame C-terminal V5-tag, a poly(A) sequence, and a zeocin resistance cassette (Zeo^R) was inserted at the ORF56/57 locus in VZV ORF9cDHFR by BAC recombineering. (B) Further modification of the wild-type ORF9 (9c.9-WT) inserted at the 56/57 locus include, a small 52 residue (9c.9-C1) or large 102 residue (9c.9-C2) carboxy-terminal deletion, a small 49 residue (9c.9-N1) or large 99 residue (9c.9-N2) amino-terminal deletion, and one mutant with deletions at both termini so the ORF contained only the conserved homolgy region (9c.9-CR). The "residues" column lists the amino acids that will be translated according to the specific mutations. Created with BioRender.com.

We then prepared whole cell lysates from MeWo cells infected with each ectopic mutant virus in the presence and absence of 100 nM TMP. We probed the same blot for ORF9cDHFRp with a rabbit antibody to ORF9 and the second copy of ORF9-V5p with a mouse antibody to V5 (**Fig 25**). In the presence of TMP, ORF9cDHFRp could be readily detected by an ORF9 antibody at the expected size of about 55 kDa for all but the C2 (1-250) mutant. This was consistent with our previous protein analysis (**Fig 10**) in which we observed multiple bands and a slightly leaky

phenotype for ORF9cDHFRp in the absence of TMP. The multi-banding pattern of ORF9 is expected due to multiple phosphorylation states of ORF9p, though the intensity of the lower bands indicated a much lower concentration compared to Fig 10. Lower molecular weight bands in the C2 and N1 lanes corresponding to the protein from the ectopic ORF9-V5 gene are observable at very low concentrations and do not appear to be affected by TMP presence. The lack of bands in the other lanes might suggest the ORF9 antibody is not capable of binding the mutant protein or the protein concentrations are below the level of detection.

Probing with an antibody against the V5-tag revealed imperfect results and the image contrast has been raised considerably so bands were visible. Proteins bands were inconsistent and appeared to be very low in concentration. 9c.9-WT did not show identical sized bands under both TMP conditions which was unexpected because production of the ectopic mutant should not be influenced by TMP. 9c.9-CR did not show a clear band under either TMP condition which may indicate the combined N- and C-terminal deletions generated an unstable protein that was rapidly turned over. Protein bands corresponding to mutants 9c.9-C2, -C1, and -N1 were visible and matched the approximate protein sizes according to the deleted residues and addition of the V5-tag (see Fig 25 caption) but were rather low in concentration making the results difficult to discern. The 9c.9-N2 mutant showed bands slightly larger and smaller than the expected size and the discrepancy is unclear. Bands in the 9c.9-C1 mutant were unexpected because there was no ORF9cDHFRp detected top blot to indicate the virus replicating and produce sufficient protein concentrations for detection. 9c.9-N1 was the only mutant to show the multiple bands that is expected of ORF9. The ORF47 phosphorylation site remains intact in this mutant from aa 84-87 and multiple bands were shown. 9c.9-C1 and -C2 were expected to show multiple bands as they

also include these amino acids, but it is possible these bands are below the concentrations required for detection.

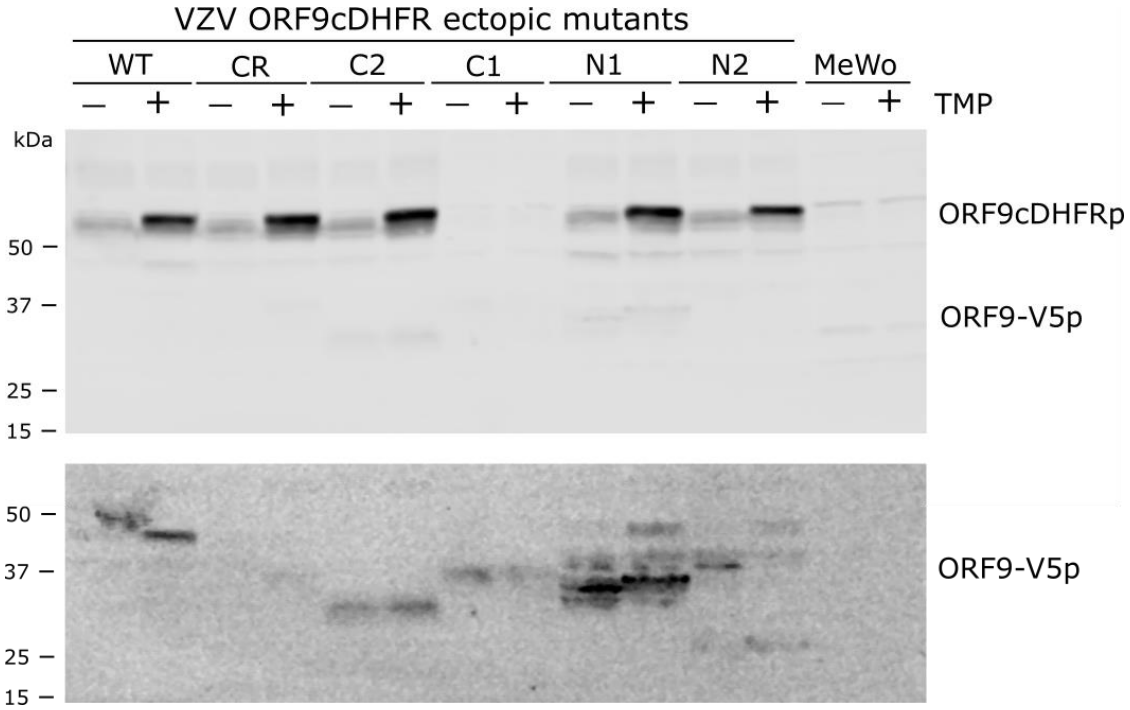

Figure 25: Protein analysis of ORF9 genetic mutants expressed from ORF56/57 locus.

Whole cell lysates were probed with an ORF9 antibody (top) or V5 antibody (bottom) after a 1000 PFU VZV infections for 72-h in MeWo cells in the presence (+) and absence (-) of 100 nM TMP. The mutants are descibed in Fig 20b and uninfected MeWo cell lysates were prepared as an uninfected cell control. Both top and bottom panels were acquired from the same blot on a linear scale. The contrast of the bottom panel was increased to better display the low concentration protein bands from the ectopic ORF9-V5 mutated genes. Estimated mutant protein sizes are 9c.9-WT (40 kDa), -CR (19 kDa), -C2 (29 kDa), -C1 (35 kDa), -N1 (35 kDa), and -N2 (30 kDa).

We next determined the growth capacity of each mutant in the presence and absence of TMP. The parent virus in these growth curves was derived from the VZV BAC containing a GFP fusion to ORF23 (VZV GFP-ORF23) [85]. Growth of VZV ORF9cDHFR was shown previously

and reached approximately $5x10^4$ plaques over the 4-d infection with TMP (**Fig 7a**) which is consistent with parent VZV GFP-ORF23 here with or without TMP (**Fig 26**). The 9c.9-WT virus showed a 2x reduction in growth compared to the parent virus under both TMP conditions (**Fig 26a**). C-terminal deletion mutants 9c.9-C1 and -C2 showed similar growth capacities under 100 nM TMP conditions and reached plaque counts nearly equivalent to the parent virus, though this might have been an artifact of the 0-d infecting virus concentrations (**Fig 26b/c**). Although each virus was titered and thought to be initiated at 100 pfu/well (diluted from enumerated stock concentrations of C1 - 2400 pfu/µl and C2 – 1500 pfu/µl), the actual starting concentrations of the C1 and C2 virus appeared to be about 10x higher. Despite this, the growth kinetics thereafter appear to fall in with the expected growth kinetics and may indicate a titration error in the 0-d samples alone. In the absence of TMP, both 9c.9-C1 and -C2 showed 2x reduced growth by 4-d. The N-terminal mutants 9c.9-N1 and -N2 showed fewer plaques under both TMP conditions by 4-d, corresponding to a 2x reduction with TMP and 4x reduction without TMP (**Fig 26d/e**). Finally, the 9c.9-CR mutant grew similar to the parent when TMP was present and showed 3x reduced growth in the absence of TMP (**Fig 26f**). Post-hoc analysis suggested none of the reductions in growth were significant when compared to the parent with or without TMP.

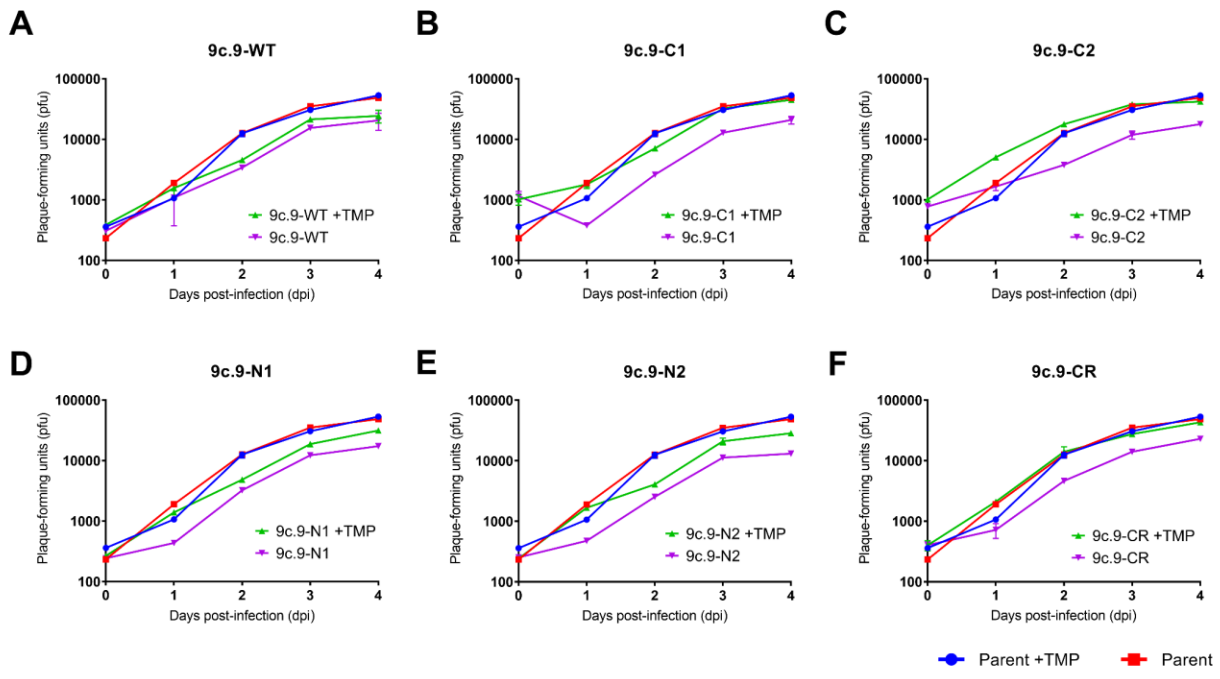

Figure 26: Growth analysis of ORF9 ectopic mutants derived from VZV ORF9cDHFR.

Conditional growth analysis of ORF9 ectopic mutants from Fig 20b or parent virus (VZV GFP-ORF23) after initating low multiplicity infections in the presence and absence of 100 nM TMP. Growth over a 4-d period shows VZV ORF9cDHFR with ectopically inserted (A) WT ORF9, (B) C1 small or (C) C2 large C-terminal deletion from ORF9, (D) N1 small or (E) N2 large N-terminal from ORF9, and (F) C- and N-terminal deletions (CR) leaving only the conserved homology region of ORF9. Infections by the mutants in the presence of TMP (green) are compared to infections without TMP (purple), and also compared to parent with (blue) or without (red) TMP. Mutants are described in Fig 20b.

7.2.2 Establishing latent VZV infection in hESC-neurons without acyclovir

The essential function of ORF4p in VZV replication has been documented [286,292]. Our studies showed VZV ORF4nDHFR was effective at inhibiting VZV growth in the absence of TMP, showing little to no spread of infectious virus (**Fig 7b/d and 11**). We considered this virus might be used to initiate a quiescent infection for the study of VZV latency and reactivation as an

alternative to past methods that used ACV to inhibit sporadic lytic infections. ARPE cells infected with cell-free VZV ORF4nDHFR were first examined to differentiate infection in the presence and absence of TMP over a 7-d infection (**Fig 27**). In VZV ORF4nDHFR, GFP is fused to the protein from ORF23 which encodes the minor capsid protein and therefore should not reach high concentrations until later infection times. The presence of GFP fluorescence therefore indicates the virus is undergoing lytic replication. Without TMP, no GFP fluorescence was detectable after a 7-d infection in ARPE cells (**Fig 27a**). In contrast, cell cultures that were infected with 100nM TMP produced large infectious centers with indications of syncytia that form after extensive lytic infection (**Fig 27b**). Additionally, a 10-d infection was initiated in the absence of TMP, then 100nM TMP was added to the media. Adding TMP resulted in the expression of GFP fluorescence by 2-d, indicating that lytic replication had resumed (**Fig 27c**). This suggests that in the absence of TMP, the genome persists but is not silenced as heterochromatin in ARPE cells. We suggest this means VZV DNA remained present in host nuclei, but only initiated abortive infections that never underwent a complete replication cycle due to the absence of ORF4nDHFRp. Once TMP was added to the medium, the stabilization of ORF4nDHFRp allowed VZV replication to resume unabated.

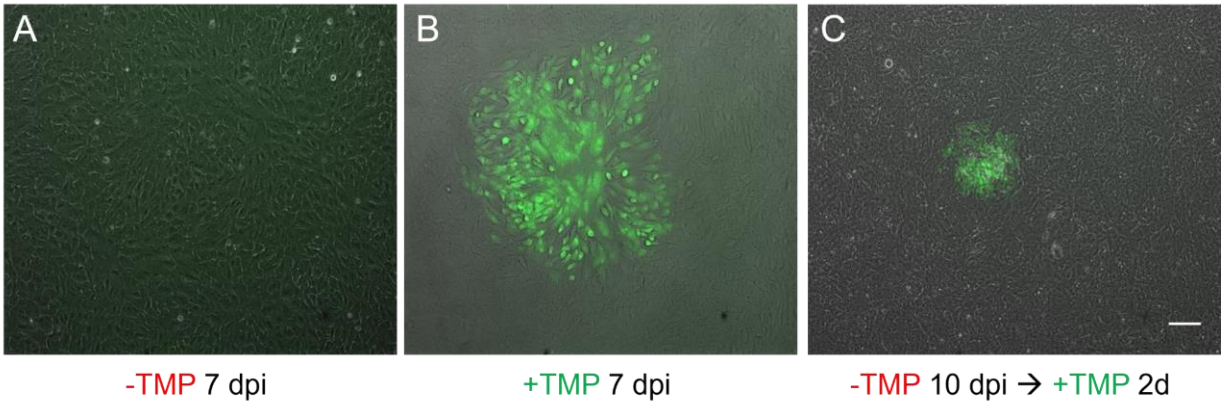

Figure 27: Cell-free VZV ORF4nDHFR establishes a quiescent infection in skin cells without TMP.

ARPE-19 cells are infected with 500 PFU cell-free VZV ORF4nDHFR for 7-days (A) without TMP, (B) with 100 nM TMP, or (C) without TMP for 10-days followed by addition of TMP to growth media for 2-days that initates a lytic infection as shown by increase in fluorescent GFP fused VZV ORF23 protein. Images acquired with a 10X (NA 0.3) air objective. Scale bar = 100 µM.

We next sought to determine if VZV ORF4nDHFR could initiate lytic and quiescent infections in hESC-derived neurons depending on the provision of TMP. hESC-derived neuospheres were first plated for 21-d so the neuospheres could adhere, differentiate into terminal neuron cultures, and develop axonal and dendritic projections. Low multiplicity cell-free infections were then initiated on the hESC-derived neurons (**Fig 28**). By 5-dpi in the presence of 100 nM TMP, GFP fluoresence was observable in many large and small neurons and indicated possible trafficking of virus between neuron clusters by neurite connections and an expansion of virus growth (**Fig 28a**). Fluoresence remained observable at 8-d (**Fig 28b**) and continued to expand, eventually resulting in morphological changes suggestive of cytopathic effects in the infected neurons by 10-d (**Fig 28c**), similar to that reported in our previous studies [85]. In contrast, all cultures infected with cell free VZV ORF4nDHFR in the absence of TMP resulted in no fluoresence over the entire 10-d infection in both large neuron clusters (**Fig 28d/e**) and in the

network of projecting axons (**Fig 28f**). This suggested that VZV ORF4nDHFR did not replicate under nonpermissive conditions.

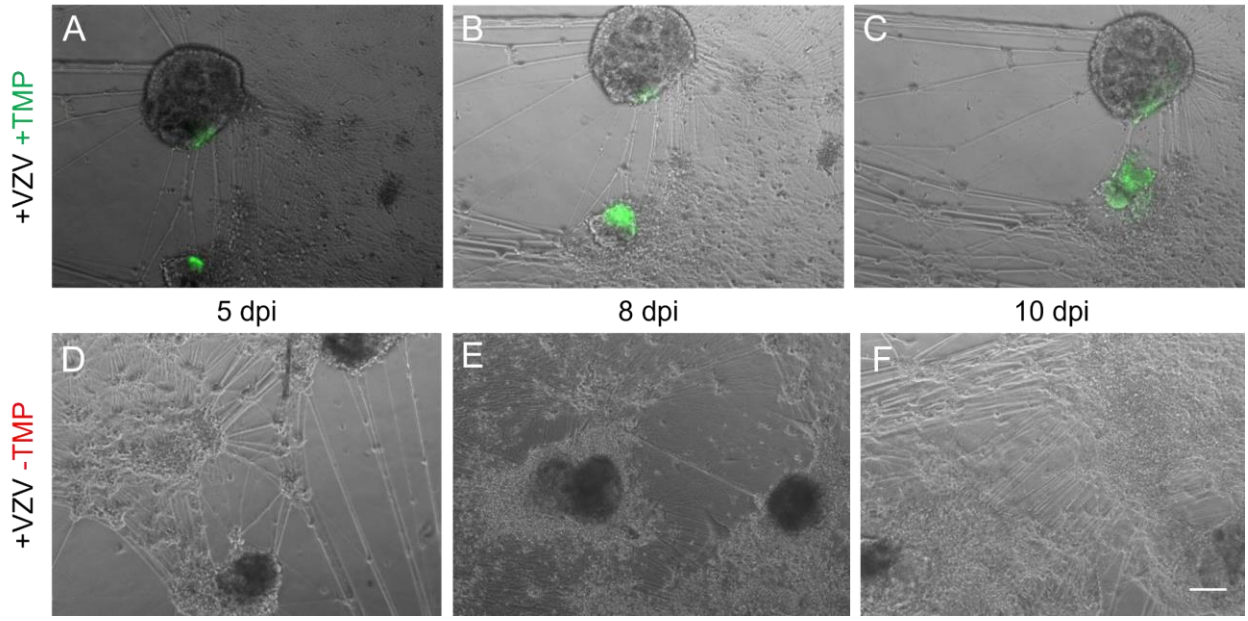

Figure 28: Cell-free VZV ORF4nDHFR initiates a quiescent infection in hESC-derived neurons without TMP.

Cultures hESC-derived neurons were infected with cell-free VZV ORF4nDHFR with 100 nM TMP (A-C) or without TMP (D-F) and were live imaged at 5-, 8-, or 10-dpi. VZV infection is demostrated by GFP fluoresence from a fusion to the capsid protein from ORF23. Panels A-C represent the same culture imaged at different times and D-F are different regions to the same culture to show a lack of GFP. Images acquired with a 10X (NA 0.3) air objective. Scale bar = 100 µM.

A lack of GFP expression did not confirm that experimental latency had been established. In the case of the ARPE cell infections (**Fig 28c**), the reversal of halted lytic replication by TMP addition to the media resulted in renewed growth and GFP expression. This suggested that the virus was undergoing a continuous abortive infection in ARPE cells resulting from destabilized ORF4nDHFRp without a complete silencing as heterochromatin. To determine if hESC-derived

neurons were undergoing a similar abortive infection or had established experimental latency in neurons, neurons were again plated 21-d to allow differentiation and infections were initiated with 1000 PFU of cell-free VZV ORF4nDHFR in the absence of TMP. After a 15-d infection without TMP, the neuron cultures were treated in two ways. One group received new neuron basal growth media containing 100 nM TMP, which was then visualized for GFP fluorescence at 2-d (**Fig 29a**) and 5-d (**Fig 29b**). None of these cultures developed visible fluorescence, suggesting the virus unable to initiate a lytic infection as was the case in ARPE cells. The other treatment group received media containing 100nM TMP and 20mM sodium butyrate (NaB). NaB is a type-1 histone deacetylase inhibitor that acts to counter the formation of repressive heterochromatin and has been shown to reactivate latent VZV DNA and initiate a lytic replication [128]. When TMP and NaB were applied to infected neuron cultures together, observation at 2-d (**Fig 29b**) and 5-d (**Fig 29d**) resulted in several positions in 9 of 12 cultures that developed GFP fluorescence as early as 2-d, suggesting that lytic VZV replication was initiated. By 5-d, the infection had spread within the neuron sphere to indicates productive replication was underway and capable of undergoing cell-cell spread.

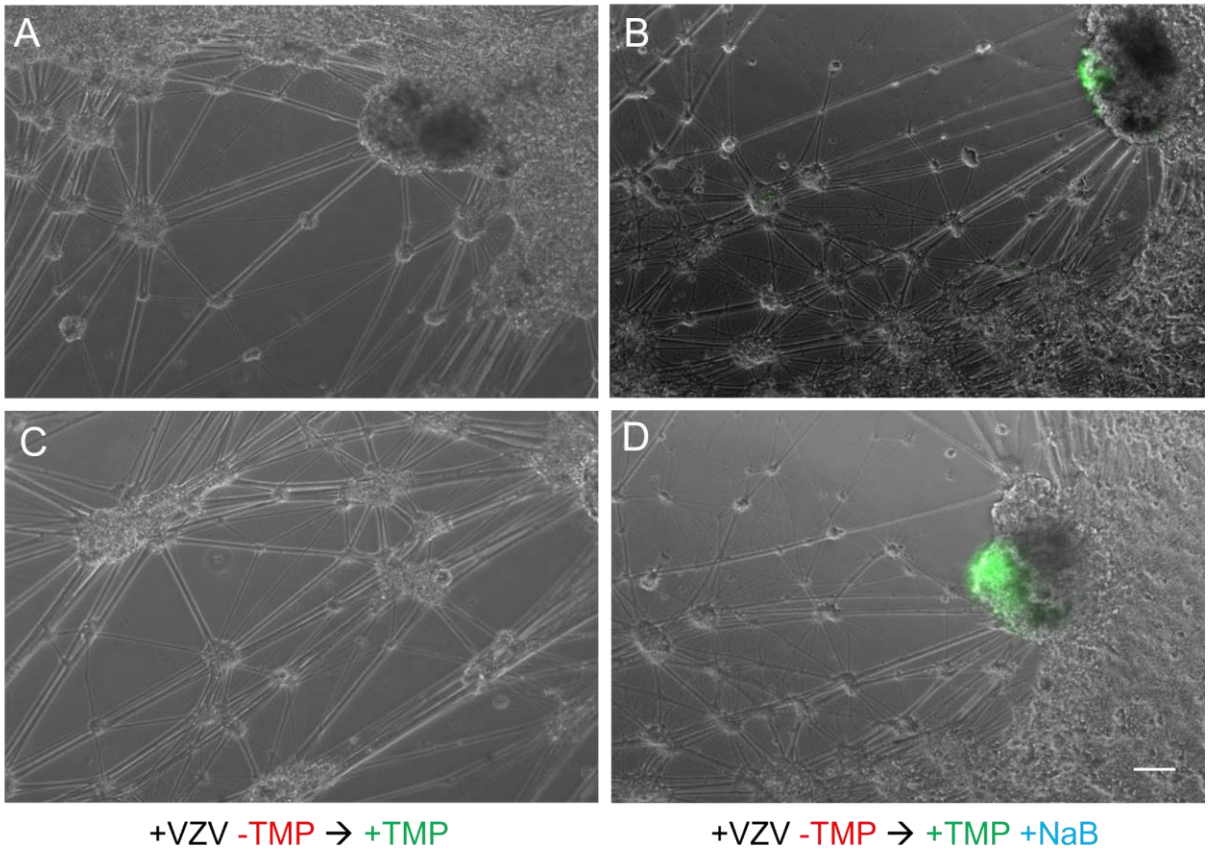

Figure 29: VZV ORF4nDHFR reactivation on neurons requires TMP and NaB.

hESC-derived neurospheres were seeded in 24-well plates for 21-d before infection with 1000 PFU cell-free VZV ORF4nDHFR for 15-d without TMP. To 12-wells, 100 nM TMP was added to growth media and observed at (A) 2-d and (C) 5-d and displayed no GFP fluoresence to indicate VZV lytic growth. To the other 12-wells, 100 nM TMP and 20 mM sobium butyrate (NaB) was added and observed at (B) 2-d and (D) 5-d and showed GFP fluoresence in 9 of 12 wells that indicated lytic replication was initated and spreading.

7.3 Discussion

The study of VZV essential gene function and the mechanisms governing latency and reactivation are traditionally difficult to study for VZV. Application of the growth conditional

viruses generated by the DHFR degron system may help simplify such studies. To determine if gene function analyses with this system were feasible, we developed several ORF9 recombinant mutants in the VZV ORF9cDHFR background. Overall, the approach showed some success, although the slight leakiness of VZV ORF9cDHFR and poor detection of the ectopic ORF9 mutant proteins complicated interpretation of the results. Detection of the ectopic gene products with a V5 antibody was not immediately clear and requires optimization, though most the bands that were visible fell within the expected protein sizes. This suggested some production of the ectopic proteins occurred. It is unclear if issues that contributed to reduced protein concentrations occurred at the level of transcription or translation. Growth of 9c.9-WT under both TMP conditions was considerably reduced compared to the control, suggesting ORF9 expression from two loci may be having an inhibitory effect on virus replication. The N-terminal mutants 9c.9-N1 and -N2 also showed reduced growth even in the presence of TMP which suggests that the ectopic mutants interfered with virus growth, possibly by a dominant negative effect. Their growth defects in the absence of TMP were therefore less clear compared to the C-terminal mutants. The putative NLS is within the first 50 residues and its removal might initiate excessive accumulation of mutated protein in the cytoplasm that interfered with cytoplasmic processes. The 9c.9-CR mutant, which is missing similar residues at both N- and C-termini, did not show the most severe growth reduction as expected and may indicate that the severely truncated protein was inactive.

While experiments may be designed where both ORF9 proteins functionally compete, for the purpose of investigating ORF9 mutants in the context of infection, modifying the system for conditional expression of the ectopic mutants could be beneficial. A tetracycline on system where the mutant gene is conditionally expressed could prevent co-expression of the DHFR modified ORF9 with the downstream mutant. Alternatively, other degron systems have been described that

rely on ligand-induced destabilization [312] rather than the induced stabilization method of the DHFR system. Theoretically, these systems may be combined to swap protein stabilization allowing only one protein to be active at a time. This, however, would not overcome the leakiness of ORF9cDHFRp without TMP which is a critical step for such experiments. While the studies here were not as successful as we had hoped, they give context to using the DHFR system for the study of gene functional domains and identify important considerations for modifying this system.

VZV ORF4nDHFR infection of hESC-derived neurons represents the first time DHFR degron VZV have been used to study latency and reactivation. VZV ORF4nDHFR is considerably more tightly regulated by TMP than VZV ORF9cDHFR and ORF63cDHFR and provides a novel method for preventing sporadic lytic infections when establishing model latency. Upon infection with this virus, non-lytic infections are default in non-neuronal cells which traditionally undergo lytic replication in both cell culture and SCID-hu mouse studies [17,40,122,313]. Lytic replication can be conditionally initiated by TMP that is capable of cell-cell spread and morphological changes associated with advanced VZV infections. Quiescent and lytic infections were also demonstrated in neuron cultures, but one major difference between the cell types was apparent; infection of non-neuronal cells was abortive whereas neuron infections suggested experimental latency had been established. This was demonstrated by addition of TMP alone or in combination with a putative reactivation stimulus.

While these experiments can conclude the ability of VZV ORF4nDHFR to establish experimental latency, we acknowledge that quantitative assessment is lacking in these studies. Transcriptome profiling of infected skin cells and neurons under both TMP conditions may provide more conclusive evidence of the level of viral gene expression in non-neuronal and neuronal cells. If our suspicion is correct, we may find that in the absence of TMP, the non-neuronal cells would

still express some lytic immediate-early and early transcripts and possibly proteins, while the latent state would rather express the VLT RNAs. It would be beneficial to determine if latency is virus-dose dependent, as appears to be the case for establishing latency by axonal tip infections in microfluidic chambers [128]. Reactivation efficiency should also be compared between VZV ORF4nDHFR and classic methods of experimental latency/reactivation, and gene expression may be compared between these methods before and after experimental reactivation.

8.0 Summary and Future Perspectives

We have presented a novel method for generating recombinant VZV with essential gene mutations. The DHFR degron system simplifies mutant virus derivation over traditional complementation methods. The relatively few cell lines that support robust VZV replication severely limits options for generating complementing cell lines and only a few mutants by this method have been described [30,101,107]. The degron system allows mutant generation in any cell line that supports VZV growth. The highly cell-associated nature of VZV has also restricted use of complementing cells for many applications in which the complementing cell might interfere. Conditional degradation of individual proteins provides more acute control over presence and function of the target protein. Using a self-excisable VZV BAC [101], DHFR degron mutants were described for essential immediate-early regulatory proteins IE4 and IE63, and late tegument protein ORF9p. However, the DHFR degron system is not without caveats. Attempts to target other essential proteins involved in transcriptional activation and DNA replication generated VZV that were not replication-conditional or not viable, which indicated that the DHFR degron system is gene dependent. Although, we reported that IE62 was not replication conditional when the DHFR was fused to either terminus, slight modifications to virus development have been made and we now appear to have a working VZV ORF62nDHFR that is undergoing characterization (Kinchington, unpublished data). VZV ORF9cDHFR and ORF63cDHFR exhibited slightly leaky phenotypes where the protein was detectable by antibody probed even in the absence of TMP. This may result from poor access of ubiquitin ligases to the protein or sequestration of the protein away from the proteasome. Nevertheless, the DHFR degron system is a promising method for mutant VZV generation but is only one of several degrons currently available [312]. Other systems utilize

ligand-induced degradation or auxin-inducible degrons which may provide and alternative approach for genes that did not work with DHFR. The ligand-induced degron developed by the Wandless group works much the same as DHFR, but instead relies on providing the Shield-1 ligand, which generates a confirmational change in the degron that reveals key residues necessary for proteasomal degradation [314]. This degron is only 19 aa and therefore much smaller than the 160 aa of DHFR but has been shown to only work efficiently at C-termini. Auxin-inducible systems were derived from plants and requires the introduction of a component of the plant E3 ubiquitin ligase complex, F-box transport inhibitor response protein 1 (TIR1), to be functional in eukaryotes [315]. Given our ability to extensively modify the VZV genome in BACs, we may be able to generate VZV that contain all the necessary components to make this system functional in the rat. Versions of these degrons range from about 65-130 aa and proteins appear to be depleted about 1-h after providing auxin [315]. Currently, however, the DHFR system remains the best characterized for use in mammalian cells and rat models.

We then exploited the three growth conditional VZV in rat models of postherpetic neuralgia. Foot- and whisker pad inoculation with VZV ORF9cDHFR indicated that productive replication was not required for induction of pain behaviors. However, gene expression events during early infection played a critical role in generating hypersensitivity as shown by the VZV ORF4nDHFR animal experiments. These findings were reproduced in an additional footpad experiment that used alternative assembly deficient mutant VZV Δ54S [30] and early transcriptional mutant VZV ORF63cDHFR. Future experiments might determine if DNA replication is essential for the induction of pain behaviors. Based on past evidence, we hypothesized DNA replication is dispensable for pain induction as VZV DNA replication did not occur in several rat tissues [246] and ACV does not affect the pain outcome in VZV-inoculated

rats [235]. We inserted degron sequences on several essential genes involved in DNA replication but have not yet derived a working virus. Two genes we have not yet explored are the DNA polymerase subunit from ORF28 and processivity factor from ORF16. If our hypothesis that DNA replication is dispensable for hypersensitivity is correct, it would narrow the window of VZV infection processes required for pain induction to those preceding DNA replication. This would also substantially reduce the protein candidates for direct involvement in establishing a pain phenotype. The experiments here only established that IE4 and IE63 are involved in pain processes but did not establish a direct role for either protein. Direct involvement could be addressed by insertion of these genes into an HSV or AAV vector that allows for protein activity outside the context of VZV infection. HSV vectors have been previously exploited by our lab for delivery of human proenkephalin in the rat footpad model [245]. It is important to note that while we continue to limit VZV by blocking critical stages in the life cycle, we cannot rule out that proteins produced at later infection times do not contribute to or enhance pain mechanisms during clinical reactivation. Another question we have not yet addressed in the rat model is: how does VZV activity at the periphery affect pain outcomes? Stereotactic inoculation of VZV into the TG and subsequent assessment of pain at the whisker pad has concluded that events in the ganglion are involved in establishing pain behaviors [238]. Could VZV that are unable to traffic to ganglia still develop a limited pain phenotype? Developing a such virus that replicates efficiently might prove difficult, though herpesvirus axonal trafficking is starting to be understood through PRV experiments that have identified components involved in retrograde transport [50,316,317]. A much easier solution may be to purify proteins that have been identified as essential to the pain outcome, such as IE4 and IE63, and inject them into the foot- or whisker pad and assess pain behavior development. Alternatively, AAV vectors that replicate efficiently in skin may deliver

genes of interest. These studies may give context to the contribution of signals originating from the periphery in pain development.

We have been unable to conclusively detect the VZV transcription of ORF4, ORF63, and ORF63 within the ganglia of peripherally inoculated rats. Analysis of host gene expression in the DRG after footpad inoculation clearly indicates marked shift in certain genes associated with pain pathways [246]. It is possible these changes were transduced by signals originating at the periphery, but pain assessment after stereotactic inoculation of the TG provides the most compelling evidence that ganglionic infection events directly contribute to pain behaviors [238]. The lack of VZV detection in innervating ganglia is a major shortcoming for our analyses because we do not have conclusive evidence that the VZV ORF4nDHFR and ORF63cDHFR reach the ganglion in the absence of TMP. As part of the tegument it is possible IE4 and IE63 support capsid motility [37], though neither protein has been assigned any such function. Possibly, transcript purification methods such as SureSelect or single-cell transcriptomics in combination with next generation sequencing can overcome the limitations of the qPCR methods we have described to definitively locate these genes in the rat ganglion. The newly available transgenic reporter rat that expresses a tdTomato gene after Cre recombinase exposure may provide a model for clarification of the distribution of VZV in the rat TG and DRG and may reveal non-neuronal tissues that become infected. We have generated a recombinant VZV that expresses Cre recombinase to work with this model and have begun characterizing *in vitro* and *in vivo* infections. Although *in vitro* infections have resulted in tdTomato detection, *in vivo* analyses have not been successful. Because the delivery of infectious VZV includes associated cells that have made abundant Cre protein, it is possible that the expression of tdTomato in cell culture results from secreted Cre protein acting on rat cells independent of VZV infection. This is also a concern for analysis of the inoculation site

tissues in which we have detected tdTomato in 28-dpi footpad tissue. A cell-free infection experiment would be necessary to explore these concerns and would be simple to do *in vitro*, though reaching sufficient titers for *in vivo* use may be limiting. Detection of tdTomato within TG or DRG would also validate VZV infection *in vivo* as the cells delivered with the inoculum cannot reach the ganglion, but we have been unable to locate any instance of tdTomato in these tissues so far. In future experiments we may start by simply increasing the infectious titer and harvest ganglia at timepoints later than 28-dpi. If ganglia detection still proves difficult, we may also use cell sorting techniques to isolate tdTomato fluorescent rat cells following *in vivo* inoculation. This would be particularly relevant for ganglia because it may allow quantification of infected rat cells which is expected to be low and thus difficult to detect by screening tissue sections. Sorted tdTomato cells may then be analyzed by modern transcriptomic techniques as have been detailed in recent years for herpesviruses [55,318]. Finally, as an alternative approach to determine if specific VZV transcripts are made within rat tissues, we may recombine the T2A/Cre expression cassette after immediate-early and early genes of interest. In these recombinant VZV, tdTomato fluorescence would report transcription of the specific VZV genes from their wild-type promoters.

The use of the DHFR degron system for gene function studies presents a step forward for essential VZV gene experimentation. The ectopic mutant viruses generated from VZV ORF9cDHFR are a proof of principle but will require further modification to be effective. One current drawback is the concurrent production of ORF9cDHFRp and the mutated ORF9p under TMP conditions. Growth analysis of the ectopic N-terminal mutants suggest the deletion mutants may be interfering with ORF9cDHFRp required for growth. This is shown by a considerable growth reduction under both TMP conditions for 9c.9-N1 and -N2. It may be beneficial to place the ectopic mutant gene under an inducible promoter to avoid potential mutant protein interference

or dominant negative effects. Alternatively, it may be possible to recombine a different degron onto the ectopic mutants in place of the V5-tag, which would function by ligand-induced degradation [312]. This would allow for swapping of the stabilized proteins. While either method would add complexity, it is likely unavoidable to reduce pitfalls uncontrolled from dual protein function. The growth analysis here may have revealed dominant negative effects of the mutant ORF9p and if a dual degron system were used competitive binding experiments would still be available. Pulldown assays may be completed to determine if N-terminal mutants 9c.9-N1 or -N2 have a greater binding affinity and may reveal other important sequences in the protein. Because of the DHFR system success in SVV and now VZV, the opportunity for application to other related viruses should not be overlooked. This system might benefit some of the neuroinvasive studies that are carried out with PRV.

Finally, the use of VZV ORF4nDHFR for the establishment of experimental latency and reactivation in hESC-derived neurons is encouraging. Established methods of establishing latency suffer from sporadic lytic infections and potential lower reactivation efficiency with ACV. The studies presented here show that VZV ORF4nDHFR is efficient at establishing quiescent infections in both skin and neuronal cell types. Infection in skin cells appears to be abortive while neurons appear to establish a latent infection that is capable of reactivating. However, these analyses were only qualitative and quantitative assessments are required to confirm these conclusions. Quantitative studies may indicate if establishing experimental latency with VZV ORF4nDHFR is dose-dependent and how dose might affect reactivation frequency and efficiency. It is also important to establish a transcriptional profile for different TMP conditions to further assess differences in abortive versus latent infections in this model. Alternative neuron culture systems have been described using induced pluripotent stem cells and may provide more pure

compositions of certain neuron cell types for assessment [319]. Recent studies using such neurons have suggested that the neurons may first undergo an initial lytic infection that is less severe and may facilitate establishment of latency. It would be interesting to determine the infection outcome of a virus like VZV ORF4nDHFR that cannot undertake the initial lytic infection and how that might affect latency.

References

1. Kolb, A.W., Lewin, A.C., Moeller Trane, R., McLellan, G.J., and Brandt, C.R. (2017) Phylogenetic and recombination analysis of the herpesvirus genus varicellovirus. *BMC Genomics*, 18 (1), 887.

2. Gray, W.L., Starnes, B., White, M.W., and Mahalingam, R. (2001) The DNA sequence of the simian varicella virus genome. *Virology*, 284 (1), 123–130.

3. Cohen, J.I. (2010) The Varicella-Zoster Virus Genome, in *Assessment & Evaluation in Higher Education*, vol. 37, pp. 1–14.

4. Sheldrick, P., and Berthelot, N. (1974) Inverted Repetitions in the Chromosome of Herpes Simplex Virus. *Cold Spring Harb. Symp. Quant. Biol.*, 39, 667–678.

5. Ecker, J.R., and Hyman, R.W. (1982) Varicella zoster virus DNA exists as two isomers. *Proc. Natl. Acad. Sci. U. S. A.*, 79 (1), 156–160.

6. Kinchington, P.R., Reinhold, W.C., Casey, T.A., Straus, S.E., Hay, J., and Ruyechan, W.T. (1985) Inversion and circularization of the varicella-zoster virus genome. *J. Virol.*, 56 (1), 194–200.

7. Hayward, G.S., Jacob, R.J., Wadsworth, S.C., and Roizman, B. (1975) Anatomy of herpes simplex virus DNA: evidence for four populations of molecules that differ in the relative orientations of their long and short components. *Proc. Natl. Acad. Sci. U. S. A.*, 72 (11), 4243–4247.

8. Mahiet, C., Ergani, A., Huot, N., Alende, N., Azough, A., Salvaire, F., Bensimon, A., Conseiller, E., Wain-Hobson, S., Labetoulle, M., and Barradeau, S. (2012) Structural Variability of the Herpes Simplex Virus 1 Genome In Vitro and In Vivo. *J. Virol.*, 86 (16), 8592–8601.

9. Stow, N.D., and Davison, A.J. (1986) Identification of a Varicella-Zoster Virus Origin of DNA Replication and Its Activation by Herpes Simplex Virus Type 1 Gene Products. *J. Gen. Virol.*, 67 (8), 1613–1623.

10. Stow, N.D. (1982) Localization of an origin of DNA replication within the TRS/IRS repeated region of the herpes simplex virus type 1 genome. *EMBO J.*, 1 (7), 863–867.

11. Jackson, S.A., and DeLuca, N.A. (2003) Relationship of herpes simplex virus genome

configuration to productive and persistent infections. *Proc. Natl. Acad. Sci.*, 100 (13), 7871–7876.

12. Mellerick, D.M., and Fraser, N.W. (1987) Physical state of the latent herpes simplex virus genome in a mouse model system: Evidence suggesting an episomal state. *Virology*, 158 (2), 265–275.

13. Zhang, Z., Selariu, A., Warden, C., Huang, G., Huang, Y., Zaccheus, O., Cheng, T., Xia, N., and Zhu, H. (2010) Genome-Wide Mutagenesis Reveals That ORF7 Is a Novel VZV Skin-Tropic Factor. *PLoS Pathog.*, 6 (7), e1000971.

14. Moffat, J.F., Zerboni, L., Sommer, M.H., Heineman, T.C., Cohen, J.I., Kaneshima, H., and Arvin, A.M. (1998) The ORF47 and ORF66 putative protein kinases of varicella-zoster virus determine tropism for human T cells and skin in the SCID-hu mouse. *Microbiology*, 95 (20), 11969–11974.

15. Hu, H., and Cohen, J.I. (2005) Varicella-zoster virus open reading frame 47 (ORF47) protein is critical for virus replication in dendritic cells and for spread to other cells. *Virology*, 337 (2), 304–311.

16. Besser, J., Sommer, M.H., Zerboni, L., Bagowski, C.P., Ito, H., Moffat, J., Ku, C.-C., and Arvin, A.M. (2003) Differentiation of varicella-zoster virus ORF47 protein kinase and IE62 protein binding domains and their contributions to replication in human skin xenografts in the SCID-hu mouse. *J. Virol.*, 77 (10), 5964–74.

17. Besser, J., Ikoma, M., Fabel, K., Sommer, M.H., Zerboni, L., Grose, C., and Arvin, A.M. (2004) Differential Requirement for Cell Fusion and Virion Formation in the Pathogenesis of Varicella-Zoster Virus Infection in Skin and T Cells. *J. Virol.*, 78 (23), 13293–13305.

18. Felser, J.M., Kinchington, P.R., Inchauspe, G., Straus, S.E., and Ostrove, J.M. (1988) Cell lines containing varicella-zoster virus open reading frame 62 and expressing the "IE" 175 protein complement ICP4 mutants of herpes simplex virus type 1. *J. Virol.*, 62 (6), 2076–82.

19. Thompson, R., Honess, R.W., Taylor, L., Morran, J., and Davison, A.J. (1987) Varicella-zoster virus specifies a thymidylate synthetase. *J. Gen. Virol.*, 68 (5), 1449–1455.

20. Gáspár, G., De Clercq, E., and Neyts, J. (2002) Human Herpesvirus 8 Gene Encodes a Functional Thymidylate Synthase. *J. Virol.*, 76 (20), 10530–10532.

21. Cox, E., Reddy, S., Iofin, I., and Cohen, J.I. (1998) Varicella-Zoster Virus ORF57, Unlike Its Pseudorabies Virus UL3.5 Homolog, Is Dispensable for Viral Replication in Cell Culture. *Virology*, 250 (1), 205–209.

22. Kaufer, B.B., Smejkal, B., and Osterrieder, N. (2010) The varicella-zoster virus ORFS/L (ORF0) gene is required for efficient viral replication and contains an element involved in DNA cleavage. *J. Virol.*, 84 (22), 11661–9.

23. Cohen, J.I., and Seidel, K.E. (1995) Varicella-zoster virus open reading frame 1 encodes a membrane protein that is dispensable for growth of VZV in vitro. *Virology*, 206 (2), 835–842.

24. Sato, H., Pesnicak, L., and Cohen, J.I. (2002) Varicella-Zoster Virus Open Reading Frame 2 Encodes a Membrane Phosphoprotein That Is Dispensable for Viral Replication and for Establishment of Latency. *J. Virol.*, 76 (7), 3575–3578.

25. Cohen, J.I., and Seidel, K.E. (1993) Generation of varicella-zoster virus (VZV) and viral mutants from cosmid DNAs: VZV thymidylate synthetase is not essential for replication in vitro. *Proc. Natl. Acad. Sci.*, 90 (15), 7376–7380.

26. Reddy, S.M., Cox, E., Iofin, I., Soong, W., and Cohen, J.I. (1998) Varicella-Zoster Virus (VZV) ORF32 Encodes a Phosphoprotein That Is Posttranslationally Modified by the VZV ORF47 Protein Kinase. *J. Virol.*, 72 (10), 8083–8088.

27. Kut, E., and Rasschaert, D. (2004) Assembly of Marek's disease virus (MDV) capsids using recombinant baculoviruses expressing MDV capsid proteins. *J. Gen. Virol.*, 85 (4), 769–774.

28. del Rio, T., Ch'ng, T.H., Flood, E.A., Gross, S.P., and Enquist, L.W. (2005) Heterogeneity of a Fluorescent Tegument Component in Single Pseudorabies Virus Virions and Enveloped Axonal Assemblies. *J. Virol.*, 79 (7), 3903–3919.

29. Cohen, G.H., Ponce de Leon, M., Diggelmann, H., Lawrence, W.C., Vernon, S.K., and Eisenberg, R.J. (1980) Structural analysis of the capsid polypeptides of herpes simplex virus types 1 and 2. *J. Virol.*, 34 (2), 521–31.

30. Visalli, M.A., House, B.L., Selariu, A., Zhu, H., and Visalli, R.J. (2014) The Varicella-Zoster Virus Portal Protein Is Essential for Cleavage and Packaging of Viral DNA. *J. Virol.*, 88 (14), 7973–7986.

31. Wang, W., Cheng, T., Zhu, H., and Xia, N. (2015) Insights into the function of tegument proteins from the varicella zoster virus. *Sci. China Life Sci.*, 58 (8), 739–749.

32. Luxton, G.W.G., Haverlock, S., Coller, K.E., Antinone, S.E., Pincetic, A., and Smith, G.A. (2005) Targeting of herpesvirus capsid transport in axons is coupled to association with specific sets of tegument proteins. *Proc. Natl. Acad. Sci.*, 102 (16), 5832–5837.

33. Wolfstein, A., Nagel, C.H., Radtke, K., Döhner, K., Allan, V.J., and Sodeik, B. (2006) The inner tegument promotes herpes simplex virus capsid motility along microtubules in vitro. *Traffic*, 7 (2), 227–237.

34. Coller, K.E., and Smith, G.A. (2008) Two Viral Kinases are Required for Sustained Long Distance Axon Transport of a Neuroinvasive Herpesvirus. *Traffic*, 9 (9), 1458–1470.

35. Radtke, K., Kieneke, D., Wolfstein, A., Michael, K., Steffen, W., Scholz, T., Karger, A., and Sodeik, B. (2010) Plus- and minus-end directed microtubule motors bind simultaneously to herpes simplex virus capsids using different inner tegument structures. *PLoS Pathog.*, 6 (7), 1–20.

36. Sandbaumhüter, M., Döhner, K., Schipke, J., Binz, A., Pohlmann, A., Sodeik, B., and Bauerfeind, R. (2013) Cytosolic herpes simplex virus capsids not only require binding inner tegument protein pUL36 but also pUL37 for active transport prior to secondary envelopment. *Cell. Microbiol.*, 15 (2), 248–269.

37. Kinchington, P.R., Bookey, D., and Turse, S.E. (1995) The transcriptional regulatory proteins encoded by varicella-zoster virus open reading frames (ORFs) 4 and 63, but not ORF 61, are associated with purified virus particles. *J. Virol.*, 69 (7), 4274–82.

38. Kinchington, P.R., Fite, K., Seman, A., and Turse, S.E. (2001) Virion Association of IE62, the Varicella-Zoster Virus (VZV) Major Transcriptional Regulatory Protein, Requires Expression of the VZV Open Reading Frame 66 Protein Kinase. *J. Virol.*, 75 (19), 9106–9113.

39. Spengler, M., Niesen, N., Grose, C., Ruyechan, W.T., and Hay, J. (2001) Interactions among structural proteins of varicella zoster virus. *Arch.Virol.Suppl*, (0939–1983), 71–79.

40. Che, X., Reichelt, M., Sommer, M.H., Rajamani, J., Zerboni, L., and Arvin, A.M. (2008) Functions of the ORF9-to-ORF12 Gene Cluster in Varicella-Zoster Virus Replication and in the Pathogenesis of Skin Infection. *J. Virol.*, 82 (12), 5825–5834.

41. Oliver, S.L., Yang, E., and Arvin, A.M. (2016) Varicella-Zoster Virus Glycoproteins: Entry, Replication, and Pathogenesis. *Curr. Clin. Microbiol. Reports*, 3 (4), 204–215.

42. Kennedy, P.G.E., Graner, M.W., Gunaydin, D., Bowlin, J., Pointon, T., and Yu, X. (2020) Varicella-Zoster Virus infected human neurons are resistant to apoptosis. *J. Neurovirol.*, 26 (3), 330–337.

43. Kennedy, P.G.E., and Mogensen, T.H. (2021) Varicella-zoster virus infection of neurons derived from neural stem cells. *Viruses*, 13 (3), 1–9.

44. Muggeridge, M.I. (2000) Characterization of cell-cell fusion mediated by herpes simplex virus 2 glycoproteins gB, gD, gH and gL in transfected cells. *J. Gen. Virol.*, 81 (8), 2017–2027.

45. Haan, K.M., Kyeong Lee, S., and Longnecker, R. (2001) Different functional domains in the cytoplasmic tail of glycoprotein B are involved in Epstein-Barr virus-induced membrane fusion. *Virology*, 290 (1), 106–114.

46. Xu, J., Yao, K., Dou, J., Qin, J., Xu, W.R., Chen, Y., Yin, Q.Z., and Zhou, F. (2007) Human herpesvirus 7 glycoprotein B (gB), gH, gL, gO can mediate cell fusion. *Prog. Biochem. Biophys.*, 34 (11), 1202–1209.

47. Pertel, P.E., Fridberg, A., Parish, M.L., and Spear, P.G. (2001) Cell fusion induced by herpes simplex virus glycoproteins gB, gD, and gH-gL requires a gD receptor but not necessarily heparan sulfate. *Virology*, 279 (1), 313–324.

48. Jacquet, A., Haumont, M., Chellun, D., Massaer, M., Tufaro, F., Bollen, A., and Jacobs, P. (1998) The varicella zoster virus glycoprotein B (gB) plays a role in virus binding to cell surface heparan sulfate proteoglycans. *Virus Res.*, 53 (2), 197–207.

49. Cole, N.L., and Grose, C. (2003) Membrane fusion mediated by herpesvirus glycoproteins: The paradigm of varicella-zoster virus. *Rev. Med. Virol.*, 13 (4), 207–222.

50. Zaichick, S. V., Bohannon, K.P., Hughes, A., Sollars, P.J., Pickard, G.E., and Smith, G.A. (2013) The herpesvirus VP1/2 protein is an effector of dynein-mediated capsid transport and neuroinvasion. *Cell Host Microbe*, 13 (2), 193–203.

51. Honess, R.W., and Roizman, B. (1974) Regulation of herpesvirus macromolecular synthesis. I. Cascade regulation of the synthesis of three groups of viral proteins. *J. Virol.*, 14 (1), 8–19.

52. McKnight, J.L., Kristie, T.M., and Roizman, B. (1987) Binding of the virion protein mediating alpha gene induction in herpes simplex virus 1-infected cells to its cis site requires cellular proteins. *Proc. Natl. Acad. Sci.*, 84 (20), 7061–7065.

53. Preston, C.M., Frame, M.C., and Campbell, M.E.M. (1988) A complex formed between cell components and an HSV structural polypeptide binds to a viral immediate early gene regulatory DNA sequence. *Cell*, 52 (3), 425–434.

54. Gerster, T., and Roeder, R.G. (1988) A herpesvirus trans-activating protein interacts with transcription factor OTF-1 and other cellular proteins. *Proc. Natl. Acad. Sci.*, 85 (17), 6347–6351.

55. Braspenning, S.E., Sadaoka, T., Breuer, J., Verjans, G.M.G.M., Ouwendijk, W.J.D., and Depledge, D.P. (2020) Decoding the Architecture of the Varicella-Zoster Virus Transcriptome. *MBio*, 11 (5).

56. Lebrun, M., Thelen, N., Thiry, M., Riva, L., Ote, I., Condé, C., Vandevenne, P., Di Valentin, E., Bontems, S., and Sadzot-Delvaux, C. (2014) Varicella-zoster virus induces the formation of dynamic nuclear capsid aggregates. *Virology*, 454–455 (1), 311–327.

57. Granzow, H., Klupp, B.G., Fuchs, W., Veits, J., Osterrieder, N., and Mettenleiter, T.C. (2001) Egress of Alphaherpesviruses: Comparative Ultrastructural Study. *J. Virol.*, 75 (8), 3675–3684.

58. Skepper, J.N., Whiteley, A., Browne, H., and Minson, A. (2001) Herpes Simplex Virus Nucleocapsids Mature to Progeny Virions by an Envelopment → Deenvelopment → Reenvelopment Pathway. *J. Virol.*, 75 (12), 5697–5702.

59. Riva, L., Thiry, M., Bontems, S., Joris, A., Piette, J., Lebrun, M., and Sadzot-Delvaux, C. (2013) ORF9p phosphorylation by ORF47p is crucial for the formation and egress of varicella-zoster virus viral particles. *J. Virol.*, 87 (5), 2868–81.

60. Harson, R., and Grose, C. (1995) Egress of varicella-zoster virus from the melanoma cell: a tropism for the melanocyte. *J. Virol.*, 69 (8), 4994–5010.

61. Kyratsous, C.A., and Silverstein, S.J. (2009) Components of Nuclear Domain 10 Bodies Regulate Varicella-Zoster Virus Replication. *J. Virol.*, 83 (9), 4262–4274.

62. Reichelt, M., Wang, L., Sommer, M., Perrino, J., Nour, A.M., Sen, N., Baiker, A., Zerboni, L., and Arvin, A.M. (2011) Entrapment of Viral Capsids in Nuclear PML Cages Is an Intrinsic Antiviral Host Defense against Varicella-Zoster Virus. *PLoS Pathog.*, 7 (2), e1001266.

63. Reichelt, M., Brady, J., and Arvin, A.M. (2009) The replication cycle of varicella-zoster virus: analysis of the kinetics of viral protein expression, genome synthesis, and virion assembly at the single-cell level. *J. Virol.*, 83 (8), 3904–18.

64. Zhong, S., Salomoni, P., and Pandolfi, P.P. (2000) The transcriptional role of PML and the nuclear body. *Nat. Cell Biol.*, 2 (5), E85–E90.

65. Bernardi, R., and Pandolfi, P.P. (2007) Structure, dynamics and functions of promyelocytic leukaemia nuclear bodies. *Nat. Rev. Mol. Cell Biol.*, 8 (12), 1006–1016.

66. Wang, L., Oliver, S.L., Sommer, M., Rajamani, J., Reichelt, M., and Arvin, A.M. (2011) Disruption of PML Nuclear Bodies Is Mediated by ORF61 SUMO-Interacting Motifs and

Required for Varicella-Zoster Virus Pathogenesis in Skin. *PLoS Pathog.*, 7 (8), e1002157.

67. Moriuchi, H., Moriuchi, M., Straus, S.E., and Cohen, J.I. (1993) Varicella-zoster virus (VZV) open reading frame 61 protein transactivates VZV gene promoters and enhances the infectivity of VZV DNA. *J. Virol.*, 67 (7), 4290–4295.

68. Moriuchi, H., Moriuchi, M., and Cohen, J.I. (1995) Proteins and cis-acting elements associated with transactivation of the varicella-zoster virus (VZV) immediate-early gene 62 promoter by VZV open reading frame 10 protein. *J. Virol.*, 69 (8), 4693–4701.

69. Ouwendijk, W.J.D., Flowerdew, S.E., Wick, D., Horn, A.K.E., Sinicina, I., Strupp, M., Osterhaus, A.D.M.E., Verjans, G.M.G.M., and Hüfner, K. (2012) Immunohistochemical detection of intra-neuronal VZV proteins in snap-frozen human ganglia is confounded by antibodies directed against blood group A1-associated antigens. *J. Neurovirol.*, 18 (3), 172–180.

70. Zerboni, L., Sobel, R.A., Lai, M., Triglia, R., Steain, M., Abendroth, A., and Arvin, A. (2012) Apparent Expression of Varicella-Zoster Virus Proteins in Latency Resulting from Reactivity of Murine and Rabbit Antibodies with Human Blood Group A Determinants in Sensory Neurons. *J. Virol.*, 86 (1), 578–583.

71. Hyman, R.W., Ecker, J.R., and Tenser, R.B. (1983) VARICELLA-ZOSTER VIRUS RNA IN HUMAN TRIGEMINAL GANGLIA. *Lancet*, 322 (8354), 814–816.

72. Croen, K.D., Ostrove, J.M., Dragovic, L.J., and Straus, S.E. (1988) Patterns of gene expression and sites of latency in human nerve ganglia are different for varicella-zoster and herpes simplex viruses. *Proc. Natl. Acad. Sci. U. S. A.*, 85 (24), 9773–9777.

73. Meier, J.L., Holman, R.P., Croen, K.D., Smialek, J.E., and Straus, S.E. (1993) Varicella-zoster virus transcription in human trigeminal ganglia. *Virology*, 193 (1), 193–200.

74. Cohrs, R.J., Barbour, M., and Gilden, D.H. (1996) Varicella-zoster virus (VZV) transcription during latency in human ganglia: detection of transcripts mapping to genes 21, 29, 62, and 63 in a cDNA library enriched for VZV RNA. *J. Virol.*, 70 (5), 2789–2796.

75. Mahalingam, R., Wellish, M., Cohrs, R., Debrus, S., Piette, J., Rentier, B., and Gilden, D.H. (1996) Expression of protein encoded by varicella-zoster virus open reading frame 63 in latently infected human ganglionic neurons. *Proc. Natl. Acad. Sci. U. S. A.*, 93 (5), 2122–2124.

76. Cohrs, R.J., Srock, K., Barbour, M.B., Owens, G., Mahalingam, R., Devlin, M.E., Wellish, M., and Gilden, D.H. (1994) Varicella-zoster virus (VZV) transcription during latency in human ganglia: construction of a cDNA library from latently infected human trigeminal

ganglia and detection of a VZV transcript. *J. Virol.*, 68 (12), 7900–7908.

77. Cohrs, R.J., Barbour, M.B., Mahalingam, R., Wellish, M., and Gilden, D.H. (1995) Varicella-zoster virus (VZV) transcription during latency in human ganglia: prevalence of VZV gene 21 transcripts in latently infected human ganglia. *J. Virol.*, 69 (4), 2674–2678.

78. Cohrs, R.J., and Gilden, D.H. (2007) Prevalence and abundance of latently transcribed varicella-zoster virus genes in human ganglia. *J. Virol.*, 81 (6), 2950–2956.

79. Cohrs, R.J., Gilden, D.H., Kinchington, P.R., Grinfeld, E., and Kennedy, P.G.E. (2003) Varicella-Zoster Virus Gene 66 Transcription and Translation in Latently Infected Human Ganglia. *J. Virol.*, 77 (12), 6660–6665.

80. Mador, N., Goldenberg, D., Cohen, O., Panet, A., and Steiner, I. (1998) Herpes Simplex Virus Type 1 Latency-Associated Transcripts Suppress Viral Replication and Reduce Immediate-Early Gene mRNA Levels in a Neuronal Cell Line. *J. Virol.*, 72 (6), 5067–5075.

81. Umbach, J.L., Kramer, M.F., Jurak, I., Karnowski, H.W., Coen, D.M., and Cullen, B.R. (2008) MicroRNAs expressed by herpes simplex virus 1 during latent infection regulate viral mRNAs. *Nature*, 454 (7205), 780–783.

82. Shen, W., Sa e Silva, M., Jaber, T., Vitvitskaia, O., Li, S., Henderson, G., and Jones, C. (2009) Two Small RNAs Encoded within the First 1.5 Kilobases of the Herpes Simplex Virus Type 1 Latency-Associated Transcript Can Inhibit Productive Infection and Cooperate To Inhibit Apoptosis. *J. Virol.*, 83 (18), 9131–9139.

83. Depledge, D.P., Ouwendijk, W.J.D., Sadaoka, T., Braspenning, S.E., Mori, Y., Cohrs, R.J., Verjans, G.M.G.M., and Breuer, J. (2018) A spliced latency-associated VZV transcript maps antisense to the viral transactivator gene 61. *Nat. Commun.*, 9 (1), 1167.

84. Ouwendijk, W.J.D., Depledge, D.P., Rajbhandari, L., Lenac Rovis, T., Jonjic, S., Breuer, J., Venkatesan, A., Verjans, G.M.G.M., and Sadaoka, T. (2020) Varicella-zoster virus VLT-ORF63 fusion transcript induces broad viral gene expression during reactivation from neuronal latency. *Nat. Commun.*, 11 (1).

85. Markus, A., Grigoryan, S., Sloutskin, A., Yee, M.B., Zhu, H., Yang, I.H., Thakor, N. V., Sarid, R., Kinchington, P.R., and Goldstein, R.S. (2011) Varicella-zoster virus (VZV) infection of neurons derived from human embryonic stem cells: direct demonstration of axonal infection, transport of VZV, and productive neuronal infection. *J. Virol.*, 85 (13), 6220–33.

86. Grigoryan, S., Kinchington, P.R., Yang, I.H., Selariu, A., Zhu, H., Yee, M., and Goldstein, R.S. (2012) Retrograde axonal transport of VZV: Kinetic studies in hESC-derived neurons.

J. Neurovirol., 18 (6), 462–470.

87. Depledge, D.P., Sadaoka, T., and Ouwendijk, W.J.D. (2018) Molecular aspects of varicella-zoster virus latency. *Viruses*, 10 (7).

88. Cliffe, A.R. (2019) DNA Damage Meets Neurotrophin Signaling: A Delicate Balancing AKT to Maintain Virus Latency. *Mol. Cell*, 74 (3), 411–413.

89. Ambagala, A.P., Bosma, T., Ali, M.A., Poustovoitov, M., Chen, J.J., Gershon, M.D., Adams, P.D., and Cohen, J.I. (2009) Varicella-Zoster Virus Immediate-Early 63 Protein Interacts with Human Antisilencing Function 1 Protein and Alters Its Ability To Bind Histones H3.1 and H3.3. *J. Virol.*, 83 (1), 200–209.

90. Kollias, C.M., Huneke, R.B., Wigdahl, B., and Jennings, S.R. (2015) Animal models of herpes simplex virus immunity and pathogenesis. *J. Neurovirol.*, 21 (1), 8–23.

91. Gabel, C.A., Dubey, L., Steinberg, S.P., Sherman, D., Gershon, M.D., and Gershon, A.A. (1989) Varicella-zoster virus glycoprotein oligosaccharides are phosphorylated during posttranslational maturation. *J. Virol.*, 63 (10), 4264–4276.

92. Chen, J.J., Gershon, A.A., Li, Z.S., Lungu, O., and Gershon, M.D. (2003) Latent and lytic infection of isolated guinea pig enteric ganglia by varicella zoster virus. *J. Med. Virol.*, 70 (SUPPL. 1), 71–78.

93. Gershon, A.A., Chen, J., and Gershon, M.D. (2008) A Model of Lytic, Latent, and Reactivating Varicella-Zoster Virus Infections in Isolated Enteric Neurons. *J. Infect. Dis.*, 197 (s2), S61–S65.

94. Mahalingam, R., Gershon, A., Gershon, M., Cohen, J.I., Arvin, A., Zerboni, L., Zhu, H., Gray, W., Messaoudi, I., and Traina-Dorge, V. (2019) Current In Vivo Models of Varicella-Zoster Virus Neurotropism. *Viruses*, 11 (6), 502.

95. Ku, C.-C., Padilla, J.A., Grose, C., Butcher, E.C., and Arvin, A.M. (2002) Tropism of Varicella-Zoster Virus for Human Tonsillar CD4+ T Lymphocytes That Express Activation, Memory, and Skin Homing Markers. *J. Virol.*, 76 (22), 11425–11433.

96. Ku, C.-C., Besser, J., Abendroth, A., Grose, C., and Arvin, A.M. (2005) Varicella-Zoster Virus Pathogenesis and Immunobiology: New Concepts Emerging from Investigations with the SCIDhu Mouse Model. *J. Virol.*, 79 (5), 2651–2658.

97. Zerboni, L., Ku, C.-C., Jones, C.D., Zehnder, J.L., and Arvin, A.M. (2005) Varicella-zoster virus infection of human dorsal root ganglia in vivo. *Proc. Natl. Acad. Sci.*, 102 (18), 6490–6495.

98. Cohen, J.I., Cox, E., Pesnicak, L., Srinivas, S., and Krogmann, T. (2004) The Varicella-Zoster Virus Open Reading Frame 63 Latency-Associated Protein Is Critical for Establishment of Latency. *J. Virol.*, 78 (21), 11833–11840.

99. Sato, H., Pesnicak, L., and Cohen, J.I. (2003) Use of a rodent model to show that varicella-zoster virus ORF61 is dispensable for establishment of latency. *J. Med. Virol.*, 70 (SUPPL. 1), S79–S81.

100. Fleetwood-Walker, S.M., Quinn, J.P., Wallace, C., Blackburn-Munro, G., Kelly, B.G., Fiskerstrand, C.E., Nash, A.A., and Dalziel, R.G. (1999) Behavioural changes in the rat following infection with varicella-zoster virus. *J. Gen. Virol.*, 80 (Pt 9) (9), 2433–2436.

101. Tischer, B.K., Kaufer, B.B., Sommer, M., Wussow, F., Arvin, A.M., and Osterrieder, N. (2007) A self-excisable infectious bacterial artificial chromosome clone of varicella-zoster virus allows analysis of the essential tegument protein encoded by ORF9. *J. Virol.*, 81 (23), 13200–8.

102. Tischer, B.K., von Einem, J., Kaufer, B., and Osterrieder, N. (2006) Two-step red-mediated recombination for versatile high-efficiency markerless DNA manipulation in Escherichia coli. *Biotechniques*, 40 (2), 191–7.

103. Nagaike, K., Mori, Y., Gomi, Y., Yoshii, H., Takahashi, M., Wagner, M., Koszinowski, U., and Yamanishi, K. (2004) Cloning of the varicella-zoster virus genome as an infectious bacterial artificial chromosome in Escherichia coli. *Vaccine*, 22 (29–30), 4069–74.

104. Zhang, Z., Rowe, J., Wang, W., Sommer, M., Arvin, A., Moffat, J., and Zhu, H. (2007) Genetic Analysis of Varicella-Zoster Virus ORF0 to ORF4 by Use of a Novel Luciferase Bacterial Artificial Chromosome System. *J. Virol.*, 81 (17), 9024–9033.

105. Balliet, J.W., Min, J.C., Cabatingan, M.S., and Schaffer, P.A. (2005) Site-Directed Mutagenesis of Large DNA Palindromes: Construction and In Vitro Characterization of Herpes Simplex Virus Type 1 Mutants Containing Point Mutations That Eliminate the oriL or oriS Initiation Function. *J. Virol.*, 79 (20), 12783–12797.

106. Balliet, J.W., and Schaffer, P.A. (2006) Point Mutations in Herpes Simplex Virus Type 1 oriL, but Not in oriS, Reduce Pathogenesis during Acute Infection of Mice and Impair Reactivation from Latency. *J. Virol.*, 80 (1), 440–450.

107. Cohen, J.I., Krogmann, T., Ross, J.P., Pesnicak, L., and Prikhod'ko, E.A. (2005) Varicella-zoster virus ORF4 latency-associated protein is important for establishment of latency. *J. Virol.*, 79 (11), 6969–75.

108. Iwamoto, M., Björklund, T., Lundberg, C., Kirik, D., and Wandless, T.J. (2010) A general

chemical method to regulate protein stability in the mammalian central nervous system. *Chem. Biol.*, 17 (9), 981–8.

109. Warner, B.E., Yee, M.B., Zhang, M., Hornung, R.S., Kaufer, B.B., Visalli, R.J., Kramer, P.R., Goins, W.F., and Kinchington, P.R. (2021) Varicella-zoster virus early infection but not complete replication is required for the induction of chronic hypersensitivity in rat models of postherpetic neuralgia. *PLOS Pathog.*, 17 (7), e1009689.

110. Finger, R., Hughes, J.P., Meade, B.J., Pelletier, A.R., and Palmer, C.T. (1994) Age-specific incidence of chickenpox. *Public Health Rep.*, 109 (6), 750–755.

111. Riera-Montes, M., Bollaerts, K., Heininger, U., Hens, N., Gabutti, G., Gil, A., Nozad, B., Mirinaviciute, G., Flem, E., Souverain, A., Verstraeten, T., and Hartwig, S. (2017) Estimation of the burden of varicella in Europe before the introduction of universal childhood immunization. *BMC Infect. Dis.*, 17 (1), 1–16.

112. Gershon, A.A., Breuer, J., Cohen, J.I., Cohrs, R.J., Gershon, M.D., Gilden, D., Grose, C., Hambleton, S., Kennedy, P.G.E., Oxman, M.N., Seward, J.F., and Yamanishi, K. (2015) Varicella zoster virus infection. *Nat. Rev. Dis. Prim.*, 1 (July), 1–19.

113. Chen, T.M., George, S., Woodruff, C.A., and Hsu, S. (2002) Clinical manifestations of varicella-zoster virus infection. *Dermatol. Clin.*, 20 (2), 267–82.

114. Kennedy, P.G.E., and Gershon, A.A. (2018) Clinical features of varicella-zoster virus infection. *Viruses*, 10 (11), 1–11.

115. Preblud, S.R. (1986) Varicella: Complications and costs. *Pediatrics*, 78 (4 II SUPPL.), 728–735.

116. Mandal, B.K., Mukherjee, P.P., Murphy, C., Mukherjee, R., and Naik, T. (1998) Adult Susceptibility to Varicella in the Tropics Is a Rural Phenomenon Due to the Lack of Previous Exposure. *J. Infect. Dis.*, 178 (s1), S52–S54.

117. Gregorakos, L., Myrianthefs, P., Markou, N., Chroni, D., and Sakagianni, E. (2002) Severity of illness and outcome in adult patients with primary varicella pneumonia. *Respiration*, 69 (4), 330–334.

118. Leclair, J.M., Zaia, J.A., Levin, M.J., Congdon, R.G., and Goldmann, D.A. (1980) Airborne Transmission of Chickenpox in a Hospital. *N. Engl. J. Med.*, 302 (8), 450–453.

119. Grose, C. (1981) Variation on a theme by Fenner: the pathogenesis of chickenpox. *Pediatrics*, 68 (5), 735–737.

120. Whitley, R.J., and Roizman, B. (2001) Herpes simplex virus infections. *Lancet (London, England)*, 357 (9267), 1513–8.

121. Tsolia, M., Gershon, A.A., Steiberg, S.P., and Gelb, L. (1990) Live attenuated varicella vaccine: Evidence that the virus is attenuated and the importance of skin lesions in transmission of varicella-zoster virus. *J. Pediatr.*, 116 (2), 184–189.

122. Zerboni, L., Sen, N., Oliver, S.L., and Arvin, A.M. (2014) Molecular mechanisms of varicella zoster virus pathogenesis. *Nat. Rev. Microbiol.*, 12 (3), 197–210.

123. Abendroth, A., Morrow, G., Cunningham, A.L., and Slobedman, B. (2001) Varicella-Zoster Virus Infection of Human Dendritic Cells and Transmission to T Cells: Implications for Virus Dissemination in the Host. *J. Virol.*, 75 (13), 6183–6192.

124. Moffat, J.F., Stein, M.D., Kaneshima, H., and Arvin, A.M. (1995) Tropism of varicella-zoster virus for human CD4+ and CD8+ T lymphocytes and epidermal cells in SCID-hu mice. *J. Virol.*, 69 (9), 5236–5242.

125. Ku, C.-C., Zerboni, L., Ito, H., Graham, B.S., Wallace, M., and Arvin, A.M. (2004) Varicella-zoster virus transfer to skin by T Cells and modulation of viral replication by epidermal cell interferon-alpha. *J. Exp. Med.*, 200 (7), 917–25.

126. Myers, M.I., Peltier, A.C., and Li, J. (2013) Evaluating dermal myelinated nerve fibers in skin biopsy. *Muscle Nerve*, 47 (1), 1–11.

127. Muraki, R., Iwasaki, T., Sata, T., Sato, Y., and Kurata, T. (1996) Hair follicle involvement in herpes zoster: pathway of viral spread from ganglia to skin. *Virchows Arch.*, 428–428 (4–5), 275–280.

128. Markus, A., Lebenthal-Loinger, I., Yang, I.H., Kinchington, P.R., and Goldstein, R.S. (2015) An In Vitro Model of Latency and Reactivation of Varicella Zoster Virus in Human Stem Cell-Derived Neurons. *PLoS Pathog.*, 11 (6), 1–22.

129. Mahalingam, R., Wellish, M., Soike, K., White, T., Kleinschmidt-DeMasters, B.K., and Gilden, D.H. (2001) Simian varicella virus infects ganglia before rash in experimentally infected monkeys. *Virology*, 279 (1), 339–342.

130. Furuta, Y., Takasu, T., Fukuda, S., Sato-Matsumura, K.C., Inuyama, Y., Hondo, R., and Nagashima, K. (1992) Detection of varicella-zoster virus DNA in human geniculate ganglia by polymerase chain reaction. *J. Infect. Dis.*, 166 (5), 1157–1159.

131. Furuta, Y., Takasu, T., Suzuki, S., Fukuda, S., Inuyama, Y., and Nagashima, K. (1997) Detection of latent varicella-zoster virus infection in human vestibular and spiral ganglia. *J.*

Med. Virol., 51 (3), 214–216.

132. Gilden, D.H., Gesser, R., Smith, J., Wellish, M., Laguardia, J.J., Cohrs, R.J., and Mahalingam, R. (2001) Presence of VZV and HSV-1 DNA in human nodose and celiac ganglia. *Virus Genes*, 23 (2), 145–147.

133. Chen, J.J., Gershon, A.A., Li, Z., Cowles, R.A., and Gershon, M.D. (2011) Varicella zoster virus (VZV) infects and establishes latency in enteric neurons. *J. Neurovirol.*, 17 (6), 578–589.

134. Gershon, A.A., Chen, J., Davis, L., Krinsky, C., Cowles, R., Reichard, R., and Gershon, M. (2012) Latency of varicella zoster virus in dorsal root, cranial, and enteric ganglia in vaccinated children. *Trans. Am. Clin. Climatol. Assoc.*, 123 (2), 17–35.

135. Richter, E.R., Dias, J.K., Gilbert II, J.E., and Atherton, S.S. (2009) Distribution of Herpes Simplex Virus Type 1 and Varicella Zoster Virus in Ganglia of the Human Head and Neck. *J. Infect. Dis.*, 200 (12), 1901–1906.

136. Nagel, M.A., Rempel, A., Huntington, J., Kim, F., Choe, A., and Gilden, D. (2014) Frequency and Abundance of Alphaherpesvirus DNA in Human Thoracic Sympathetic Ganglia. *J. Virol.*, 88 (14), 8189–8192.

137. Maple, P.A.C., Haedicke, J., Quinlivan, M., Steinberg, S.P., Gershon, A.A., Brown, K.E., and Breuer, J. (2016) The differences in short- and long-term varicella-zoster virus (VZV) immunoglobulin G levels following varicella vaccination of healthcare workers measured by VZV fluorescent-antibody-to-membrane-antigen assay (FAMA), VZV time-resolved fluorescence immuno. *Epidemiol. Infect.*, 144 (11), 2345–2353.

138. Wiese-Posselt, M., Siedler, A., Mankertz, A., Sauerbrei, A., Hengel, H., Wichmann, O., and Poethko-Müller, C. (2017) Varicella-zoster virus seroprevalence in children and adolescents in the pre-varicella vaccine era, Germany. *BMC Infect. Dis.*, 17 (1), 1–9.

139. Forbes, H.J., Bhaskaran, K., Thomas, S.L., Smeeth, L., Clayton, T., and Langan, S.M. (2014) Quantification of risk factors for herpes zoster: population based case-control study. *BMJ*, 348 (May), g2911.

140. Marra, F., Parhar, K., Huang, B., and Vadlamudi, N. (2020) Risk Factors for Herpes Zoster Infection: A Meta-Analysis. *Open Forum Infect. Dis.*, 7 (1), 1–8.

141. Marin, M., Harpaz, R., Zhang, J., Wollan, P.C., Bialek, S.R., and Yawn, B.P. (2016) Risk Factors for Herpes Zoster Among Adults. *Open Forum Infect. Dis.*, 3 (3), ofw119.

142. Johnson, R.W., Alvarez-Pasquin, M.-J., Bijl, M., Franco, E., Gaillat, J., Clara, J.G.,

Labetoulle, M., Michel, J.-P., Naldi, L., Sanmarti, L.S., and Weinke, T. (2015) Herpes zoster epidemiology, management, and disease and economic burden in Europe: a multidisciplinary perspective. *Ther. Adv. Vaccines*, 3 (4), 109–120.

143. Joesoef, R.M., Harpaz, R., Leung, J., and Bialek, S.R. (2012) Chronic Medical Conditions as Risk Factors for Herpes Zoster. *Mayo Clin. Proc.*, 87 (10), 961–967.

144. Yawn, B.P., and Gilden, D. (2013) The global epidemiology of herpes zoster. *Neurology*, 81 (10), 928–930.

145. Weiskopf, D., Weinberger, B., and Grubeck-Loebenstein, B. (2009) The aging of the immune system. *Transpl. Int.*, 22 (11), 1041–1050.

146. Zorzoli, E., Pica, F., Masetti, G., Franco, E., Volpi, A., and Gabutti, G. (2018) Herpes zoster in frail elderly patients: prevalence, impact, management, and preventive strategies. *Aging Clin. Exp. Res.*, 30 (7), 693–702.

147. Verjans, G.M.G.M., Hintzen, R.Q., van Dun, J.M., Poot, A., Milikan, J.C., Laman, J.D., Langerak, A.W., Kinchington, P.R., and Osterhaus, A.D.M.E. (2007) Selective retention of herpes simplex virus-specific T cells in latently infected human trigeminal ganglia. *Proc. Natl. Acad. Sci.*, 104 (9), 3496–3501.

148. Weinberg, A., and Levin, M.J. (2010) VZV T cell-mediated immunity. *Curr. Top. Microbiol. Immunol.*, 342 (October), 341–57.

149. Vukmanovic-Stejic, M., Sandhu, D., Seidel, J.A., Patel, N., Sobande, T.O., Agius, E., Jackson, S.E., Fuentes-Duculan, J., Suárez-Fariñas, M., Mabbott, N.A., Lacy, K.E., Ogg, G., Nestle, F.O., Krueger, J.G., Rustin, M.H.A., and Akbar, A.N. (2015) The Characterization of Varicella Zoster Virus–Specific T Cells in Skin and Blood during Aging. *J. Invest. Dermatol.*, 135 (7), 1752–1762.

150. Oxman, M.N., Levin, M.J., Johnson, G.R., Schmader, K.E., Straus, S.E., Gelb, L.D., Arbeit, R.D., Simberkoff, M.S., Gershon, A.A., Davis, L.E., Weinberg, A., Boardman, K.D., Williams, H.M., Zhang, J.H., Peduzzi, P.N., Beisel, C.E., Morrison, V.A., Guatelli, J.C., Brooks, P.A., Kauffman, C.A., Pachucki, C.T., Neuzil, K.M., Betts, R.F., Wright, P.F., Griffin, M.R., Brunell, P., Soto, N.E., Marques, A.R., Keay, S.K., Goodman, R.P., Cotton, D.J., Gnann, J.W., Loutit, J., Holodniy, M., Keitel, W.A., Crawford, G.E., Yeh, S.-S., Lobo, Z., Toney, J.F., Greenberg, R.N., Keller, P.M., Harbecke, R., Hayward, A.R., Irwin, M.R., Kyriakides, T.C., Chan, C.Y., Chan, I.S.F., Wang, W.W.B., Annunziato, P.W., Silber, J.L., and Shingles Prevention Study Group (2005) A vaccine to prevent herpes zoster and postherpetic neuralgia in older adults. *N. Engl. J. Med.*, 352 (22), 2271–84.

151. Blennow, O., Fjaertoft, G., Winiarski, J., Ljungman, P., Mattsson, J., and Remberger, M.

(2014) Varicella-Zoster Reactivation after Allogeneic Stem Cell Transplantation without Routine Prophylaxis-The Incidence Remains High. *Biol. Blood Marrow Transplant.*, 20 (10), 1646–1649.

152. Vermont, C.L., Jol-van der Zijde, E.C.M., Hissink Muller, P., Ball, L.M., Bredius, R.G.M., Vossen, A.C., and Lankester, A.C. (2014) Varicella zoster reactivation after hematopoietic stem cell transplant in children is strongly correlated with leukemia treatment and suppression of host T-lymphocyte immunity. *Transpl. Infect. Dis.*, 16 (2), 188–194.

153. Leung, T.F., Chik, K.W., Li, C.K., Lai, H., Shing, M.M.K., Chan, P.K.S., Lee, V., and Yuen, P.M.P. (2000) Incidence, risk factors and outcome of varicella-zoster virus infection in children after haematopoietic stem cell transplantation. *Bone Marrow Transplant.*, 25 (2), 167–172.

154. Kho, M.M.L., Roest, S., Bovée, D.M., Metselaar, H.J., Hoek, R.A.S., van der Eijk, A.A., Manintveld, O.C., Roodnat, J.I., and van Besouw, N.M. (2021) Herpes Zoster in Solid Organ Transplantation: Incidence and Risk Factors. *Front. Immunol.*, 12 (March), 1–9.

155. Kwon, D.E., Lee, H.S., Lee, K.H., La, Y., Han, S.H., and Song, Y.G. (2021) Incidence of herpes zoster in adult solid organ transplant recipients: A meta-analysis and comprehensive review. *Transpl. Infect. Dis.*, (March), 1–12.

156. Pergam, S.A., and Limaye, A.P. (2019) Varicella zoster virus in solid organ transplantation: Guidelines from the American Society of Transplantation Infectious Diseases Community of Practice. *Clin. Transplant.*, 33 (9), 1–12.

157. Miller, C.S., and Danaher, R.J. (2008) Asymptomatic shedding of herpes simplex virus (HSV) in the oral cavity. *Oral Surgery, Oral Med. Oral Pathol. Oral Radiol. Endodontology*, 105 (1), 43–50.

158. Rooney, B. V., Crucian, B.E., Pierson, D.L., Laudenslager, M.L., and Mehta, S.K. (2019) Herpes Virus Reactivation in Astronauts During Spaceflight and Its Application on Earth. *Front. Microbiol.*, 10 (feburay), 1–9.

159. van Velzen, M., Ouwendijk, W.J.D., Selke, S., Pas, S.D., van Loenen, F.B., Osterhaus, A.D.M.E., Wald, A., and Verjans, G.M.G.M. (2013) Longitudinal study on oral shedding of herpes simplex virus 1 and varicella-zoster virus in individuals infected with HIV. *J. Med. Virol.*, 85 (9), 1669–77.

160. Mehta, S.K., Cohrs, R.J., Forghani, B., Zerbe, G., Gilden, D.H., and Pierson, D.L. (2004) Stress-induced subclinical reactivation of varicella zoster virus in astronauts. *J. Med. Virol.*, 72 (1), 174–179.

161. Gershon, A.A., Chen, J., and Gershon, M.D. (2015) Use of Saliva to Identify Varicella Zoster Virus Infection of the Gut. *Clin. Infect. Dis.*, 61 (4), 536–544.

162. Gershon, M., and Gershon, A. (2018) Varicella-Zoster Virus and the Enteric Nervous System. *J. Infect. Dis.*, 218 (2), S113–S119.

163. Talbird, S.E., La, E.M., Mauskopf, J., Altland, A., Daniels, V., and Wolfson, L.J. (2018) Understanding the role of exogenous boosting in modeling varicella vaccination. *Expert Rev. Vaccines*, 17 (11), 1021–1035.

164. Forbes, H., Douglas, I., Finn, A., Breuer, J., Bhaskaran, K., Smeeth, L., Packer, S., Langan, S.M., Mansfield, K.E., Marlow, R., Whitaker, H., and Warren-Gash, C. (2020) Risk of herpes zoster after exposure to varicella to explore the exogenous boosting hypothesis: self controlled case series study using UK electronic healthcare data. *BMJ*, 368, l6987.

165. Guzzetta, G., Poletti, P., Merler, S., and Manfredi, P. (2016) The Epidemiology of Herpes Zoster after Varicella Immunization under Different Biological Hypotheses: Perspectives from Mathematical Modeling. *Am. J. Epidemiol.*, 183 (8), 765–773.

166. Thomas, S.L., Wheeler, J.G., and Hall, A.J. (2002) Contacts with varicella or with children and protection against herpes zoster in adults: A case-control study. *Lancet*, 360 (9334), 678–682.

167. Goldman, G.S., and King, P.G. (2013) Review of the United States universal varicella vaccination program: Herpes zoster incidence rates, cost-effectiveness, and vaccine efficacy based primarily on the Antelope Valley Varicella Active Surveillance Project data. *Vaccine*, 31 (13), 1680–1694.

168. Thomas, S.L., and Hall, A.J. (2004) What does epidemiology tell us about risk factors for herpes zoster? *Lancet Infect. Dis.*, 4 (1), 26–33.

169. Reynolds, M.A., Chaves, S.S., Harpaz, R., Lopez, A.S., and Seward, J.F. (2008) The Impact of the Varicella Vaccination Program on Herpes Zoster Epidemiology in the United States: A Review. *J. Infect. Dis.*, 197 (s2), S224–S227.

170. Harpaz, R., Leung, J.W., Brown, C.J., and Zhou, F.J. (2015) Psychological stress as a trigger for herpes zoster: Might the conventional wisdom be wrong? *Clin. Infect. Dis.*, 60 (5), 781–785.

171. Soh, H., Chun, J., Han, K., Park, S., Choi, G., Kim, J., Lee, J., Im, J.P., and Kim, J.S. (2019) Increased risk of herpes zoster in young and metabolically healthy patients with inflammatory bowel disease: A nationwide population-based study. *Gut Liver*, 13 (3), 333–341.

172. Forbes, H.J., Thomas, S.L., Smeeth, L., Clayton, T., Farmer, R., Bhaskaran, K., and Langan, S.M. (2016) A systematic review and meta-analysis of risk factors for postherpetic neuralgia. *Pain*, 157 (1), 30–54.

173. Forbes, H.J., Bhaskaran, K., Thomas, S.L., Smeeth, L., Clayton, T., Mansfield, K., Minassian, C., and Langan, S.M. (2016) Quantification of risk factors for postherpetic neuralgia in herpes zoster patients. *Neurology*, 87 (1), 94–102.

174. Gilden, D.H., Dueland, A.N., Devlin, M.E., Mahalingam, R., and Cohrs, R. (1992) Varicella-zoster virus reactivation without rash. *J. Infect. Dis.*, 166 Suppl (May), S30-4.

175. Gilden, D.H., Wright, R.R., Schneck, S.A., Gwaltney, J.M., and Mahalingam, R. (1994) Zoster sine herpete, a clinical variant. *Ann. Neurol.*, 35 (5), 530–3.

176. Nagel, M.A., and Gilden, D. (2013) Complications of varicella zoster virus reactivation. *Curr. Treat. Options Neurol.*, 15 (4), 439–453.

177. Reichelt, M., Zerboni, L., and Arvin, A.M. (2008) Mechanisms of varicella-zoster virus neuropathogenesis in human dorsal root ganglia. *J. Virol.*, 82 (8), 3971–83.

178. Gowrishankar, K., Steain, M., Cunningham, A.L., Rodriguez, M., Blumbergs, P., Slobedman, B., and Abendroth, A. (2010) Characterization of the host immune response in human Ganglia after herpes zoster. *J. Virol.*, 84 (17), 8861–70.

179. Esiri, M.M., and Tomlinson, A.H. (1972) Herpes zoster. Demonstration of virus in trigeminal nerve and ganglion by immunofluorescence and electron microscopy. *J. Neurol. Sci.*, 15 (1), 35–48.

180. Dworkin, R.H., Gnann, J.W., Oaklander, A.L., Raja, S.N., Schmader, K.E., and Whitley, R.J. (2008) Diagnosis and Assessment of Pain Associated With Herpes Zoster and Postherpetic Neuralgia. *J. Pain*, 9 (1 SUPPL.), 37–44.

181. Marin, M., Güris, D., Chaves, S.S., Schmid, S., Seward, J.F., and Advisory Committee on Immunization Practices, C. for D.C. and P. (CDC) (2007) Prevention of varicella: recommendations of the Advisory Committee on Immunization Practices (ACIP). *MMWR. Recomm. reports Morb. Mortal. Wkly. report. Recomm. reports*, 56 (RR-4), 1–40.

182. Levin, M.J., Schmader, K.E., Gnann, J.W., Mcneil, S.A., Vesikari, T., Betts, R.F., Keay, S., Stek, J.E., Bundick, N.D., Su, S.C., Zhao, Y., Li, X., Chan, I.S.F., Annunziato, P.W., and Parrino, J. (2013) Varicella-zoster virus-specific antibody responses in 50-59-year-old recipients of zoster vaccine. *J. Infect. Dis.*, 208 (9), 1386–1390.

183. Tseng, H.F., Harpaz, R., Luo, Y., Hales, C.M., Sy, L.S., Tartof, S.Y., Bialek, S., Hechter,

R.C., and Jacobsen, S.J. (2016) Declining Effectiveness of Herpes Zoster Vaccine in Adults Aged ≥60 Years. *J. Infect. Dis.*, 213 (12), 1872–1875.

184. Lal, H., Cunningham, A.L., Godeaux, O., Chlibek, R., Diez-Domingo, J., Hwang, S.-J., Levin, M.J., McElhaney, J.E., Poder, A., Puig-Barberà, J., Vesikari, T., Watanabe, D., Weckx, L., Zahaf, T., and Heineman, T.C. (2015) Efficacy of an Adjuvanted Herpes Zoster Subunit Vaccine in Older Adults. *N. Engl. J. Med.*, 372 (22), 2087–2096.

185. Dooling, K.L., Guo, A., Patel, M., Lee, G.M., Moore, K., Belongia, E.A., and Harpaz, R. (2018) Recommendations of the Advisory Committee on Immunization Practices for Use of Herpes Zoster Vaccines. *MMWR. Morb. Mortal. Wkly. Rep.*, 67 (3), 103–108.

186. Cunningham, A.L., and Heineman, T. (2017) Vaccine profile of herpes zoster (HZ/su) subunit vaccine. *Expert Rev. Vaccines*, 16 (7), 661–670.

187. Cunningham, A.L., Heineman, T.C., Lal, H., Godeaux, O., Chlibek, R., Hwang, S.-J., McElhaney, J.E., Vesikari, T., Andrews, C., Choi, W.S., Esen, M., Ikematsu, H., Choma, M.K., Pauksens, K., Ravault, S., Salaun, B., Schwarz, T.F., Smetana, J., Abeele, C. Vanden, Van den Steen, P., Vastiau, I., Weckx, L.Y., and Levin, M.J. (2018) Immune Responses to a Recombinant Glycoprotein E Herpes Zoster Vaccine in Adults Aged 50 Years or Older. *J. Infect. Dis.*, 217 (11), 1750–1760.

188. Kawai, K., Gebremeskel, B.G., and Acosta, C.J. (2014) Systematic review of incidence and complications of herpes zoster: towards a global perspective. *BMJ Open*, 4 (6), e004833.

189. Esposito, S., Franco, E., Gavazzi, G., de Miguel, A.G., Hardt, R., Kassianos, G., Bertrand, I., Levant, M.-C., Soubeyrand, B., and López Trigo, J.A. (2018) The public health value of vaccination for seniors in Europe. *Vaccine*, 36 (19), 2523–2528.

190. Patterson, B.J., Chen, C.C., McGuiness, C.B., Glasser, L.I., Sun, K., and Buck, P.O. (2021) Early examination of real-world uptake and second-dose completion of recombinant zoster vaccine in the United States from October 2017 to September 2019. *Hum. Vaccines Immunother.*, 00 (00), 1–6.

191. Haanpää, M., Laippala, P., and Nurmikko, T. (1999) Pain and somatosensory dysfunction in acute herpes zoster. *Clin. J. Pain*, 15 (2), 78–84.

192. Haanpää, M., Laippala, P., and Nurmikko, T. (2000) Allodynia and Pinprick Hypesthesia in Acute Herpes Zoster, and the Development of Postherpetic Neuralgia. *J. Pain Symptom Manage.*, 20 (1), 50–58.

193. Dworkin, R.H., Nagasako, E.M., Johnson, R.W., and Griffin, D.R.J. (2001) Acute pain in herpes zoster: the famciclovir database project. *Pain*, 94 (1), 113–119.

194. Drolet, M., Brisson, M., Schmader, K.E., Levin, M.J., Johnson, R., Oxman, M.N., Patrick, D., Blanchette, C., and Mansi, J.A. (2010) The impact of herpes zoster and postherpetic neuralgia on health-related quality of life: a prospective study. *C. Can. Med. Assoc. J.*, 182 (16), 1731–6.

195. Asada, H. (2019) VZV-specific cell-mediated immunity, but not humoral immunity, correlates inversely with the incidence of herpes zoster and the severity of skin symptoms and zoster-associated pain: The SHEZ study. *Vaccine*, 37 (44), 6776–6781.

196. Decroix, J., Partsch, H., Gonzalez, R., Mobacken, H., Goh, C.L., Walsh, J.B., Shukla, S., and Naisbett, B. (2000) Factors influencing pain outcome in herpes zoster: An observational study with valaciclovir. *J. Eur. Acad. Dermatology Venereol.*, 14 (1), 23–33.

197. Johnson, R.W., Wasner, G., Saddier, P., and Baron, R. (2008) Herpes zoster and postherpetic neuralgia: optimizing management in the elderly patient. *Drugs Aging*, 25 (12), 991–1006.

198. Petersen, K.L., and Rowbotham, M.C. (2010) Natural history of sensory function after herpes zoster. *Pain*, 150 (1), 83–92.

199. Nurmikko, T., and Bowsher, D. (1990) Somatosensory findings in postherpetic neuralgia. *J. Neurol. Neurosurg. Psychiatry*, 53 (2), 135–141.

200. Jung, B.F., Johnson, R.W., Griffin, D.R.J., and Dworkin, R.H. (2004) Risk factors for postherpetic neuralgia in patients with herpes zoster. *Neurology*, 62 (9), 1545–1551.

201. Borkar, D.S., Tham, V.M., Esterberg, E., Ray, K.J., Vinoya, A.C., Parker, J. V., Uchida, A., and Acharya, N.R. (2013) Incidence of Herpes Zoster Ophthalmicus: Results from the Pacific Ocular Inflammation Study. *Ophthalmology*, 120 (3), 451–456.

202. Tran, K.D., Falcone, M.M., Choi, D.S., Goldhardt, R., Karp, C.L., Davis, J.L., and Galor, A. (2016) Epidemiology of Herpes Zoster Ophthalmicus Recurrence and Chronicity. *Ophthalmology*, 123 (7), 1469–1475.

203. Davis, A.R., and Sheppard, J. (2019) Herpes Zoster Ophthalmicus Review and Prevention. *Eye Contact Lens*, 45 (5), 286–291.

204. Sutherland, J.P., Steain, M., Buckland, M.E., Rodriguez, M., Cunningham, A.L., Slobedman, B., and Abendroth, A. (2019) Persistence of a T Cell Infiltrate in Human Ganglia Years After Herpes Zoster and During Post-herpetic Neuralgia. *Front. Microbiol.*, 10 (September), 2117.

205. Schünemann, S., Mainka, C., and Wolff, M.H. (1999) No acute varicella-zoster virus

replication in peripheral blood mononuclear cells during postherpetic neuralgia. *Acta Virol.*, 43 (6), 337—340.

206. Mainka, C., Fuß, B., Geiger, H., Höfelmayr, H., and Wolff, M.H. (1998) Characterization of viremia at different stages of Varicella-zoster virus infection. *J. Med. Virol.*, 56 (1), 91–98.

207. De Jong, M.D., Weel, J.F.L., Schuurman, T., Wertheim-Van Dillen, P.M.E., and Boom, R. (2000) Quantitation of varicella-zoster virus DNA in whole blood, plasma, and serum by PCR and electrochemiluminescence. *J. Clin. Microbiol.*, 38 (7), 2568–2573.

208. Ito, M., Nishihara, H., Mizutani, K. ichi, Kitamura, K., Ihara, T., Kamiya, H., and Sakurai, M. (1995) Detection of varicella-zoster virus (VZV) DNA in throat swabs and peripheral blood mononuclear cells of immunocompromised patients with herpes zoster by polymerase chain reaction. *Clin. Diagn. Virol.*, 4 (2), 105–112.

209. Chen, N., Li, Q., Yang, J., Zhou, M., Zhou, D., and He, L. (2014) Antiviral treatment for preventing postherpetic neuralgia. *Cochrane database Syst. Rev.*, 2014 (2), CD006866.

210. Acosta, E.P., and Balfour, H.H. (2001) Acyclovir for treatment of postherpetic neuralgia: efficacy and pharmacokinetics. *Antimicrob. Agents Chemother.*, 45 (10), 2771–4.

211. Watson, C.P.N., Morshead, C., Van der Kooy, D., Deck, J., and Evans, R.J. (1988) Post-herpetic neuralgia: Post-mortem analysis of a case. *Pain*, 34 (2), 129–138.

212. Watson, C.P.N., Deck, J.H., Morshead, C., Van der Kooy, D., and Evans, R.J. (1991) Post-herpetic neuralgia: Further post-mortem studies of cases with and without pain. *Pain*, 44 (2), 105–117.

213. Ji, R.-R., Chamessian, A., and Zhang, Y.-Q. (2016) Pain regulation by non-neuronal cells and inflammation. *Science (80-.).*, 354 (6312), 572–577.

214. Mahalingam, R., Wellish, M., Brucklier, J., and Gilden, D.H. (1995) Persistence of varicella-zoster virus DNA in elderly patients with postherpetic neuralgia. *J. Neurovirol.*, 1 (1), 130–133.

215. Vafai, A., Wellish, M., and Gilden, D.H. (1988) Expression of varicella-zoster virus in blood mononuclear cells of patients with postherpetic neuralgia. *Proc. Natl. Acad. Sci. U. S. A.*, 85 (8), 2767–2770.

216. Oaklander, A.L. (2001) The density of remaining nerve endings in human skin with and without postherpetic neuralgia after shingles. *Pain*, 92 (1–2), 139–45.

217. Opstelten, W., McElhaney, J., Weinberger, B., Oaklander, A.L., and Johnson, R.W. (2010) The impact of varicella zoster virus: chronic pain. *J. Clin. Virol.*, 48 Suppl 1 (SUPPL 1), S8-13.

218. Rowbotham, M.C., Yosipovitch, G., Connolly, M.K., Finlay, D., Forde, G., and Fields, H.L. (1996) Cutaneous innervation density in the allodynic form of postherpetic neuralgia. *Neurobiol. Dis.*, 3 (3), 205–214.

219. Watson, P.N.C., Evans, R.J., Watt, V.R., and Birkett, N. (1988) Post-herpetic neuralgia: 208 cases. *Pain*, 35 (3), 289–297.

220. Devor, M. (2018) Rethinking the causes of pain in herpes zoster and postherpetic neuralgia: the ectopic pacemaker hypothesis. *PAIN Reports*, 3 (6), e702.

221. Delaney, A., Colvin, L.A., Fallon, M.T., Dalziel, R.G., Mitchell, R., and Fleetwood-Walker, S.M. (2009) Postherpetic neuralgia: from preclinical models to the clinic. *Neurotherapeutics*, 6 (4), 630–7.

222. Wood, K.C., Blackwell, J.M., and Geffen, M.N. (2017) Cortical inhibitory interneurons control sensory processing. *Curr. Opin. Neurobiol.*, 46, 200–207.

223. Latremoliere, A., and Woolf, C.J. (2009) Central sensitization: a generator of pain hypersensitivity by central neural plasticity. *J. pain*, 10 (9), 895–926.

224. Ahmed, S.V., Hamada, H., Jayawarna, C., and Chandra, S. (2012) Shingles with secondary asymptomatic CNS involvement! *Case Reports*, 2012 (may29 1), bcr0320126041–bcr0320126041.

225. Gilden, D., Nagel, M.A., Cohrs, R.J., and Mahalingam, R. (2013) The Variegate Neurological Manifestations of Varicella Zoster Virus Infection. *Curr. Neurol. Neurosci. Rep.*, 13 (9), 374.

226. Elion, G.B. (1983) The biochemistry and mechanism of action of acyclovir. *J. Antimicrob. Chemother.*, 12 (SUPPL. B), 9–17.

227. Shafran, S.D., Tyring, S.K., Ashton, R., Decroix, J., Forszpaniak, C., Wade, A., Paulet, C., and Candaele, D. (2004) Once, twice, or three times daily famciclovir compared with aciclovir for the oral treatment of herpes zoster in immunocompetent adults: A randomized, multicenter, double-blind clinical trial. *J. Clin. Virol.*, 29 (4), 248–253.

228. Tyring, S., Barbarash, R.A., Nahlik, J.E., Cunningham, A., Marley, J., Heng, M., Jones, T., Rea, T., Boon, R., and Saltzman, R. (1995) Famciclovir for the treatment of acute herpes zoster: effects on acute disease and postherpetic neuralgia. A randomized, double-blind,

placebo-controlled trial. Collaborative Famciclovir Herpes Zoster Study Group. *Ann. Intern. Med.*, 123 (2), 89–96.

229. Saint-Leéger, E., Caumes, E., Breton, G., Douard, D., Saiag, P., Huraux, J.M., Bricaire, F., Agut, H., and Fillet, A.M. (2001) Clinical and virologic characterization of acyclovir-resistant varicella-zoster viruses isolated from 11 patients with acquired immunodeficiency syndrome. *Clin. Infect. Dis.*, 33 (12), 2061–2067.

230. Piret, J., and Boivin, G. (2016) Antiviral resistance in herpes simplex virus and varicella-zoster virus infections. *Curr. Opin. Infect. Dis.*, 29 (6), 654–662.

231. Smith, K.J. (1991) Acyclovir-Resistant Varicella Zoster Responsive to Foscarnet. *Arch. Dermatol.*, 127 (7), 1069.

232. Dworkin, R.H., Johnson, R.W., Breuer, J., Gnann, J.W., Levin, M.J., Backonja, M., Betts, R.F., Gershon, A.A., Haanpää, M.L., McKendrick, M.W., Nurmikko, T.J., Oaklander, A.L., Oxman, M.N., Langston, D.P., Petersen, K.L., Rowbotham, M.C., Schmader, K.E., Stacey, B.R., Tyring, S.K., Wijck, A.J.M. van, Wallace, M.S., Wassilew, S.W., and Whitley, R.J. (2007) Recommendations for the Management of Herpes Zoster. *Clin. Infect. Dis.*, 44 (Supplement_1), S1–S26.

233. Schutzer-Weissmann, J., and Farquhar-Smith, P. (2017) Post-herpetic neuralgia – A review of current management and future directions. *Expert Opin. Pharmacother.*, 18 (16), 1739–1750.

234. Jaggi, A.S., Jain, V., and Singh, N. (2011) Animal models of neuropathic pain. *Fundam. Clin. Pharmacol.*, 25 (1), 1–28.

235. Dalziel, R.G., Bingham, S., Sutton, D., Grant, D., Champion, J.M., Dennis, S.A., Quinn, J.P., Bountra, C., and Mark, M.A. (2004) Allodynia in rats infected with varicella zoster virus--a small animal model for post-herpetic neuralgia. *Brain Res. Brain Res. Rev.*, 46 (2), 234–42.

236. Garry, E.M., Delaney, A., Anderson, H.A., Sirinathsinghji, E.C., Clapp, R.H., Martin, W.J., Kinchington, P.R., Krah, D.L., Abbadie, C., and Fleetwood-Walker, S.M. (2005) Varicella zoster virus induces neuropathic changes in rat dorsal root ganglia and behavioral reflex sensitisation that is attenuated by gabapentin or sodium channel blocking drugs. *Pain*, 118 (1–2), 97–111.

237. Stinson, C., Deng, M., Yee, M.B., Bellinger, L.L., Kinchington, P.R., and Kramer, P.R. (2017) Sex differences underlying orofacial varicella zoster associated pain in rats. *BMC Neurol.*, 17 (1), 95.

238. Kramer, P.R., Strand, J., Stinson, C., Bellinger, L.L., Kinchington, P.R., Yee, M.B., Umorin, M., and Peng, Y.B. (2017) Role for the Ventral Posterior Medial/Posterior Lateral Thalamus and Anterior Cingulate Cortex in Affective/Motivation Pain Induced by Varicella Zoster Virus. *Front. Integr. Neurosci.*, 11 (October), 27.

239. Fuchs, P.N., and McNabb, C.T. (2012) The place escape/avoidance paradigm: a novel method to assess nociceptive processing. *J. Integr. Neurosci.*, 11 (1), 61–72.

240. Prochazkova, M., Terse, A., Amin, N.D., Hall, B., Utreras, E., Pant, H.C., and Kulkarni, A.B. (2013) Activation of cyclin-dependent kinase 5 mediates orofacial mechanical hyperalgesia. *Mol. Pain*, 9 (1), 1–12.

241. Chaplan, S.R., Bach, F.W., Pogrel, J.W., Chung, J.M., and Yaksh, T.L. (1994) Quantitative assessment of tactile allodynia in the rat paw. *J. Neurosci. Methods*, 53 (1), 55–63.

242. Hargreaves, K., Dubner, R., Brown, F., Flores, C., and Joris, J. (1988) A new and sensitive method for measuring thermal nociception in cutaneous hyperalgesia. *Pain*, 32 (1), 77–88.

243. Sadzot-Delvaux, C., Debrus, S., Nikkels, A., Piette, J., and Rentier, B. (1995) Varicella-zoster virus latency in the adult rat is a useful model for human latent infection. *Neurology*, 45 (12 SUPPL. 8).

244. Kinchington, P.R., and Goins, W.F. (2011) Varicella zoster virus-induced pain and post-herpetic neuralgia in the human host and in rodent animal models. *J. Neurovirol.*, 17 (6), 590–9.

245. Guedon, J.-M.G., Zhang, M., Glorioso, J.C., Goins, W.F., and Kinchington, P.R. (2014) Relief of pain induced by varicella-zoster virus in a rat model of post-herpetic neuralgia using a herpes simplex virus vector expressing enkephalin. *Gene Ther.*, 21 (7), 694–702.

246. Guedon, J.-M.G., Yee, M.B., Zhang, M., Harvey, S.A.K., Goins, W.F., and Kinchington, P.R. (2015) Neuronal changes induced by Varicella Zoster Virus in a rat model of postherpetic neuralgia. *Virology*, 482, 167–80.

247. Hasnie, F.S., Breuer, J., Parker, S., Wallace, V., Blackbeard, J., Lever, I., Kinchington, P.R., Dickenson, A.H., Pheby, T., and Rice, A.S.C. (2007) Further characterization of a rat model of varicella zoster virus-associated pain: Relationship between mechanical hypersensitivity and anxiety-related behavior, and the influence of analgesic drugs. *Neuroscience*, 144 (4), 1495–508.

248. Wallace, V.C.J., Segerdahl, A.R., Lambert, D.M., Vandevoorde, S., Blackbeard, J., Pheby, T., Hasnie, F., and Rice, A.S.C. (2007) The effect of the palmitoylethanolamide analogue, palmitoylallylamide (L-29) on pain behaviour in rodent models of neuropathy. *Br. J.*

Pharmacol., 151 (7), 1117–1128.

249. Medhurst, S.J., Collins, S.D., Billinton, A., Bingham, S., Dalziel, R.G., Brass, A., Roberts, J.C., Medhurst, A.D., and Chessell, I.P. (2008) Novel histamine H3 receptor antagonists GSK189254 and GSK334429 are efficacious in surgically-induced and virally-induced rat models of neuropathic pain. *Pain*, 138 (1), 61–69.

250. Guedon, J.-M.G., Wu, S., Zheng, X., Churchill, C.C., Glorioso, J.C., Liu, C.-H., Liu, S., Vulchanova, L., Bekker, A., Tao, Y.-X., Kinchington, P.R., Goins, W.F., Fairbanks, C.A., and Hao, S. (2015) Current Gene Therapy using Viral Vectors for Chronic Pain. *Mol. Pain*, 11 (1), s12990-015–0018.

251. Liesegang, T.J. (2008) Herpes Zoster Ophthalmicus. Natural History, Risk Factors, Clinical Presentation, and Morbidity. *Ophthalmology*, 115 (2 SUPPL.), 3–12.

252. Shiraki, K., Toyama, N., Shiraki, A., and Yajima, M. (2018) Age-dependent trigeminal and female-specific lumbosacral increase in herpes zoster distribution in the elderly. *J. Dermatol. Sci.*, 90 (2), 166–171.

253. Stinson, C., Logan, S.M., Bellinger, L.L., Rao, M., Kinchington, P.R., and Kramer, P.R. (2019) Estradiol Acts in Lateral Thalamic Region to Attenuate Varicella Zoster Virus Associated Affective Pain. *Neuroscience*, 414, 99–111.

254. Kramer, P., Rao, M., Stinson, C., Bellinger, L.L., Kinchington, P.R., and Yee, M.B. (2018) Aromatase derived estradiol within the thalamus modulates pain induced by varicella zoster virus. *Front. Integr. Neurosci.*, 12 (October), 1–14.

255. Hornung, R., Pritchard, A., Kinchington, P.R., and Kramer, P.R. (2020) Reduced activity of GAD67 expressing cells in the reticular thalamus enhance thalamic excitatory activity and varicella zoster virus associated pain. *Neurosci. Lett.*, 736 (May), 135287.

256. Hornung, R., Pritchard, A., Kinchington, P.R., and Kramer, P.R. (2020) Comparing Gene Expression in the Parabrachial and Amygdala of Diestrus and Proestrus Female Rats after Orofacial Varicella Zoster Injection. *Int. J. Mol. Sci.*, 21 (16), 5749.

257. Sadzot-Delvaux, C., Merville-Louis, M.P., Delrée, P., Marc, P., Piette, J., Moonen, G., and Rentier, B. (1990) An in vivo model of varicella-zoster virus latent infection of dorsal root ganglia. *J. Neurosci. Res.*, 26 (1), 83–9.

258. Steain, M., Sutherland, J.P., Rodriguez, M., Cunningham, A.L., Slobedman, B., and Abendroth, A. (2014) Analysis of T cell responses during active varicella-zoster virus reactivation in human ganglia. *J. Virol.*, 88 (5), 2704–16.

259. Annunziato, P., LaRussa, P., Lee, P., Steinberg, S., Lungu, O., Gershon, A.A., and Silverstein, S. (1998) Evidence of latent varicella-zoster virus in rat dorsal root ganglia. *J. Infect. Dis.*, 178 Suppl (5 SUPPL.), S48-51.

260. Kennedy, P.G.E., Grinfeld, E., Bontems, S., and Sadzot-Delvaux, C. (2001) Varicella-Zoster virus gene expression in latently infected rat dorsal root ganglia. *Virology*, 289 (2), 218–23.

261. Grinfeld, E., Sadzot-Delvaux, C., and Kennedy, P.G.E. (2004) Varicella-Zoster virus proteins encoded by open reading frames 14 and 67 are both dispensable for the establishment of latency in a rat model. *Virology*, 323 (1), 85–90.

262. Qiu, Y., Hao, M.L., Cheng, X.T., and Hua, Z. (2020) Bioinformatics Analysis of Genes and Mechanisms in Postherpetic Neuralgia. *Pain Res. Manag.*, 2020.

263. Xu, X., Yang, X., Zhang, P., Chen, X., Liu, H., and Li, Z. (2012) Effects of exogenous galanin on neuropathic pain state and change of galanin and its receptors in DRG and SDH after sciatic nerve-pinch injury in rat. *PLoS One*, 7 (5), 1–10.

264. Magnussen, C., Hung, S.-P., and Ribeiro-da-Silva, A. (2015) Novel expression pattern of neuropeptide Y immunoreactivity in the peripheral nervous system in a rat model of neuropathic pain. *Mol. Pain*, 11 (1), 31.

265. Jarvis, M.F., Honore, P., Shieh, C.C., Chapman, M., Joshi, S., Zhang, X.F., Kort, M., Carroll, W., Marron, B., Atkinson, R., Thomas, J., Liu, D., Krambis, M., Liu, Y., McGaraughty, S., Chu, K., Roeloffs, R., Zhong, C., Mikusa, J.P., Hernandez, G., Gauvin, D., Wade, C., Zhu, C., Pai, M., Scanio, M., Shi, L., Drizin, I., Gregg, R., Matulenko, M., Hakeem, A., Gross, M., Johnson, M., Marsh, K., Wagoner, P.K., Sullivan, J.P., Faltynek, C.R., and Krafte, D.S. (2007) A-803467, a potent and selective Nav1.8 sodium channel blocker, attenuates neuropathic and inflammatory pain in the rat. *Proc. Natl. Acad. Sci. U. S. A.*, 104 (20), 8520–8525.

266. Tsujino, H., Kondo, E., Fukuoka, T., Dai, Y., Tokunaga, A., Miki, K., Yonenobu, K., Ochi, T., and Noguchi, K. (2000) Activating transcription factor 3 (ATF3) induction by axotomy in sensory and motoneurons: A novel neuronal marker of nerve injury. *Mol. Cell. Neurosci.*, 15 (2), 170–182.

267. Maratou, K., Wallace, V.C.J., Hasnie, F.S., Okuse, K., Hosseini, R., Jina, N., Blackbeard, J., Pheby, T., Orengo, C., Dickenson, A.H., McMahon, S.B., and Rice, A.S.C. (2009) Comparison of dorsal root ganglion gene expression in rat models of traumatic and HIV-associated neuropathic pain. *Eur. J. Pain*, 13 (4), 387–398.

268. Oaklander, A.L., Romans, K., Horasek, S., Stocks, A., Hauer, P., and Meyer, R.A. (1998)

Unilateral postherpetic neuralgia is associated with bilateral sensory neuron damage. *Ann. Neurol.*, 44 (5), 789–795.

269. Alvarez, F.K., de Siqueira, S.R.D.T., Okada, M., Teixeira, M.J., and de Siqueira, J.T.T. (2007) Evaluation of the sensation in patients with trigeminal post-herpetic neuralgia. *J. Oral Pathol. Med.*, 36 (6), 347–50.

270. Studahl, M., Petzold, M., and Cassel, T. (2013) Disease burden of herpes zoster in Sweden - predominance in the elderly and in women - a register based study. *BMC Infect. Dis.*, 13 (1), 586.

271. Muñoz-Quiles, C., López-Lacort, M., Orrico-Sánchez, A., and Díez-Domingo, J. (2018) Letter to the editor regarding "The role of age-sex interaction in the development of post-herpetic neuralgia." *Hum. Vaccines Immunother.*, 14 (4), 906–908.

272. Amicizia, D., Domnich, A., Arata, L., Zoli, D., Zotti, C.M., Cacello, E., Gualano, M.R., Gasparini, R., and Panatto, D. (2017) The role of age-sex interaction in the development of post-herpetic neuralgia. *Hum. Vaccines Immunother.*, 13 (2), 376–378.

273. Wei, S., Li, X., Wang, H., Liu, Q., and Shao, L. (2019) Analysis of the Risk Factors for Postherpetic Neuralgia. *Dermatology*, 235 (5), 426–433.

274. Goh, C.L., and Khoo, L. (1997) A retrospective study of the clinical presentation and outcome of herpes zoster in a tertiary dermatology outpatient referral clinic. *Int. J. Dermatol.*, 36 (9), 667–72.

275. Rowbotham, M., Harden, N., Stacey, B., Bernstein, P., and Magnus-Miller, L. (1998) Gabapentin for the treatment of postherpetic neuralgia: a randomized controlled trial. *JAMA*, 280 (21), 1837–42.

276. Pappagallo, M. (2003) Newer antiepileptic drugs: Possible uses in the treatment of neuropathic pain and migraine. *Clin. Ther.*, 25 (10), 2506–2538.

277. Takahashi, M., Okuno, Y., Otsuka, T., Osame, J., and Takamizawa, A. (1975) Development of a live attenuated varicella vaccine. *Biken J.*, 18 (1), 25–33.

278. Igarashi, H., Koizumi, K., Kaneko, R., Ikeda, K., Egawa, R., Yanagawa, Y., Muramatsu, S., Onimaru, H., Ishizuka, T., and Yawo, H. (2016) A Novel Reporter Rat Strain That Conditionally Expresses the Bright Red Fluorescent Protein tdTomato. *PLoS One*, 11 (5), e0155687.

279. Pomp, O., Brokhman, I., Ziegler, L., Almog, M., Korngreen, A., Tavian, M., and Goldstein, R.S. (2008) PA6-induced human embryonic stem cell-derived neurospheres: A new source

of human peripheral sensory neurons and neural crest cells. *Brain Res.*, 1230, 50–60.

280. Sloutskin, A., and Goldstein, R.S. (2014) Laboratory preparation of Varicella-Zoster Virus: Concentration of virus-containing supernatant, use of a debris fraction and magnetofection for consistent cell-free VZV infections. *J. Virol. Methods*, 206, 128–132.

281. Szpara, M.L., Tafuri, Y.R., and Enquist, L.W. (2011) Preparation of Viral DNA from Nucleocapsids. *J. Vis. Exp.*, (54), 2–7.

282. Moffat, J.F., Zerboni, L., Kinchington, P.R., Grose, C., Kaneshima, H., and Arvin, A.M. (1998) Attenuation of the vaccine Oka strain of varicella-zoster virus and role of glycoprotein C in alphaherpesvirus virulence demonstrated in the SCID-hu mouse. *J. Virol.*, 72 (2), 965–74.

283. Gerk, P.M. (2011) Quantitative immunofluorescent blotting of the Multidrug Resistance-associated Protein 2 (MRP2). *J. Pharmacol. Toxicol. Methods*, 63 (3), 279–282.

284. Eisfeld, A.J., Turse, S.E., Jackson, S.A., Lerner, E.C., and Kinchington, P.R. (2006) Phosphorylation of the varicella-zoster virus (VZV) major transcriptional regulatory protein IE62 by the VZV open reading frame 66 protein kinase. *J. Virol.*, 80 (4), 1710–23.

285. Kinchington, P.R., Inchauspe, G., Subak-Sharpe, J.H., Robey, F., Hay, J., and Ruyechan, W.T. (1988) Identification and characterization of a varicella-zoster virus DNA-binding protein by using antisera directed against a predicted synthetic oligopeptide. *J. Virol.*, 62 (3), 802–9.

286. Sato, B., Sommer, M., Ito, H., and Arvin, A.M. (2003) Requirement of varicella-zoster virus immediate-early 4 protein for viral replication. *J. Virol.*, 77 (22), 12369–72.

287. Kukkar, A., Singh, N., and Jaggi, A.S. (2014) Attenuation of neuropathic pain by sodium butyrate in an experimental model of chronic constriction injury in rats. *J. Formos. Med. Assoc.*, 113 (12), 921–928.

288. Russo, R., De Caro, C., Avagliano, C., Cristiano, C., La Rana, G., Mattace Raso, G., Berni Canani, R., Meli, R., and Calignano, A. (2016) Sodium butyrate and its synthetic amide derivative modulate nociceptive behaviors in mice. *Pharmacol. Res.*, 103, 279–291.

289. Verweij, M.C., Wellish, M., Whitmer, T., Malouli, D., Lapel, M., Jonjić, S., Haas, J.G., DeFilippis, V.R., Mahalingam, R., and Früh, K. (2015) Varicella Viruses Inhibit Interferon-Stimulated JAK-STAT Signaling through Multiple Mechanisms. *PLoS Pathog.*, 11 (5), e1004901.

290. Cai, M., Wang, S., Xing, J., and Zheng, C. (2011) Characterization of the nuclear import

and export signals, and subcellular transport mechanism of varicella-zoster virus ORF9. *J. Gen. Virol.*, 92 (Pt 3), 621–6.

291. Stellberger, T., Häuser, R., Baiker, A., Pothineni, V.R., Haas, J., and Uetz, P. (2010) Improving the yeast two-hybrid system with permutated fusions proteins: the Varicella Zoster Virus interactome. *Proteome Sci.*, 8 (1), 8.

292. Defechereux, P., Debrus, S., Baudoux, L., Rentier, B., and Piette, J. (1997) Varicella-zoster virus open reading frame 4 encodes an immediate-early protein with posttranscriptional regulatory properties. *J. Virol.*, 71 (9), 7073–9.

293. Defechereux, P., Melen, L., Baudoux, L., Merville-Louis, M.P., Rentier, B., and Piette, J. (1993) Characterization of the regulatory functions of varicella-zoster virus open reading frame 4 gene product. *J. Virol.*, 67 (7), 4379–85.

294. Ote, I., Lebrun, M., Vandevenne, P., Bontems, S., Medina-Palazon, C., Manet, E., Piette, J., and Sadzot-Delvaux, C. (2009) Varicella-zoster virus IE4 protein interacts with SR proteins and exports mRNAs through the TAP/NXF1 pathway. *PLoS One*, 4 (11), e7882.

295. Debrus, S., Sadzot-Delvaux, C., Nikkels, A.F., Piette, J., and Rentier, B. (1995) Varicella-zoster virus gene 63 encodes an immediate-early protein that is abundantly expressed during latency. *J. Virol.*, 69 (5), 3240–5.

296. Huang, Y., Zhang, J., Halawa, M.A., and Yao, S. (2014) Nuclear localization signals of varicella zoster virus ORF4. *Virus Genes*, 48 (2), 243–51.

297. Bontems, S., Di Valentin, E., Baudoux, L., Rentier, B., Sadzot-Delvaux, C., and Piette, J. (2002) Phosphorylation of varicella-zoster virus IE63 protein by casein kinases influences its cellular localization and gene regulation activity. *J. Biol. Chem.*, 277 (23), 21050–60.

298. Stevenson, D., Xue, M., Hay, J., and Ruyechan, W.T. (1996) Phosphorylation and nuclear localization of the varicella-zoster virus gene 63 protein. *J. Virol.*, 70 (1), 658–62.

299. Mao, Y., Zhou, J., Liu, X., Gu, E., Zhang, Z., and Tao, W. (2019) Comparison of Different Histone Deacetylase Inhibitors in Attenuating Inflammatory Pain in Rats. *Pain Res. Manag.*, 2019.

300. Ambagala, A.P.N., and Cohen, J.I. (2007) Varicella-Zoster virus IE63, a major viral latency protein, is required to inhibit the alpha interferon-induced antiviral response. *J. Virol.*, 81 (15), 7844–51.

301. Sommer, M.H., Zagha, E., Serrano, O.K., Ku, C.C., Zerboni, L., Baiker, A., Santos, R., Spengler, M., Lynch, J., Grose, C., Ruyechan, W., Hay, J., and Arvin, A.M. (2001)

Mutational analysis of the repeated open reading frames, ORFs 63 and 70 and ORFs 64 and 69, of varicella-zoster virus. *J. Virol.*, 75 (17), 8224–39.

302. Mitchell, B.M., Bloom, D.C., Cohrs, R.J., Gilden, D.H., and Kennedy, P.G.E. (2003) Herpes simplex virus-1 and varicella-zoster virus latency in ganglia. *J. Neurovirol.*, 9 (2), 194–204.

303. Cohen, J.I. (2010) Rodent models of varicella-zoster virus neurotropism. *Curr. Top. Microbiol. Immunol.*, 342 (4), 277–89.

304. Blackbeard, J., Wallace, V.C.J., O'Dea, K.P., Hasnie, F., Segerdahl, A., Pheby, T., Field, M.J., Takata, M., and Rice, A.S.C. (2012) The correlation between pain-related behaviour and spinal microgliosis in four distinct models of peripheral neuropathy. *Eur. J. Pain*, 16 (10), 1357–1367.

305. Tunnicliffe, R.B., Schacht, M., Levy, C., Jowitt, T.A., Sandri-Goldin, R.M., and Golovanov, A.P. (2015) The structure of the folded domain from the signature multifunctional protein ICP27 from herpes simplex virus-1 reveals an intertwined dimer. *Sci. Rep.*, 5 (1), 11234.

306. Zerboni, L., Reichelt, M., Jones, C.D., Zehnder, J.L., Ito, H., and Arvin, A.M. (2007) Aberrant infection and persistence of varicella-zoster virus in human dorsal root ganglia in vivo in the absence of glycoprotein I. *Proc. Natl. Acad. Sci. U. S. A.*, 104 (35), 14086–91.

307. Knickelbein, J.E., Khanna, K.M., Yee, M.B., Baty, C.J., Kinchington, P.R., and Hendricks, R.L. (2008) Noncytotoxic Lytic Granule-Mediated CD8+ T Cell Inhibition of HSV-1 Reactivation from Neuronal Latency. *Science (80-.).*, 322 (5899), 268–271.

308. Pereira, R.A., Simon, M.M., and Simmons, A. (2000) Granzyme A, a noncytolytic component of CD8(+) cell granules, restricts the spread of herpes simplex virus in the peripheral nervous systems of experimentally infected mice. *J. Virol.*, 74 (2), 1029–32.

309. Riva, L., Thiry, M., Lebrun, M., L'homme, L., Piette, J., and Sadzot-Delvaux, C. (2015) Deletion of the ORF9p Acidic Cluster Impairs the Nuclear Egress of Varicella-Zoster Virus Capsids. *J. Virol.*, 89 (4), 2436–2441.

310. Kenyon, T.K., Homan, E., Storlie, J., Ikoma, M., and Grose, C. (2003) Comparison of varicella-zoster virus ORF47 protein kinase and casein kinase II and their substrates. *J. Med. Virol.*, 70 (SUPPL. 1), 95–102.

311. Cilloniz, C., Jackson, W., Grose, C., Czechowski, D., Hay, J., and Ruyechan, W.T. (2007) The varicella-zoster virus (VZV) ORF9 protein interacts with the IE62 major VZV transactivator. *J. Virol.*, 81 (2), 761–774.

312. Natsume, T., and Kanemaki, M.T. (2017) Conditional Degrons for Controlling Protein Expression at the Protein Level. *Annu. Rev. Genet.*, 51, 83–102.

313. Baiker, A., Bagowski, C., Ito, H., Sommer, M., Zerboni, L., Fabel, K., Hay, J., Ruyechan, W., and Arvin, A.M. (2004) The Immediate-Early 63 Protein of Varicella-Zoster Virus: Analysis of Functional Domains Required for Replication In Vitro and for T-Cell and Skin Tropism in the SCIDhu Model In Vivo. *J. Virol.*, 78 (3), 1181–1194.

314. Bonger, K.M., Chen, L., Liu, C.W., and Wandless, T.J. (2011) Small-molecule displacement of a cryptic degron causes conditional protein degradation. *Nat. Chem. Biol.*, 7 (8), 531–537.

315. Holland, A.J., Fachinetti, D., Han, J.S., and Cleveland, D.W. (2012) Inducible, reversible system for the rapid and complete degradation of proteins in mammalian cells. *Proc. Natl. Acad. Sci.*, 109 (49), E3350–E3357.

316. Huffmaster, N.J., Sollars, P.J., Richards, A.L., Pickard, G.E., and Smith, G.A. (2015) Dynamic ubiquitination drives herpesvirus neuroinvasion. *Proc. Natl. Acad. Sci. U. S. A.*, 112 (41), 12818–23.

317. Richards, A.L., Sollars, P.J., Pitts, J.D., Stults, A.M., Heldwein, E.E., Pickard, G.E., and Smith, G.A. (2017) The pUL37 tegument protein guides alpha-herpesvirus retrograde axonal transport to promote neuroinvasion. *PLoS Pathog.*, 13 (12), 1–32.

318. Depledge, D.P., and Wilson, A.C. (2020) Using Direct RNA Nanopore Sequencing to Deconvolute Viral Transcriptomes. *Curr. Protoc. Microbiol.*, 57 (1), e99.

319. Yu, X., Seitz, S., Pointon, T., Bowlin, J.L., Cohrs, R.J., Jonjić, S., Haas, J., Wellish, M., and Gilden, D. (2013) Varicella zoster virus infection of highly pure terminally differentiated human neurons. *J. Neurovirol.*, 19 (1), 75–81.